



CORPES¹³

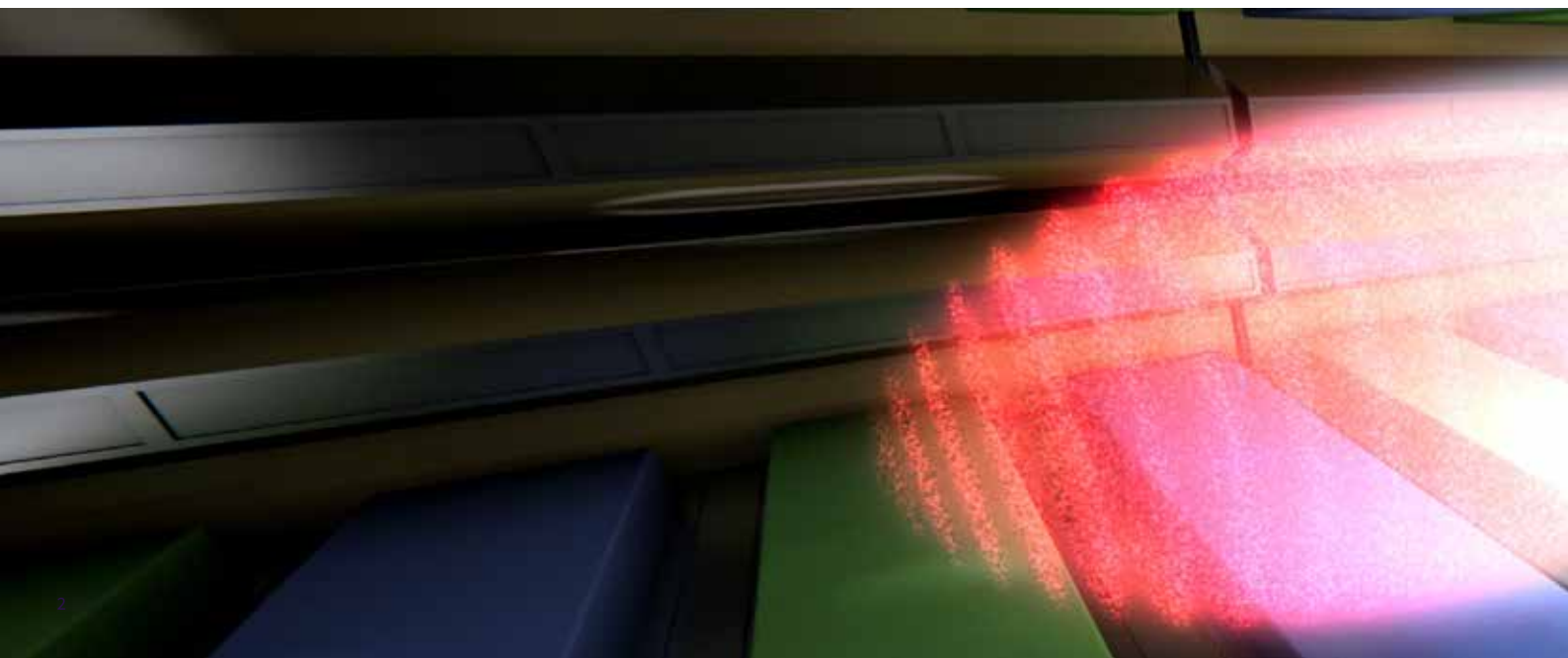
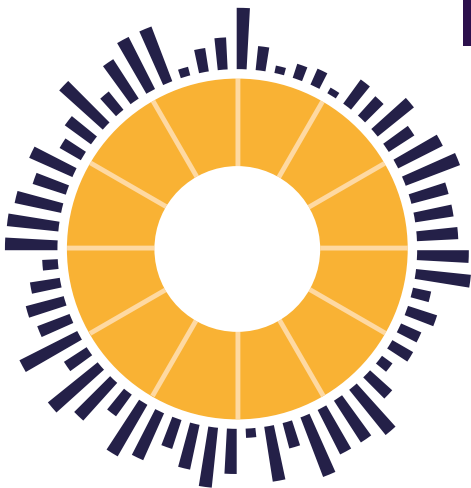
International workshop on strong *correlations*
and angle-resolved photoemission spectroscopy

29 July – 2 August 2013
Hamburg, Germany

PROGRAMME

PARTNERS

We thank our partners for their kind support.



GREETINGS

Dear attendees of the CORPES¹³ workshop,

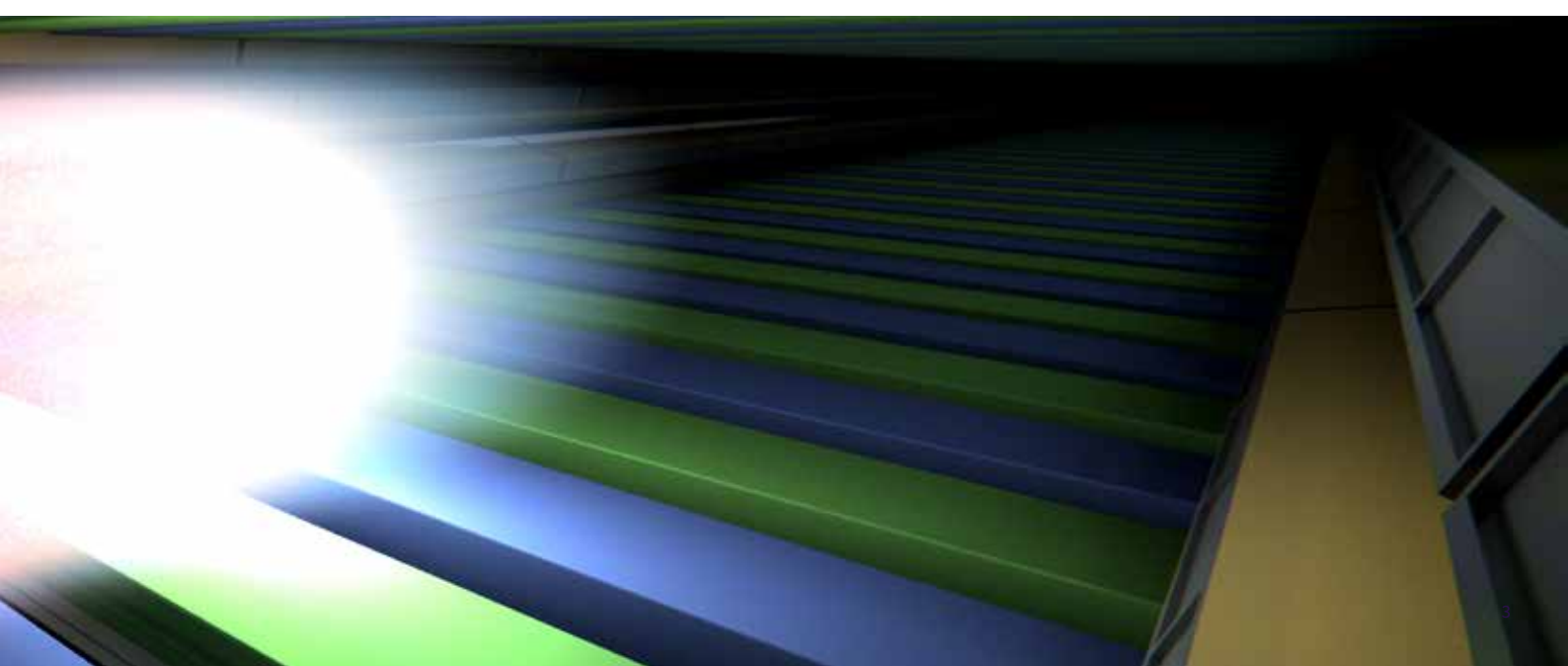
On behalf of the European XFEL and of the whole physics community in Hamburg, I am very pleased to welcome all participants to CORPES¹³.

The physics of strongly correlated electron systems still poses formidable challenges to our understanding, and photoemission spectroscopy has been a central and very important tool to shed some light on these systems. The emergence of new, powerful X-ray sources, such as free-electron lasers, offers new possibilities for the study of these fascinating systems. In particular, the exploration of time-dependent response, well below the ps time scale, can greatly benefit from the very intense ultrashort pulses of the new sources. This is why we are very happy to host the CORPES meeting and look forward to getting fresh ideas and new perspectives from the experts converging here from all over the world.

I hope that, besides gaining new insights, starting new collaborations, and nurturing novel ideas, all participants enjoy getting a direct impression of the progress of European XFEL construction and appreciate the vast offerings of cultural and sightseeing opportunities provided by Hamburg.

Massimo Altarelli

Managing Director and
Chairman of the European XFEL Management Board



CONTENTS

WORKSHOP

1 Week in overview

Mo Monday

Tu Tuesday

We Wednesday

Th Thursday

Fr Friday

P1 Poster Session 1

P2 Poster Session 2

2 Location & Hamburg

3 Participants

4 Author index



The international workshop CORPES¹³ discusses characteristics of correlated quantum matter and the photoemission process itself. It covers novel experimental techniques, prospects and challenges brought up by new light sources, and innovative theoretical ideas.

SCOPE

CORPES¹³ is held to advance our understanding of strongly correlated materials, using angle-resolved photoemission spectroscopy as a unique tool to access electronic structures and many-body theory to work out the underlying concepts and mechanisms. The programme is a balanced fusion of currently well-established and newly emerging topics, with ample time for discussions.

HOST AND VENUE

Host of CORPES¹³ is European XFEL in Hamburg. The workshop will take place on the premises of DESY.

PUBLISHER

European X-Ray Free-Electron Laser Facility GmbH
Albert-Einstein-Ring 19
22761 Hamburg

DESIGN

Dirk Rathje, Hamburg

INTERNATIONAL WORKSHOP ON STRONG CORRELATIONS AND ANGLE-RESOLVED PHOTOEMISSION SPECTROSCOPY

INVITED SPEAKERS

J. W. Allen, E. B. Fernández, F. Baumberger, S. Biermann, T.-C. Chiang, T. Das, A. Fujimori, C. Giannetti, M. Haverkort, C. Kim, W. Ku, G. Landolt, C. Monney, T. Okuda, E. Razzoli, E. Rotenberg, A. Santander-Syro, T. Shimojima, M. Sing, R. Valenti, D. Vyalikh, M. Weinelt, W. Wurth, X.-J. Zhou

INTERNATIONAL PROGRAMME COMMITTEE

M. Potthoff (Chair), P. Aebi, V. Brouet, D. Dessau, K. Matho, S. Molodtsov, L. Patthey, K. Shimada, T. Tohyama

ORGANIZERS

S. Molodtsov (Chair), S. Bertini, J. Buck, A. Cavalleri, W. Drube, I. Gembalies, M. Izquierdo, A. Lichtenstein, A. Scherz, W. Wurth

TOPICS

SPECTROSCOPIC INVESTIGATIONS OF CORRELATED ELECTRON MATERIALS

d- and f-electron systems; doped Mott insulators, unconventional superconductors; charge- and spin-density wave systems; surfaces, polar surfaces, interfaces, multilayers; low-dimensional systems, nanostructures; topological insulators and strong spin-orbit coupled materials; graphene

MANY-BODY THEORY OF CORRELATED ELECTRONS IN SOLIDS

Spectral function of lattice-fermion models; ab initio approaches to single-electron excitations; dynamical mean-field theory and beyond; GW, weak- and intermediate-coupling methods; low-energy effective theories; electron-boson coupling; quantum criticality and competing orders; non-Fermi-liquid behavior; novel methods

THE PHOTOEMISSION PROCESS

One-step model including electron correlations; low and high photon energies; high intensities, multi-photon processes, non-linear phenomena; theory of time-dependent spectroscopy; modeling of pump-probe processes; transition matrix elements and final-state effects

ADVANCES IN PHOTOEMISSION TECHNIQUES

Time-resolved and two-photon measurements; ultra-high resolution spectroscopies; bulk-sensitive photoemission; spin-resolved techniques; new possibilities provided by UV and X-ray free electron lasers

RELATIONS TO OTHER PHOTON-BASED TECHNIQUES

Resonant soft X-ray scattering and inelastic X-ray scattering; X-ray absorption spectroscopy; inverse photoemission



LINEAR SCHEDULE

We will preserve the workshop spirit, that means a linear schedule with no parallel sessions and ample time for discussion after each presentation as well as between sessions.



ORAL AND POSTER PRESENTATIONS

Applicants to the workshop will be selected to give either oral or poster presentations, with the latter being given significant weight to the program including short oral poster “flash sessions”.



BRINGING TOGETHER EXPERTS AND NEWCOMERS

It is intended to bring together experts and newcomers in the field, to learn from one another, and to foster collaborations.

WEEK IN OVERVIEW

1

SUNDAY 28 JULY

All talks take place in the DESY Main Auditorium.

The poster sessions take place in a tent in front of the Main Auditorium.

(Map on page 82)

17:00 **Registration & Reception in the DESY Main Auditorium.**

MONDAY 29 JULY

9:00		Opening
9:20	Mo.01	J. Allen <i>University of Michigan</i>
9:50	Mo.02	T. Wehling <i>University of Bremen</i>
10:15	Mo.03	M. Mulazzi <i>Universität Würzburg</i>
10:40	Mo.04	M. Haverkort <i>MPI for Solid State Research</i>
11:10		Coffee break
11:50	Mo.05	D. Dessau <i>University of Colorado</i>
12:15	Mo.06	A. Fujimori <i>University of Tokyo</i>
12:45		Lunch break
14:30	Mo.07	G. Landolt <i>Swiss Light Source</i>
15:00	Mo.08	I. Vobornik <i>CNR-IOM, TASC Laboratory, Sincrotrone Trieste</i>
15:25	Mo.09	Y. Tanaka <i>University of Tokyo</i>
15:50	P1.XX	Flash Poster Session 1
16:50		Coffee break
17:30	Mo.10	E. Rotenberg <i>Lawrence Berkeley National Laboratory</i>
18:00	Mo.11	F. Manghi <i>University of Modena and RE</i>
18:25	Mo.12	D. Qian <i>Shanghai Jiao Tong University</i>
18:50	P1.XX	Poster Session 1 (incl. snacks & drinks)

TUESDAY 30 JULY

9:00	Tu.01	F. Baumberger <i>University of Geneva</i>
9:30	Tu.02	E. Lahoud <i>Technion - Israel's Institute of Technology</i>
9:55	Tu.03	J. Miwa <i>Aarhus University</i>
10:20	Tu.04	J. Schäfer <i>University of Würzburg</i>
10:45		Coffee break
11:30	Tu.05	J. Braun <i>LMU Munich</i>
11:55	Tu.06	E. Krasovskii <i>The University of the Basque Country</i>
12:20	Tu.07	M. Lindroos <i>Tampere University of Technology</i>
12:45		Lunch break
14:30	Tu.08	T. Chiang <i>University of Illinois at Urbana-Champaign</i>
15:00	Tu.09	B. M. Wojek <i>KTH Royal Institute of Technology</i>
15:25	Tu.10	C. Kim <i>Yonsei University</i>
15:55	P2.XX	Flash Poster Session 2
16:55		Coffee break
17:30	Tu.11	T. Okuda <i>Hiroshima Synchrotron Radiation Center</i>
18:00	Tu.12	Z. Zhu <i>University of British Columbia</i>
18:25	Tu.13	V. N. Strocov <i>Paul Scherrer Institute</i>
18:50	P2.XX	Poster Session 2 (incl. snacks & drinks)

WEDNESDAY 31 JULY

9:00	We.01	M. Sing <i>University of Würzburg</i>
9:30	We.02	K. Held <i>Vienna University of Technology</i>
9:55	We.03	T. Zhang <i>Fudan University</i>
10:20		Coffee break
11:00	We.04	M. Eckstein <i>University of Hamburg, CFEL</i>
11:25	We.05	D. Manske <i>Max Planck Institute for Solid State Research</i>
11:50	We.06	A. Mishchenko <i>RIKEN Emergent Materials Department</i>
12:15	We.07	B. Moritz <i>SLAC National Accelerator Laboratory</i>
12:40		Lunch break
13:45		Excursion & Conference Dinner

THURSDAY 1 AUGUST

9:00	Th.01	A. Santander-Syro <i>CSNSM - Université Paris-Sud</i>
9:30	Th.02	Y. Cao <i>University of Colorado</i>
9:55	Th.03	F. O. Schumann <i>MPI für Mikrostrukturphysik</i>
10:20	Th.04	D. Vyalikh <i>University of Technology Dresden</i>
10:50		Coffee break
11:30	Th.05	R. Valenti <i>University of Frankfurt</i>
12:00	Th.06	D. Evtushinsky <i>IFW Dresden</i>
12:25	Th.07	T. Shimojima <i>University of Tokyo</i>
12:55		Lunch break
14:30	Th.08	S. Biermann <i>CPHT Ecole Polytechnique</i>
15:00	Th.09	A. M. Oleś <i>Jagellonian University and MPI</i>
15:25	Th.10	T. Das <i>Los Alamos National Laboratory</i>
15:55		Coffee break
16:30	Th.11	W. Ku <i>Brookhaven National Laboratory</i>
17:00	Th.12	R. Dhaka <i>Iowa State University</i>
17:25	Th.13	E. Bascones <i>ICMM-CSIC</i>
17:55		Best Poster Award & break
18:30	Th.14	X. Zhou <i>Chinese Academy of Sciences</i>
19:00	Th.15	E. Razzoli <i>Université de Fribourg, Switzerland</i>
19:30	Th.16	J. Fink <i>IFW Dresden</i>

FRIDAY 2 AUGUST

9:00	Fr.01	C. Giannetti <i>Università Cattolica del Sacro Cuore</i>
9:30	Fr.02	P. Werner <i>University of Fribourg</i>
9:55	Fr.03	W. Wurth <i>Universität Hamburg</i>
10:25		Coffee break
11:00	Fr.04	C. Monney <i>University of Fribourg</i>
11:30	Fr.05	J. Petersen <i>MPI & University of Oxford</i>
11:55	Fr.06	M. Weinelt <i>FU Berlin</i>
12:25		CORPES¹⁵ and close-out
13:00		Lunch break
13:45		Visit of European XFEL construction site

MONDAY 29 JULY

Mo

09:00		Opening
09:20	Mo.01 (invited)	Photoemission and theoretical studies of perpendicular electron hopping in $\text{Li}_{0.9}\text{Mo}_6\text{O}_{17}$ J. Allen <i>University of Michigan</i>
09:50	Mo.02	Excitation spectra of transition metal atoms on the Ag(100) surface controlled by Hund's exchange T. Wehling <i>University of Bremen</i>
10:15	Mo.03	Evidence of Kondo effect at the surface of the CePd₇/Pd(001) surface alloy M. Mulazzi <i>Universität Würzburg</i>
10:40	Mo.04 (invited)	Explaining the band structure of the quasi-one-dimensional purple bronze M. Haverkort <i>Max Planck Institute for Solid State Research</i>
11:05		Coffee break
11:50	Mo.05	Pairing and pair-breaking in cuprate superconductors D. Dessau <i>University of Colorado</i>
12:15	Mo.06 (invited)	Self-energy from the low to high energy scales in the electronic structure of correlated metal SrVO₃ A. Fujimori <i>University of Tokyo</i>
12:45		Lunch break

14:30	Mo.07 (invited)	Surface and bulk Rashba splittings in noncentrosymmetric BiTeI G. Landolt <i>Swiss Light Source</i>
15:00	Mo.08	Surface dynamics in TlBiSe₂ topological insulator I. Vobornik <i>CNR-IOM, TASC Laboratory, Sincrotrone Trieste</i>
15:25	Mo.09	High-resolution ARPES study of topological crystalline insulator SnTe Y. Tanaka <i>University of Tokyo</i>
15:50	P1.XX	Flash poster session
16:50		Coffee break
17:30	Mo.10 (invited)	Coexisting massive and massless Dirac fermions in symmetry broken bilayer graphene E. Rotenberg <i>Lawrence Berkeley National Laboratory</i>
18:00	Mo.11	Rientrant metallicity in the Hubbard model: the case of honeycomb nanoribbons F. Manghi <i>University of Modena and RE</i>
18:25	Mo.12	Many-body interaction in reshaped helical Dirac cone of topological insulators D. Qian <i>Shanghai Jiao Tong University</i>
18:50	P1.XX	Poster Session 1 (incl. snacks & drinks)

Mo.01

Photoemission and theoretical studies of perpendicular electron hopping in $\text{Li}_{0.9}\text{Mo}_6\text{O}_{17}$

Mo

L. Dudy *Julius-Maximilians-Universität*, J. Denlinger *Lawrence Berkeley National Laboratory*, J. W. Allen (presenter) *University of Michigan*, M. Greenblatt *Rutgers University*, O. K. Andersen *Max-Planck Institut für Festkörperforschung*, M. W. Haavorkort *Max-Planck Institute für Chemische Physik fester Stoffe*, T. Saha-Disgupta *S. N. Bose Centre for Basic Science*, S. Satpathy *University of Missouri*, Z. S. Popovic *University of Belgrade*

$\text{Li}_{0.9}\text{Mo}_6\text{O}_{17}$ is a quasi-one dimensional (quasi-1D) metal which displays spectroscopic [1, 2] and transport [3] signatures of Luttinger liquid (LL) behavior at temperatures down to at least 30K and superconductivity below $T_c = 1.9$ K. The route for 1D to 3D crossover between these two behaviors has been very challenging to elucidate because of many novel properties that are conflicting within usual 1D theoretical frameworks. A particular interesting possibility [1] is that 1D behavior is maintained down to T_c . A crucial issue is the magnitude of the perpendicular electron hopping t_{\perp} between the chains. There are actually two chains per unit cell and LDA calculations predict splitting and warping of the quasi-1D Fermi surface (FS) larger than is seen in ARPES. The research to be reported here is an experimental and theoretical collaboration consisting of high resolution angle resolved photoemission spectroscopy (ARPES) performed for T down to 6K to study the FS and NMTO band theory and downfolding to characterize the t_{\perp} hopping in detail. The theory shows that the FS is entirely governed by indirect perturbative interactions with other bonding and antibonding bands. An effort to compare the ARPES FS to that predicted using indirect interaction parameters deduced from ARPES below the Fermi energy will be described.

[1] L.Dudy et al., *J. Phys.: Condens. Matter* 25, 014007 (2013).

[2] J. Hager et al., *Phys. Rev. Lett.* 83, 186402 (2005).

[3] N. Wakeham et al., *Nature Commun.* 2, 396 (2011).

Mo.02

Excitation spectra of transition metal atoms on the Ag(100) surface controlled by Hund's exchange

T. Wehling (presenter) *University of Bremen*, S. Gardonio *University of Nova Gorica*, M. Karolak *University of Hamburg*, A. Lichtenstein *University of Hamburg*, C. Carbone *Consiglio Nazionale delle Ricerche*

We report photoemission experiments revealing the valence electron spectral function of Mn, Fe, Co and Ni atoms on the Ag(100) surface. The series of spectra shows splittings of higher energy features which decrease with the filling of the 3d shell and a highly non-monotonous evolution of spectral weight near the Fermi edge. First principles calculations demonstrate that two manifestations of Hund's exchange J are responsible for this evolution. First, there is a monotonous reduction of the effective exchange splittings with increasing filling of the 3d shell. Second, the amount of charge fluctuations and, thus, the weight of quasiparticle peaks at the Fermi level varies non-monotonously through this 3d series due to a distinct occupancy dependence of effective charging energies U_{eff} .

Mo.03

Evidence of Kondo effect at the surface of the CePd₇/Pd(001) surface alloy

M. Mulazzi (presenter) *University of Würzburg*, H. Schwab *University of Würzburg*, J. Jian *Hiroshima University*, K. Shimada *Hiroshima University*, F. Reinert *University of Würzburg*

In this contribution, I will show our results about the predominant role of the electron localisation at the surface of CePd₇. Evidence of long range ordering in the alloy was evidenced by electron diffraction after evaporation of Cerium on Pd(001) and high temperature annealing, while the stoichiometry of the alloy was inferred by Auger electron spectroscopy. By examining the f-electron spectral function, derived from resonant angle-resolved photoemission data, it was possible to identify a narrow peak near the Fermi level that we attribute to a Kondo screening of the f-electrons. Our data point out that the hybridisation between Cerium and Palladium is strongly reduced at the surface. The consequence of this weaker hybridisation is that the Kondo temperature is reduced by a factor one thousand, the charge fluctuations are removed from the excitation spectrum and the spin fluctuations remain to screen the local moment.

Mo.04

Explaining the band structure of the quasi-one-dimensional purple bronze

M. Haverkort (presenter) *Max Planck Institute for CPFS*, O. K. Andersen *Max Planck Institut for FKF*, Y. Nohara *Max Planck Institute for FKF*

The purple bronze Li_{0.9}Mo₆O₁₇ displays spectroscopic [1] and transport [2] signatures of a Tomonaga-Luttinger Liquid at temperatures down to 30 K. No crystal (Peirls) dimerization has been found, instead the material turns superconducting around 1.9 K. The crystal structure is 3D and complicated with 12 Mo atoms per primitive cell, 6 of which are inequivalent. Nonetheless, the band-structure around the Fermi energy is surprisingly simple, showing two nearly degenerate 1D bands in all existing calculations, and a single 1D band in ARPES experiments [1]. The origin of the splitting and the perpendicular dispersion of the two conduction bands has not been understood, and only the crudest t_x, t_y, t_z -Hamiltonian has been used in many-body calculations [3]. We present an ab initio DFT-NMTO Wannier-function study. With a basis of merely 6 t_{2g} -like orbitals per cell we can describe the complete bandstructure in a region of 1 eV around the Fermi energy in terms of a simple tight-binding Hamiltonian. Our Wannier orbitals are of non-bonding O-p Mo- t_{2g} character, which indicates particularly weak electron-phonon interactions and makes the absence of dimerization understandable. A detailed comparison with ARPES in a 1 eV region supports our finding that the splitting and perpendicular dispersion are caused exclusively by hybridization with the 2D bands formed by the 4 other t_{2g} orbitals and gapped around the Fermi level. The lack of splitting between the two 1D bands in ARPES seems to be caused by matrix element effects. The 2D bands are more 1D like in ARPES than in DFT and run at approximately $\pm 60^\circ$ to the 1D band at the Fermi level.

[1] L. Dudy et al., J. Phys.: Condens. Matter 25, 014007 (2013).

[2] N. Wakeham et al., Nature Comm. 1406 (2011).

[3] P. Chudzinski et al. Phys. Rev. B 86, 075147 (2012).

Mo.05

Gaps and scattering rates in cuprate superconductors

Mo

D. Dessau (presenter) *University of Colorado*, T. Reber *University of Colorado*, N. Plumb *University of Colorado/Swiss Light Source*, Y. Cao *University of Colorado*, S. Parham *University of Colorado*, Z. Sun *University of Colorado/USTC*, Q. Wang *University of Colorado/Los Alamos*, G. Arnold *University of Colorado*, H. Iwasawa *HISOR*, G. D. Gu *Brookhaven National Laboratory*, Y. Aiura *AIST*, H. Eisaki *AIST*, Y. Yoshida *AIST*

A new ARPES-based method allows us to make the first quantitative extraction of the pair-breaking scattering strengths as well as improved accuracy in gap measurements, giving new insights into the origin of pseudogaps, Fermi arcs, and superconductive pairing and prepairing in the cuprate superconductors. This gives much greater clarity to the doping phase diagram and helps us answer the critical question “What sets T_c ?”

Mo.06

Self-energy from the low to high energy scales in the electronic structure of correlated metal SrVO_3

A. Fujimori (presenter) *University of Tokyo*, T. Yoshida *University of Tokyo*, K. Yoshimatsu *KEK-IMSS*, *University of Tokyo*, H. Kumigashira *KEK-IMSS*

The perovskite oxide SrVO_3 with the d^1 electronic configuration is a typical correlated metal, and has been extensively studied theoretically and experimentally. We have made an ARPES study of SrVO_3 using in-situ prepared high-quality thin films followed by self-energy analysis [1]. Pronounced features of band renormalization have been observed: a sharp kink ~ 60 meV below the Fermi level (E_F) and a broad “high-energy kink” ~ 0.3 eV below it. The observation of these kinks, which have been observed for the high- T_c cuprates, in the normal metal SrVO_3 put constraint on the origin of the kinks in the cuprates. In order to deduce the self-energy over a wider energy range including the incoherent part ~ 1.5 eV below E_F , we have applied the Kramers-Kronig transformation to the observed spectra (the imaginary part of the Green function: $\text{Im}G$) over the wide energy range. The deduced self-energy clearly shows a large energy scale of ~ 0.7 eV arising from electron-electron interaction. The real part of the Green function ($\text{Re}G$) is found to show a “zero band” which separates the coherent and incoherent bands, in analogy to the “zero surface” mechanism of the pseudogap opening in the cuprates [2].

[1] S. Aizaki et al., Phys. Rev. Lett. 109, 056401 (2012).

[2] Y. Yamaji and M. Imada, Phys. Rev. Lett. 106, 016404 (2011).

Mo.07

Surface and bulk Rashba splittings in noncentrosymmetric BiTeI

G. Landolt (presenter) *Swiss Light Source*

In systems lacking bulk inversion symmetry the Kramer's degeneracy can be lifted by spin-orbit interaction giving rise to Dresselhaus or Rashba effects. Materials in the class of layered bismuth tellurohalides, such as BiTeI, have a layered and noncentrosymmetric structure with a giant Rashba-type splitting of the bulk bands. We present direct measurements of the bulk band structure of BiTeI measured with soft x-ray angle-resolved photoemission (ARPES), revealing the three-dimensional Fermi surface. The observed spindle torus shape bears the potential for a topological transition in the bulk by doping. Moreover, the bulk electronic structure is clearly disentangled from the two-dimensional surface electronic structure by means of high-resolution and spin-resolved ARPES measurements in the ultra-violet regime.

Mo.08

Surface dynamics in TlBiSe₂ topological insulator

I. Vobornik (presenter) *CNR-IOM, TASC Laboratory*, A. Artioli *CNR-IOM, TASC Laboratory*, M. Unnikrishnan *CNR-IOM, TASC Laboratory*, J. Fujii *CNR-IOM, TASC Laboratory*, G. Panaccione *CNR-IOM, TASC Laboratory*, G. Rossi *CNR-IOM, TASC Laboratory*

Topological insulators represent a new state of quantum matter, characterized by a finite energy gap in the bulk and gapless modes at the boundaries (edges in 2 dimensions; surfaces in 3 dimensions). These states are characterized by Dirac dispersion and spin-momentum locking that as a consequence has robustness towards impurity scattering [1]. Often, however, such surface states lay near the bulk valence/conduction bands and this configuration hinders the exploitation of the surface properties.

The ternary topological insulator TlBiSe₂ became particularly attractive since its surface state does not interfere with the bulk electronic structure, i.e. the scattering channel from the topological surface state to the bulk continuum is suppressed [2]. We studied the time evolution of the surface band structure. At difference to binary compounds, such as Bi₂Se₃ and Bi₂Te₃, whose surfaces get electron doped with time [3], TlBiSe₂ loses electrons progressively and the Dirac point shifts to lower binding energies. We also investigated the time evolution of the shallow core levels (Bi 5d, Tl 5d, Se 3d). While both bismuth and selenium exhibit single photoemission peaks, thallium has two components: one does not evolve with time, while the second one is progressively suppressed and follows the surface state time evolution. We further doped the surface with sodium and confirmed that the same surface component in Tl 5d spectrum gets progressively suppressed with doping. This indicates that a peculiar surface dynamics related to modification of Tl on the surface takes place in this ternary compound.

[1] M.Z. Hasan and C.L. Kane, *Rev. Mod. Phys.* 82, 3045–3067 (2010).

[2] K. Kuroda et al., *Phys. Rev. Lett.* 105, 146801 (2010).

[3] Z-H. Zhu et al., *Phys. Rev. Lett.* 107, 186405 (2011).

Mo.09

High-resolution ARPES study of topological crystalline insulator SnTe

Y. Tanaka (presenter) *Tohoku University*, Z. Ren *Osaka University*, T. Sato *Tohoku University*, T. Takahashi *Tohoku University*, K. Segawa *Osaka University*, Y. Ando *Osaka University*

Topological insulators materialize a topological quantum state of matter where unusual gapless metallic states protected by the time-reversal symmetry (TRS) emerge at the edge or surface. The discovery has stimulated intensive researches to search for a different type of topological materials. Recently a new type of topological material has been theoretically predicted and named “topological crystalline insulator” (TCI), where the metallic surface states are protected not by the TRS, but by the point group symmetry (mirror symmetry) of crystal. In this paper, we report our recent high-resolution ARPES results on one of TCI candidates, tin telluride (SnTe), showing the first definitive experimental evidence for the existence of TCI state in this material [1]. We also report a systematic ARPES study on the evolution of the electronic states across the topological phase transition in the solid-solution system of (Pb,Sn)Te [2].

[1] Y. Tanaka et al., *Nature Phys.* 8, 800 (2012).

[2] Y. Tanaka et al., arXiv:1301.1177.

Mo.10

Coexisting massive and massless Dirac fermions in symmetry broken bilayer graphene

K. S. Kim *Lawrence Berkeley National Laboratory*, A. Walter *Lawrence Berkeley National Laboratory*, L. Moreschini *Lawrence Berkeley National Laboratory*, T. Seyller *TU Chemnitz*, K. Horn *FHI-Berlin*, E. Rotenberg (presenter) *Lawrence Berkeley National Laboratory*, A. Bostwick *Lawrence Berkeley National Laboratory*

Charge carriers in bilayer graphene are widely believed to be massive Dirac fermions that have a bandgap tunable by a transverse electric field. However, a full transport gap, despite its importance for device applications, has not been clearly observed in gated bilayer graphene, a long-standing puzzle. Moreover, the low-energy electronic structure of bilayer graphene is widely held to be unstable towards symmetry breaking either by structural distortions, such as twist, strain, or electronic interactions that can lead to various ground states. Which effect dominates the physics at low energies is hotly debated. Here we show both by direct band-structure measurements and by calculations that a native imperfection of bilayer graphene, a distribution of twists whose size is as small as $\sim 0.1^\circ$, is sufficient to generate a completely new electronic spectrum consisting of massive and massless Dirac fermions. The latter is robust against strong electric fields, and has a novel topology in momentum space consisting of closed arcs having an exotic chiral pseudospin texture, which can be tuned by varying the charge density. The discovery of this unusual Dirac spectrum not only complements the framework of massive Dirac fermions, widely relevant to charge transport in bilayer graphene, but also supports the possibility of valley polarized transport [1].

[1] K.S. Kim et al., *Nature Mater.* (in press).

Mo.11

Reentrant metallicity in the Hubbard model: the case of honeycomb nanoribbons

F. Manghi (presenter) *University of Modena and RE*, F. Petocchi *SISSA*

The repulsive interaction among electrons is responsible of the failure of single particle picture and of the opening/widening of energy gaps in solids. The Hubbard model, where electrons are assumed to interact through extremely short ranged Coulomb repulsion, is the paradigm to describe this phenomenon: sufficiently large values of the on-site e-e repulsion inhibit the inter-site hopping favoring an insulating behavior. The 1-atom thick 2D honeycomb lattice (graphene) does not contradict this picture: many-body effects due to on-site Coulomb repulsion have been shown to lead, for sufficiently strong interactions, to semimetal-to-insulator transition [1] as well as to other deviations from Fermi-liquid behavior such as unconventional quasiparticle lifetimes [2], long range antiferromagnetic order [3] and spin liquid phase [4]. According to a recent ab-initio estimate [5] the screened on-site Coulomb interaction in graphene should be indeed rather close to the critical value to induce a Mott transition.

We have studied the effects of Mott-Hubbard correlation in honeycomb nanoribbons: we have considered a honeycomb lattice truncated to reproduce zigzag and armchair ribbons of different width. A true many body approach based on the Cluster Perturbation Theory [6] has been adopted to solve the problem in different correlation regimes, tuning the Hubbard U across the critical value. We show that zigzag ribbons exhibit the expected behavior: e-e repulsion inhibits double occupancies of sites and drives the system across a metal-to-insulator transition. For armchair terminated ribbons the situation is completely different and the repulsive e-e interaction is responsible of a metallic phase in ribbons that in the single-particle picture are semiconducting. This appears to be another extraordinary property of the 2-D honeycomb lattice.

[1] A. Liebsch, Phys. Rev. B 83, 035113 (2011).

[2] J. Gonzalez et al., Phys. Rev. Lett. 77, 3589 (1996).

[3] T. Paiva, Phys. Rev. B 72, 085123 (2005).

[4] Z. Meng et al. Nature (London) 464, 847 (2010).

[5] T. O. Wehling et al., Phys. Rev. Lett. 106, 236805 (2011).

[6] D. Sénéchal et al., Phys. Rev. Lett. 84, 522 (2000).

Mo.12

Many-body interaction in reshaped helical Dirac cone of topological insulators

D. Qian (presenter) *Shanghai Jiao Tong University*, L. Miao *Shanghai Jiao Tong University*, F. Liu *University of Utah*, Z. Wang *University of Utah*, J. Jia *Shanghai Jiao Tong University*

Topological insulators and graphene present two unique classes of materials, which are characterized by spin-polarized (helical) and nonpolarized Dirac cone band structures, respectively. The importance of many-body interactions that renormalize the linear bands near Dirac point in graphene has been well recognized and attracted much recent attention. However, renormalization of the helical Dirac point has not been observed in topological insulators. Here, we report the experimental observation of the renormalized quasiparticle spectrum with a skewed Dirac cone in a single Bi bilayer grown on Bi_2Te_3 substrate from angle-resolved photoemission spectroscopy. First-principles band calculations indicate that the quasiparticle spectra are likely associated with the hybridization between the extrinsic substrate-induced Dirac states of Bi bilayer and the intrinsic surface Dirac states of Bi_2Te_3 film at close energy proximity.

Without such hybridization, only single-particle Dirac spectra are observed in a single Bi bilayer grown on Bi_2Se_3 , where the extrinsic Dirac states Bi bilayer and the intrinsic Dirac states of Bi_2Se_3 are well separated in energy. The possible origins of many-body interactions are discussed. Our findings provide a means to manipulate topological surface states.

TUESDAY 30 JULY

Tu

09:00	Tu.01 (invited)	Orbital ordering, electron boson coupling and unconventional Rashba effect of a two-dimensional electron gas in SrTiO₃ F. Baumberger <i>University of Geneva</i>
09:30	Tu.02	Emergent novel metallic state in a disordered 2D Mott insulator E. Lahoud <i>Technion - Israel's Institute of Technology</i>
09:55	Tu.03	Direct band structure measurements of a buried delta-layer J. Miwa <i>Aarhus University</i>
10:20	Tu.04	Spin order in a frustrated atomic lattice on the surface of a semiconductor J. Schäfer <i>University of Würzburg</i>
10:45		Coffee break
11:30	Tu.05	Exploring the XPS-limit in soft and hard x-ray angle-resolved photoemission using fully temperature-dependent one-step theory: from simple metals to complex systems J. Braun <i>LMU Munich</i>
11:55	Tu.06	Photoelectron spectroscopy of Rashba-split and Rashba-polarized polarized states E. Krasovskii <i>The University of the Basque Country</i>
12:20	Tu.07	Dichromatic signal and spin-polarization: A study of the Au(111) surface state M. Lindroos <i>Tampere University of Technology</i>
12:45		Lunch break

14:30	Tu.08 (invited)	<p>Topological surfaces, interfaces, and films</p> <p>T. Chiang <i>University of Illinois at Urbana-Champaign</i></p>
15:00	Tu.09	<p>The (001) surface states of the topological crystalline insulator (Pb,Sn)Se</p> <p>B. M. Wojek <i>KTH Royal Institute of Technology</i></p>
15:25	Tu.10 (invited)	<p>Local orbital angular momentum and circular dichroism ARPES</p> <p>C. Kim <i>Yonsei University</i></p>
15:55	P2.XX	<p>Flash poster session 2</p>
16:55		<p>Coffee break</p>
17:30	Tu.11 (invited)	<p>Observation of spin-polarized surface states induced by spin-orbit interaction by high-resolution spin-polarized photoelectron spectroscopy</p> <p>T. Okuda <i>Hiroshima Synchrotron Radiation Center</i></p>
18:00	Tu.12	<p>Layer-by-layer entangled spin-orbital texture of the topological surface state in Bi₂Se₃</p> <p>Z. Zhu <i>University of British Columbia</i></p>
18:25	Tu.13	<p>Soft-X-ray ARPES at Swiss Light Source: From 3D materials to buried heterostructures and impurities</p> <p>V. N. Strocov <i>Paul Scherrer Institute</i></p>
18:50	P2.XX	<p>Poster Session 2 (incl. snacks & drinks)</p>

Tu.01

Orbital ordering, electron boson coupling and unconventional Rashba effect of a two-dimensional electron gas in SrTiO₃

F. Baumberger (presenter) *University of Geneva*, P. King *Cornell University*, W. Meevasana *Suranaree University of Technology*, S. McKeown Walker *University of Geneva*, A. Tamai *University of Geneva*

Two-dimensional electron gases (2DEGs) in SrTiO₃ host novel properties including high mobility, gate-tuned superconductivity, and its coexistence with ferromagnetism, and have become a paradigm for the potential of complex oxides for electronics. In this talk I will present recent angle resolved photoemission (ARPES) experiments that provide unprecedented insight into the microscopic electronic structure of this system. I will first discuss the orbital ordering induced in the 2DEG by quantum confinement and the spatial extent of the different subbands. Our data further provide direct evidence for a substantial phonon driven mass enhancement of the 2DEG states, which resolves an earlier discrepancy between the cyclotron masses observed in quantum oscillation experiments and the Fermi velocities reported from ARPES. Finally, I will present experimental evidence, combined with realistic tight-binding supercell calculations, that spin-orbit interactions play an unexpectedly large role in this system. We find that these drive an unconventional Rashba-like spin splitting of the Ti d-electron subband ladder, which is enhanced by inter-orbital charge transfer.

Tu.02

Emergent novel metallic state in a disordered 2D Mott insulator

E. Lahoud (presenter) *Technion - Israel's Institute of Technology*, A. Kanigel *Technion - Israel's Institute of Technology*, N. Meetei *Ohio State University*, K. Chaska *Technion - Israel's Institute of Technology*, N. Trivedi *Ohio State University*

It is well established that for non-interacting electrons, increasing disorder drives a metal into a gapless localized Anderson insulator. While in three dimensions a threshold in disorder must be crossed for the transition, in two dimensions and lower, the smallest amount of disorder destabilizes the metal. The nature of the metal-insulator transition in an interacting system remains unresolved. In this work we explore the effect of disorder on a strongly correlated Mott insulator without changing the carrier concentration. Angle resolved photoemission spectroscopy (ARPES) measurements on copper intercalated single crystals of the layered dichalcogenide 1T-TaS₂ reveal the presence of new delocalized states within the Mott gap. This is the first experimental realization of a novel disorder-induced metal that was theoretically predicted to exist between the Mott insulator and Anderson insulator.

Tu.03

Direct band structure measurements of a buried delta-layer

J. Miwa (presenter) *Aarhus University*, P. Hofmann *Aarhus University*, M. Simmons *University of New South Wales*, J. Wells *Norwegian University of Science and Technology*

We directly measure the band structure of a buried two dimensional electron gas (2DEG) using angle resolved photoemission spectroscopy [1]. The buried 2DEG is formed several nanometers beneath the surface of p-type silicon (001), because of a dense delta-layer of phosphorus n-type dopants which are placed there. Although the delta-layer is deeply buried, relative to the photoelectron mean free path, photoemission is still possible at very low kinetic energies, or when a resonant enhancement is invoked.

Here we present direct measurements of the band structure of the buried 2DEG using angle resolved photoemission spectroscopy (ARPES). Our measurements confirm the layer to be metallic and give direct access to the Fermi level position, as well as facilitating a direct comparison with calculations. In addition, we report the dependence of the band structure on properties such as dopant confinement and temperature, and discuss the resonant enhancement mechanism which facilitates such measurements.

[1] J. A. Miwa et al., *Phys. Rev. Lett.* (accepted), arxiv.org/abs/1210.7113.

Tu.04

Spin order in a frustrated atomic lattice on the surface of a semiconductor

J. Schäfer (presenter) *University of Würzburg*, G. Li *University of Würzburg*, P. Hoefner *University of Würzburg*, W. Hanke *University of Würzburg*, R. Claessen *University of Würzburg*

Two-dimensional electron systems can be realized at the surface of semiconductors by metal atom adsorption. An intriguing scenario emerges for submonolayer coverages, where strong electron correlations come into play. The electrons can lose their conducting properties due to the local Coulomb repulsion, leading to a Mott-insulating state. For a lattice of triangular geometry, filled with one electron and hence a single spin per atom, any antiferromagnetic spin ordering faces the problem of geometric frustration. This spurs speculations about the potential existence of long-range magnetic order or, alternatively, a spin-liquid phase.

We address this question by epitaxial Sn atom adsorption in a triangular reconstruction on a silicon substrate. Using angle-resolved photoemission, we have mapped out the many-body spectral function, which indicates a Mott-Hubbard insulator with a half-filled band. These excitation spectra are compared to theoretical simulations of the correlated electron lattice using a dynamical cluster approximation. Contrary to naive expectation, the spins are not disordered. Instead, we observe characteristic “shadow bands” induced by backfolding from a magnetic superstructure, which results from an unusual row-wise antiferromagnetic spin alignment [1]. Such magnetic order in a frustrated lattice of otherwise non-magnetic ingredients emerges from longer-ranged electron hopping between the atoms. This finding points at a novel pathway to control magnetism on surfaces.

[1] G. Li et al., *Nature Comm.*, accepted (2013).

Tu.05

Exploring the XPS-limit in soft and hard x-ray angle-resolved photoemission using fully temperature-dependent one-step theory: from simple metals to complex systems

J. Braun (presenter) *LMU Munich*, J. Minar *LMU Munich*, H. Ebert *LMU Munich*

A brief introduction to the theory of soft and hard x-ray angle-resolved photo electron spectroscopy (S-ARPES, HARPES) of solid materials is given with an emphasis on the so-called one-step-model of photoemission that describes excitation, transport to the surface and the escape into the vacuum in a coherent way. The main aspects of the theory [1, 2] and its implementation within the Munich SPR-KKR program package [3] will be reviewed. As a new feature we present a model that accounts for finite temperatures when calculating photoemission spectra on the basis of the Coherent Potential Approximation (CPA) alloy theory (alloy analogy model). Our method goes well beyond the simple, but standard Debye-Waller approach to photoemission by including in particular the temperature dependence of the effective photoemission matrix elements as well.

This allows among others to reproduce the so called XPS- or density of states limit in angle-resolved photoemission which occurs for high photon energies and/or high temperatures due to a full Brillouin zone averaging caused by phonon scattering.

In a similar way thermal displacements of atoms were successfully introduced by the authors within an alloy analogy model to calculate the Gilbert damping parameter [4]. To illustrate the applicability of the new formalism examples of soft- and hard X-ray ARPES calculations for simple metals like W(110), Pt(111) and Au(111) [5] as well as complex systems like topological insulators will be presented. The nearly quantitative agreement between experiment and theory which we found in our first applications indicates that our approach could work as a powerful analysis tool for various soft x-ray as well as hard x-ray ARPES investigations also on strongly correlated systems like cuprate or pnictide high- T_c superconductors.

[1] A. Gray et al., *Nature Mater.*, 10, 759 (2011).

[2] A. Gray et al., *Nature Mater.* 11, 957 (2012).

[3] H. Ebert et al., The Munich SPR-KKR package, version 6.3, <http://olymp.cup.uni-muenchen.de/ak/ebert/SPRKKR> (2012).

[4] H. Ebert et al., *Phys. Rev. Lett.* 107, 066603 (2011).

[5] J. Braun et al. submitted to *Phys. Rev. Lett.* (2013).

Tu.06

Photoelectron spectroscopy of Rashba-split and Rashba-polarized states

E. Krasovskii (presenter) *The University of the Basque Country*

Angle and spin-resolved photoelectron spectroscopy of systems with strong spin-orbit interaction will be considered based on the one-step theory of photoemission, in particular the Rashba effect and the surface states of topological insulators. Special attention will be paid to the spin polarization of the photocurrent from bulk continuum states, which was observed on Bi(111) [1] and W(110) [2]. A qualitative model analysis will be presented, as well as ab initio calculations for Bi(111), W(110), and Al/W(110). The role of photoemission final states and dichroism effects will be discussed.

[1] A. Kimura et al., *Phys. Rev. Lett.* 105, 076804 (2010).

[2] A. Rybkin et al., *Phys. Rev. B* 86, 035117 (2012).

Tu.07

Dichromatic signal and spin-polarization: A study of the Au(111) surface state

M. Lindroos (presenter) *Tampere University of Technology*

To measure the spin polarisation by ARPES is cumbersome and time-consuming. Thus it has been proposed that the spin polarisation could be determined from the measured or calculated dichromatic signal [1, 2].

We have investigated the dichromatic signal and the spin-polarizations of the Au(111) surface state as a function of photon energy and compared them to one another. Also the in-plane spin-polarization vectors have been studied as a function of photon energy. The angle-resolved photoemission intensity calculations are based on the one-step model and multiple-scattering theory. A fully relativistic formalism is used.

The behavior of the dichromatic signal of the Au(111) surface state at Fermi energy is complicated and we have found 13 different patterns of dichromatic signal with photon energies in the range of 7-100 eV. Comparing the dichromatic signal to the spin-polarizations $\langle S_x \rangle$, $\langle S_y \rangle$ and $\langle S_z \rangle$ it is noticed that there is no correlation between them. $\langle S_x \rangle$ and $\langle S_y \rangle$ stay almost constant as a function of photon energy but $\langle S_z \rangle$ seems to have a photon energy dependence. Apart from a few exceptions the in-plane spin-polarization vectors stay constant as a function of photon energy with the Rashba-split inner state rotating counterclockwise and the outer state rotating clockwise.

The origin of dichromatic signal is discussed. Some examples are also shown for topological insulators showing similar disagreement between spin polarization and dichromatic signal.

[1] Y.H. Wang et al., Phys. Rev. Lett. 107, 207602 (2011).

[2] H. Mirhosseini and J. Henk, Phys. Rev. Lett. 109, 036803 (2012).

Tu.08

Topological surfaces, interfaces, and films

T. Chiang (presenter) *University of Illinois at Urbana-Champaign*

Topological insulators are typically characterized by an inverted bulk band gap caused by a strong spin-orbit coupling. By analytic continuation, this gap must close at the surface and reopen outside in vacuum where the gap is noninverted (and infinite). The resulting metallic surface states, or topological states, are spin-polarized and span the bulk gap. They carry a spin current, independent of the details of the surface, which is a feature of strong interest for spintronic applications. This talk will focus on thin films of topological materials (Sb, Bi₂Se₃, and Bi₂Te₃). Thin films are basic building blocks of devices, which often involve multilayers of various materials. As the thickness of a topological insulator film is reduced to the nanoscale, the bulk bands are reduced to discrete quantum well states, and the surface/interface states associated with the two faces of the film can interact, resulting in spin mixture and formation of a tunneling gap. The detailed atomic bonding structure at each face of the film can also affect the overall electronic structure of the system. The interplay of quantum confinement, topological order, spin polarization, and surface/interface bonding and chemistry will be discussed.

Tu.09

The (001) surface states of the topological crystalline insulator (Pb,Sn)Se

B. M. Wojek (presenter) *KTH Royal Institute of Technology*, R. Buczko *Institute of Physics, Polish Academy of Sciences, Warsaw, Poland*, P. Dziawa *Polish Academy of Sciences*, M. Berntsen *KTH Royal Institute of Technology*, B. J. Kowalski *Polish Academy of Sciences*, T. Balasubramanian *Lund University*, A. Szczerbakow *Polish Academy of Sciences*, T. Story *Polish Academy of Sciences*, O. Tjernberg *KTH Royal Institute of Technology*

The prediction and experimental discovery of a topological-crystal-line-insulating (TCI) state have recently enriched the family of topological phases occurring in condensed matter. While in topological insulators time-reversal symmetry warrants the topological protection of metallic surface states, in the TCI phase, certain point-group symmetries ensure metallic channels on specific crystal surfaces.

It has been shown that the narrow-gap IV-VI semiconductors (Pb,Sn)Se and (Pb,Sn)Te undergo a transition from a normal insulator into a TCI state when the band structure is inverted at large enough Sn content and low temperatures [1, 2], where conducting surface channels are stabilized by the presence of the mirror symmetry of the crystal [3]. Here, we report on studies of (001) surfaces of (Pb,Sn)Se. Our calculations not only predict metallic surface states with a chiral spin structure for the TCI state but also gapped surface states with nonzero polarization when the system is a normal insulator.

Angle-resolved photoemission experiments provide conclusive evidence for the formation of these surface states and their evolution as a function of crystal composition and temperature. The chiral spin structure of the states is demonstrated by means of spin-resolved photoemission [1, 4].

[1] P. Dziawa et al., *Nat. Mater.* 11, 409-416 (2012).

[2] Su-Yang Xu et al., *Nat. Commun.* 3, 1192 (2012).

[3] T. H. Hsieh et al., *Nat. Commun.* 3, 982 (2012).

[4] B. M. Wojek et al., *Phys. Rev. B* 87, 115106 (2013).

Tu.10

Local orbital angular momentum and circular dichroism ARPES

C. Kim (presenter) *Yonsei University*

Orbital angular momentum (OAM), often ignored in solids (OAM quenching), is found to play an important role in the electronic structure for a broad range of materials. Combination of OAM and electron momentum produces an asymmetric charge distribution which couples with an electric field. The interaction results in a new energy scale that affects the electronic structures. The energy scale of Rashba type band splitting, found in many surface states including a topological insulator Bi_2Se_3 , can be accounted for by such interaction [1, 2]. It turns out that the newly found interaction can explain many other aspects such as chiral OAM structure in addition to the already known chiral spin structure.

Experimental detection of OAM can be achieved by using circular dichroism angle resolved photoemission (CD-ARPES). The mechanism behind the detection will be discussed in the presentation.

[1] S. R. Park, *Phys. Rev. Lett.* 108, 046805 (2012).

[2] S. R. Park, *Phys. Rev. Lett.* 107, 0156803 (2011).

Tu.11

Observation of spin-polarized surface states induced by spin-orbit interaction by high-resolution spin-polarized photoelectron spectroscopy

T. Okuda (presenter) *Hiroshima University*

Spin and angle resolved photoelectron spectroscopy (S-ARPES), in which one can measure electron energy, emitted angle (=electron momentum) and spin polarization, has contributed to understand the properties of ferromagnetic materials in the past decades.

Recent findings of the spin-polarized electronic states caused by the spin-orbit interaction at the surfaces, such as Rashba spin splitting states or topological surface states move the S-ARPES into the spotlight again.

Since the spin splitting of these systems is much smaller in energy and/or momentum than that of the exchange splitting ferromagnetic materials higher energy- and angular-resolution is eagerly desired.

The extremely low efficiency of the spin detection with the conventional spin polarimeter, however, hampers to realize the S-ARPES measurement with high energy- and angular-resolution so far.

By utilizing the higher efficiency of the spin polarimeter based on the very low energy electron diffraction (VLEED) combining with the state-of-the-art photoelectron analyzer, we have recently realized S-ARPES measurement with high energy and angular resolutions ($\Delta E \sim 10$ meV, $\Delta q \sim \pm 0.2^\circ$) [1]. Passivation of the Fe(001) target by a pre-oxidation with pure oxygen makes the stable operation of VLEED spin detector possible and overcomes the shortcoming of the traditional VLEED spin detector.

In the presentation, some applications of the high-resolution S-ARPES measurement combined with the energy- and polarization-tunability of the synchrotron radiation light for the detailed spin structures of topological insulators and Rashba spin splitting systems will be addressed. Furthermore, recent renovation of the high-resolution S-ARPES machine for the high-resolution 3D spin vectorial analysis will be also presented.

[1] T. Okuda et al., *Rev. Sci. Instrum.* 82, 103302 (2011).

Tu.12

Layer-by-layer entangled spin-orbital texture of the topological surface state in Bi_2Se_3

Z. Zhu (presenter) *University of British Columbia*, M. W. Haverkort *University of British Columbia*, I. S. Elfimov *University of British Columbia*, A. Damascelli *University of British Columbia*

With their spin-helical metallic surface state, topological insulators (TIs) define a new class of materials with strong application potential in spintronics. Technological exploitation depends on the degree of spin polarization of the topological surface state (TSS), assumed to be 100% in phenomenological models. Yet in Bi_2Se_3 , an archetypical TI material, spin- and angle-resolved photoemission spectroscopy (S-ARPES) detects a spin polarization ranging from 20 to 85%, a striking discrepancy which undermines the applicability of real TIs. We show—studying Bi_2Se_3 by polarization-dependent ARPES and density-functional theory slab calculations—that the TSS Dirac fermions are characterized by a layer-dependent entangled spin-orbital texture, which becomes apparent through quantum interference effects. This explicitly solves the puzzle of the TSS spin polarization in S-ARPES, and suggests how 100% spin polarization of photoelectrons and photocurrents can be achieved and manipulated in TI devices by using linearly polarized light.

Tu.13

Soft-X-ray ARPES at Swiss Light Source: From 3D materials to buried heterostructures and impurities

V. N. Strocov (presenter) *Paul Scherrer Institute*, M. Kobayashi *Paul Scherrer Institute and University of Tokyo*, M. Shi *Paul Scherrer Institute*, T. Schmitt *Paul Scherrer Institute*, C. Cancellieri *Paul Scherrer Institute*, M. Reinle-Schmitt *Paul Scherrer Institute*, P. Willmott *Paul Scherrer Institute*, T. Jean-Marc *University of Geneva*, M. Oshima *University of Tokyo*, A. Fujimori *University of Tokyo*, M. Tanaka *University of Tokyo*, B. Peter *TU Vienna*

A fundamental benefit of pushing the ARPES experiment into the soft-X-ray energy range is the increasing photoelectron escape depth. This gives a boost to bulk sensitivity of ARPES as well as enables access to buried heterostructures. The soft-X-ray ARPES (SX-ARPES) facility at Swiss Light Source is installed at the ADDRESS beamline [1] which delivers X-ray radiation with variable polarizations in a photon energy range from 300 to 1600 eV. High photon flux topping up 10^{13} photons/s/0.01%BW at 1 KeV combined with small spot size and grazing X-ray incidence angle experimental geometry has not only overpowered the notorious problem of small valence band cross-section but also enabled access to buried heterostructures despite the photoelectron attenuation in a few monolayers thick overlayer. At energies around 900 eV, ARPES images are routinely acquired within 5 min at a combined energy resolution of 110 meV, and within 30 min at resolution of 60 meV.

Applications of SX-ARPES to 3-dimensional (3D) materials are based on the fact that the increase of the photoelectron escape depth, by the Heisenberg uncertainty principle, improves intrinsic definition of surface-perpendicular electron momentum. We apply SX-ARPES to the paradigm transition metal dichalcogenide VSe_2 [2]. The experimental 3D band structure and Fermi surface (FS) of this material demonstrate a textbook clarity achieved by virtue of free-electron final states, their sharp definition in 3D momentum and smooth atomic-like photoemission matrix elements delivered in the soft-X-ray energy range. An intriguing feature of VSe_2 is that despite its layered quasi-2D structure this material develops 3D charge density waves (CDWs). Autocorrelation analysis of the experimental FS has revealed its pronounced out-of-plane nesting which acts as the precursor of these exotic CDWs [2].

Other application examples include polarization dependence and alternating FS shapes in pnictide HTSCs, demonstrating their 3D character and intra-cell interference effects.

The high efficiency of the new SX-ARPES facility has allowed the move from classical bulk systems to buried heterostructures. We illustrate this by resonant SX-ARPES of 2D electron gas at buried $LaAlO_3/SrTiO_3$ interfaces, which unveils different subbands and FS sheets formed by the interface states. Increase of temperature suppresses the momentum selectivity and allows determination of the 2D electron gas depth localization from variations of the SX-ARPES signal with emission angle [3]. Furthermore, we report resonant spectroscopy of Mn magnetic impurities in the paradigm magnetic semiconductor $GaMnAs$, which reveals the energy position of the ferromagnetic Mn impurity band and the mechanism of its hybridization with the 3D host $GaAs$ bands [4]. These results have immediate implications for the origin of ferromagnetism in $GaMnAs$. The whole body of our unfolding results demonstrates an immense potential of SX-ARPES to deliver a clear k-resolved picture of electronic structure from 3D materials to buried heterostructures and impurities.

[1] V. N. Strocov et al., *J. Synchrotron Rad.* 17, 631 (2010).

[2] V. N. Strocov et al., *Phys. Rev. Lett.* 109, 086401 (2012).

[3] C. Cancellieri et al., *Phys. Rev. Lett.* 110, in press (2013).

[4] M. Kobayashi et al., <http://arxiv.org/abs/1302.0063>.



WEDNESDAY 31 JULY

We

09:00	We.01 (invited)	Exploring buried interfaces of oxide heterostructures by x-ray spectroscopies M. Sing <i>University of Würzburg</i>
09:30	We.02	Oxide heterostructures: efficient solar cells and spin-orbit coupling K. Held <i>Vienna University of Technology</i>
09:55	We.03	Interface-induced superconductivity and strain-dependent spin density wave in FeSe/STO thin films T. Zhang <i>Fudan University</i>
10:20		Coffee break
11:00	We.04	Nonthermal broken symmetry states in the Hubbard model M. Eckstein <i>University of Hamburg, CFEL</i>
11:25	We.05	Density-matrix theory for time-resolved dynamics of super- conductors in non-equilibrium D. Manske <i>Max Planck Institute for Solid State Research</i>
11:50	We.06	ARPES and optical conductivity of the Hubbard-Holstein model: equilibrium and pump-probe phenomena A. Mishchenko <i>RIKEN Emergent Materials Department</i>
12:15	We.07	Correlation tuned cross-over between thermal and nonthermal states following ultrafast transient pumping B. Moritz <i>SLAC National Accelerator Laboratory</i>
12:40		Lunch break

13:45

Excursion & Conference Dinner
Departure by bus from DESY Main Auditorium

14:45

Departure of boat tour in the port of Hamburg
Landungsbrücken, pier 8 to 10, ship name to be announced

16:45

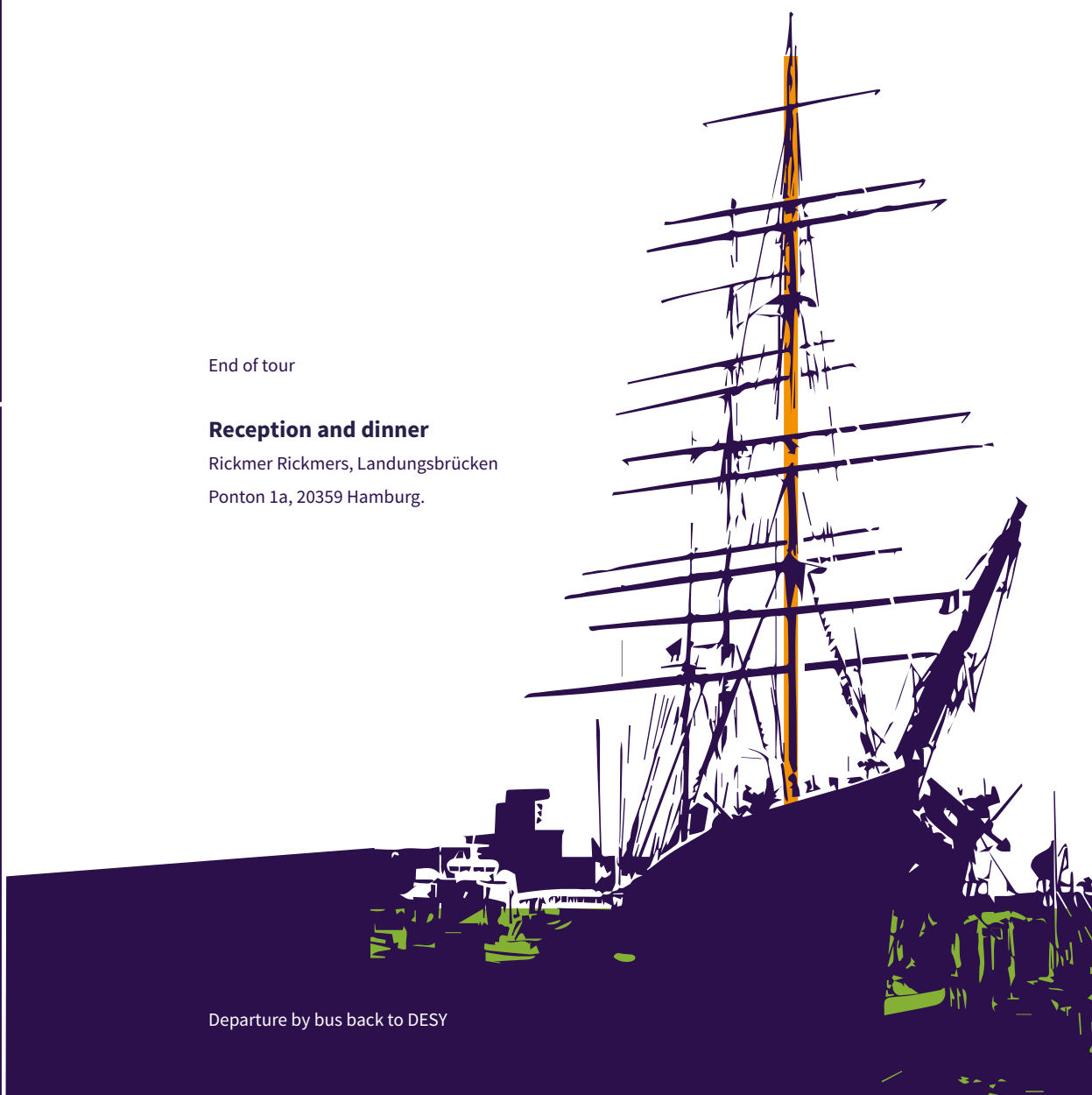
End of tour

17:00

Reception and dinner
Rickmer Rickmers, Landungsbrücken
Ponton 1a, 20359 Hamburg.

22:30

Departure by bus back to DESY



We.01

Exploring buried interfaces of oxide heterostructures by x-ray spectroscopies

M. Sing (presenter) *University of Würzburg*, R. Claessen *Würzburg*, A. Mueller *Würzburg*, J. Mannhart, S. Thiel *Augsburg*, P. R. Willmott *PSI*, M. Gorgoi *BESSY*, S. Suga *Osaka*, H. Fujiwara *Osaka*, A. Sekiyama *Osaka*, Y. Saitoh *JAEA, Japan*, A. Yamasaki *Kobe*, L.-C. Duda *Uppsala*, W. Drube *DESY*, T. Kopp *Augsburg*, N. Pavlenko *Augsburg*

Oxide heterostructures combine the electronic and magnetic properties of transition metal oxides with the potential of atomic precision heteroepitaxy, thereby paving the way towards novel interface-controlled functionalities. A case in point is the polar/non-polar interface in $\text{LaAlO}_3/\text{SrTiO}_3$, where a highly mobile two-dimensional electron system (2DES) develops at the interface beyond a critical overlayer thickness. While the microscopic mechanism for the 2DES formation is still intensely debated, it displays a number of intriguing properties including superconductivity, controllability by electric gating and the coexistence of superconductivity and ferromagnetism. Spectroscopic investigations of such 2DESs require suitable methods with sufficient interface sensitivity.

Here I will demonstrate that x-ray based spectroscopies represent valuable tools to explore the electronic structure of buried interfaces, providing information on the atomic and orbital nature of the 2DES, its sheet carrier density and spatial extent [1, 2], band bending [3], as well as the corresponding electronic dispersions and Fermi surface topology [4].

- [1] M. Sing et al., *Phys. Rev. Lett.* 102, 176805 (2009).
- [2] G. Berner et al., *Phys. Rev. B* 82, 241405(R) (2010).
- [3] G. Berner et al., submitted.
- [4] G. Berner et al., arXiv:1301.2824.

We.02

Oxide heterostructures: efficient solar cells and spin-orbit coupling

K. Held (presenter) *Vienna University of Technology*

Heterostructures made of transition metal oxides are an upcoming class of materials which may replace at some point conventional semiconductors for specific applications. We show how to exploit the unique properties of these heterostructures for high-efficiency solar cells [1]: The intrinsic electric field of polar heterostructures allows for efficiently separating the created electrons and holes. Furthermore, the heterostructure naturally provides electrical contacts through ultra-thin conducting interface layers. Last but not least, the bandgap in some heterostructures is optimal for the solar spectrum and can be tuned by using different chemical elements layer-by-layer. In the second part, I will present the theory of spin-orbit coupling in oxide heterostructures [2] which is, due to multi-orbital effects, strikingly different from the standard Rashba theory of semiconductor heterostructures: By far the biggest effect is at the crossing point of the xy and yz orbitals in case of $\text{LaAlO}_3/\text{SrTiO}_3$; and around the Γ point a spin splitting with a linear and cubic dependence on the wave vector k is possible.

- [1] E. Assmann et al., *Phys. Rev. Lett.* 110, 078701 (2013).
- [2] Z. Zhong, A. Toth, and K. Held, arXiv:1209.4705.

We

We.03

Interface-induced superconductivity and strain-dependent spin density wave in FeSe/STO thin films

D. L. Feng *Fudan University*, S. Tan *Fudan University*, T. Zhang (presenter) *Fudan University*, R. Peng *Fudan University*, H. Xu *Fudan University*, Y. Zhang *Fudan University*, Z. Ye *Fudan University*

Recently in single layer FeSe films grown on SrTiO₃ substrate, signs for superconducting transition temperature (T_c) of 65 K are reported, which may break the T_c record in iron-based high temperature superconductors (Fe-HTS's). Here by using in-situ angle resolved photoemission spectroscopy, we substantiate the presence of spin density wave (SDW) in FeSe films, a key ingredient of Fe-HTS that was missed in FeSe before, which weakens with increased thickness or reduced strain. We demonstrate that the superconductivity occurs when the electrons transferred from the oxygen-vacant substrate, which suppresses the pronounced SDW in single layer FeSe. Moreover, we establish the phase diagram of FeSe vs. lattice constant that contains all the essential physics of Fe-HTS's, and provide a comprehensive understanding of FeSe films and directions to further enhance its T_c . With the simplest structure, clean composition and single tuning parameter, FeSe thin films turn out to be ideal test beds for theories of Fe-HTS.

We.04

Nonthermal broken symmetry states in the Hubbard model

M. Eckstein (presenter) *MPSD/CFEL, University of Hamburg*, P. Werner *University of Fribourg*, N. Tsuji *University of Tokyo*

Strong perturbations of the antiferromagnetic phase of the Hubbard model, e.g., by means of interaction quenches or photo-excitation, can induce a melting of the long-range order (LRO). However, even when the excitation density exceeds the energy that would be needed to heat the system above the Neel temperature, LRO can survive for very long times [1, 2].

In the talk we address the nature of these long-lived non-thermal symmetry broken states as well as the crossover to the excitation regime in which LRO disappears already on fast timescales. At the crossover between metastable states, signatures of non-thermal critical behavior become evident through in a diverging timescale for melting of LRO, as well as through softening of the amplitude mode oscillations. The results can be carried over to superconducting and charge ordered states, and we also investigate signatures of these phenomena in time-resolved ARPES.

[1] N. Tsuji, M. Eckstein and Ph. Werner, arXiv:1210.0133.

[2] Ph. Werner, N. Tsuji and M. Eckstein, Phys. Rev. B 86, 205101 (2012).

We.05

Density-matrix theory for time-resolved dynamics of superconductors in non-equilibrium

D. Manske (presenter) *Max Planck Institute for Solid State Research, I. Eremin University Bochum*, A. Schnyder *Max Planck Institute for Solid State Research*

We study the ultrafast dynamics of unconventional superconductors from a microscopic viewpoint employing density-matrix theory. In particular, we derive and solve numerically equations of motions which allow calculating the resulting oscillations of the superconducting order parameter exactly [1]. In a next step we study the role of phonons in the non-equilibrium state and compare with time-resolved Raman scattering experiments on Bi2212 [2]. The dynamics of coherent phonons after excitation with a short intense pump pulse can be treated at a fully quantum kinetic level. We find that in the nonadiabatic regime the generation of coherent phonons is resonantly enhanced when the frequency of the order parameter oscillations is tuned to the phonon energy which might be achieved by changing the pump pulse intensity [3]. Finally, we extend our theory to 2-band superconductors and study the characteristic changes of the oscillations of the superconducting gaps due to interband coupling [4]. This allows us to contrast the ultrafast dynamics between MgB₂ and the Fe-pnictides.

[1] J. Unterhinninghofen, D. Manske, and A. Knorr, *Phys. Rev. B* 77, 180509(R) (2008).

[2] P. P. Saichu et al., *Phys. Rev. Lett.* 102, 177004 (2009).

[3] A.P. Schnyder, D. Manske, and A. Avella, *Phys. Rev. B* 84, 214513 (2011).

[4] A. Akbariet al., *Europhys. Lett.*, in press (2013).

We.06

ARPES and optical conductivity of the Hubbard-Holstein model: equilibrium and pump-probe phenomena

A. Mishchenko (presenter) *RIKEN Emergent Materials Department*

Angle resolved photoemission spectra (ARPES) [1, 2] and optical conductivity (OC) [3, 4] of the 2D Hubbard-Holstein model are calculated in the underdoped regime. The ARPES reveal either short-living quasiparticles or kink in electronic dispersion, as observed in experiments. The OC shows a three-peak structure in agreement with experimental observations. The calculations show that the energy scales of electron-electron and electron-phonon interactions are very similar and it is difficult to prove or disprove its relevance in the spectroscopic experiments with the systems in equilibrium. Hence, a pump-probe technique is an exclusive route to disentangle different interactions and evaluate its importance.

Time dynamics of the physical properties and OC of the 2D Hubbard-Holstein model is studied when undoped system is put out of equilibrium by an ultrashort powerful light pulse [5]. At nonzero electron-phonon interaction, lattice and spin subsystems oscillate with the phonon period $T_{ph} = 80$ fs. The decay time of these oscillations is about 150-200 fs, similar to the relaxation time of the charge system. We present novel theoretical results on time dynamics, consider which kind of ARPES experimental information is desirable for unambiguous theoretical conclusions, and, in particular, set up a discussion what can be extracted from the pump-probe ARPES experiments.

[1] A.S. Mishchenko and N. Nagaosa, *Phys. Rev. Lett.* 93, 036402 (2004).

[2] A.S. Mishchenko et al., *Europhys. Lett.* 95, 57007 (2011).

[3] A.S. Mishchenko et al., *Phys. Rev. Lett.* 100, 166401 (2008).

[4] G. De Filippis et al., *Phys. Rev. B* 80, 195104 (2009).

[5] G. De Filippis et al., *Phys. Rev. Lett.* 109, 176402 (2012).

We.07

Correlation tuned cross-over between thermal and nonthermal states following ultrafast transient pumping

B. Moritz (presenter) *SLAC National Accelerator Laboratory*, J. K. Freericks *Georgetown University*, T. P. Devereaux *SLAC National Accelerator Laboratory*, M. Sentef *SLAC National Accelerator Laboratory*, A. F. Kemper *Lawrence Berkeley National Laboratory*

Electron-electron mediated relaxation following excitation of a correlated system by an ultrafast electric field pump pulse leads to a dichotomy in the temporal evolution across the metal-to-insulator transition. While the metallic regime can be well characterized by evolution toward a steady-state with increased effective temperature, the insulating regime shows a breakdown in this paradigm with evolution toward a clearly nonthermal state with a complicated electronic distribution as a function of momentum. This dichotomy has been characterized by studying the changes in energy, photoemission response, and electronic distribution as a function of time with important implications for systems manifesting strong correlations subjected to investigation using strong driving fields.

THURSDAY 01 AUGUST

09:00	Th.01 (invited)	Momentum-resolved “hidden-order” gap structure, symmetries, and entropy loss in URu₂Si₂ A. Santander-Syro <i>CSNSM - Université Paris-Sud</i>
09:30	Th.02	Exotic physics from doping the Mott insulator Sr₂IrO₄ Y. Cao <i>University of Colorado</i>
09:55	Th.03	Electron pair emission: Insights on the electron correlation strength F. O. Schumann <i>Max-Planck Institut für Mikrostrukturphysik</i>
10:20	Th.04 (invited)	The dual nature of 4f electrons in rare-earth intermetallics: ARPES view D. Vyalikh <i>University of Technology Dresden</i>
10:50		Coffee break
11:30	Th.05 (invited)	Correlation effects in Fe pnictides R. Valenti <i>University of Frankfurt</i>
12:00	Th.06	ARPES on iron-based superconductors: leading role of 3d_{xz,yz} orbitals D. Evtushinsky <i>IFW Dresden</i>
12:25	Th.07 (invited)	Pseudogap formation above the superconducting dome in iron-pnictides T. Shimojima <i>University of Tokyo</i>
12:55		Lunch break

Th

14:30	Th.08 (invited)	<p>Dynamical screening, electronic polarons, and many-body satellites in SrVO₃: new surprises on an old compound from combined GW and dynamical mean field theory (“GW+DMFT”)</p> <p>S. Biermann <i>CPHT Ecole Polytechnique</i></p>
15:00	Th.09	<p>Hidden Quasiparticles and Incoherent Photoemission Spectra in Na₂IrO₃</p> <p>A. M. Oleś <i>Jagellonian University and Max-Planck-Institut für Festkörperforschung</i></p>
15:25	Th.10 (invited)	<p>Emergent Fermi liquid physics within an intermediate coupling model</p> <p>T. Das <i>Los Alamos National Laboratory</i></p>
15:55		Coffee break
16:30	Th.11 (invited)	<p>Recent theoretical developments in one-particle spectral function of strongly correlated materials</p> <p>W. Ku <i>Brookhaven National Laboratory</i></p>
17:00	Th.12	<p>Angle-resolved photoemission study of Ba(Fe_{1-x}Ru_x)₂As₂</p> <p>R. Dhaka <i>Iowa State University</i></p>
17:25	Th.13 (invited)	<p>The magnetic state of iron superconductors</p> <p>E. Bascones <i>Instituto de Ciencia de Materiales de Madrid (ICMM-CSIC)</i></p>
17:55		Best Poster Award / Coffee break
18:30	Th.14 (invited)	<p>ARPES on distinct electronic structure and high temperature superconductivity in single-layer FeSe/SrTiO₃ films</p> <p>X. Zhou <i>Chinese Academy of Sciences</i></p>
19:00	Th.15 (invited)	<p>Bandwidth renormalization in 122 iron pnictides studied by SX-ARPES</p> <p>E. Razzoli <i>Département de Physique and Fribourg Center for Nanomaterials, Université de Fribourg, Switzerland</i></p>
19:30	Th.16	<p>ARPES and TR-ARPES studies of the electronic structure of ferropnictides high-T_c superconductors</p> <p>J. Fink <i>IFW Dresden</i></p>

Th.01

Momentum-resolved “hidden-order” gap structure, symmetries, and entropy loss in URu_2Si_2

A. F. Santander-Syro (presenter) *CSNSM, Université Paris-Sud and CNRS, C. Bareille CSNSM, Université Paris-Sud and CNRS, F. L. Boariu Lehrstuhl für Experimentelle Physik VII, Universität Würzburg, H. Schwab Lehrstuhl für Experimentelle Physik VII, Universität Würzburg, P. Lejay Institut Néel, CNRS/UJF, F. Reinert Lehrstuhl für Experimentelle Physik VII, Universität Würzburg*

Due to their exceptionally strong correlations, f-electron systems present a wide realm of original phase transitions and often poorly understood states of matter. One of the most intriguing is the so-called hidden-order (HO) state forming below $T_{\text{HO}} = 17.5\text{K}$ in URu_2Si_2 . Extensive macroscopic characterizations gathered during the last 30 years show a reduction of almost 60% in the electronic specific heat across the transition, and suggest that a gap of about 10 meV opens over more than 50% of its Fermi surface. However, the identification of the associated broken symmetry and gap structure remain longstanding riddles [1-3].

In this talk, I will present our state-of-the-art ARPES measurements imaging the reconstruction of the electronic structure of URu_2Si_2 across the hidden-order transition [4-6]. We observe a change of the electronic structure symmetry from body-centred tetragonal in the paramagnetic state to simple-tetragonal in the ordered state, described by the ordering vector $Q_0=(1,0,0)$ (reciprocal-lattice units). This is accompanied by the opening of a gap of 7 meV over 70% of a large heavy-fermion Fermi surface, and the formation of four small “Fermi petals” at the incommensurate wave-vector $Q_1=(0,6,0)$ showing another gap of 5 meV with respect to the states that defined the heavy-fermion Fermi surface above T_{HO} . Furthermore, the Fermi sheets measured in the HO state are in quantitative agreement with those determined by Shubnikov–de Haas experiments. Thus, our results provide a unified microscopic picture of the large entropy loss in the HO state, of the emergence of sharp inelastic peaks in the magnetic excitation spectrum at Q_0 and the gap of magnetic excitations at Q_1 observed by inelastic neutron scattering, and of the similarity found by magneto-transport measurements between the HO phase and the high-pressure antiferromagnetic phase—which would then be a consequence of both phases having the same simple-tetragonal electronic symmetry described by the ordering vector Q_0 .

[1] T. M. Palstra et al., *Phys Rev Lett.* 55, 2727 (1985).

[2] M. B. Maple et al., *Phys. Rev. Lett.* 56, 185 (1986).

[3] J. A. Mydosh and P. M. Oppeneer, *Rev. Mod. Phys.* 83, 1301 (2011).

[4] A. F. Santander-Syro et al., *Nature Phys.* 5, 637-641 (2009).

[5] F. L. Boariu et al., *Phys. Rev. Lett.* 110, 156404 (2013).

[6] C. Bareille et al., Submitted (2013).

Th.02

Exotic Physics from Doping the Mott Insulator Sr_2IrO_4

Y. Cao (presenter) *University of Colorado, Q. Wang University of Colorado, J. Waugh University of Colorado, T. Reber University of Colorado, N. Plumb Swiss Light Source, S. Parham University of Colorado, H. X. Li University of Colorado, S. R. Park University of Colorado, T. F. Qi University of Kentucky, O. Korneta University of Kentucky, G. Cao University of Kentucky, D. Dessau University of Colorado*

Doping a Mott insulator, as in the case of high T_c cuprates, has given rise to many exotic physics in the doping diagram, such as the pseudogap and Fermi arc. An important topic in these strongly correlated systems is to distinguish the properties that are intrinsic to the Mott physics from those that are materials specific. Thus novel material systems with a Mott behavior is highly desired. Recent studies of Sr_2IrO_4 provide a new venue to look into the topic, where the spin, orbital, charge and lattice degrees of freedom interact. Using ARPES we studied the evolution of the electronic structure of Sr_2IrO_4 with both Rh and La doping. We show that the Rh substitution acts as immobile effective local holes, without a strong renormalization of the overall band structure, while La acts as an electron dopant. Particularly interesting is the lightly hole-doped regime, which showcases pseudogap and Fermi arc. Our data shows pseudogap phase is a candidate of the ground state, instead of a result of thermal fluctuation in previous theories. Scattering rate of the Fermi arc has a Marginal Fermi liquid-like behavior. We argue the observed pseudogap is a manifestation of strong short range correlations.

Th.03

Electron pair emission: Insights on the electron correlation strength

F. O. Schumann (presenter) *Max-Planck Institut für Mikrostrukturphysik*,
L. Behnke *Max-Planck Institut für Mikrostrukturphysik*, C. Li *Max-Planck Institut für Mikrostrukturphysik*, J. Kirschner *Max-Planck Institut für Mikrostrukturphysik*

The absorption of a single photon and subsequent emission of an electron is a well-established technique. An alternative pathway constitutes the emission of an electron pair upon photon absorption, this effect is known as Double Photoemission (DPE). This is experimentally accessible via coincidence spectroscopy. The power of this technique lies in the fact the very existence of a DPE intensity requires a finite electron-electron interaction [1]. This immediately leads to the question whether the intensity level provides insight into the correlation strength. A theoretical study on DPE from a strongly correlated system modeled by the Hubbard Hamiltonian gives an affirmative answer [2]. The theoretical approach of a varying the interaction strength via the Hubbard U is experimentally not possible. However, transition metal oxides like NiO are usually termed “highly” correlated due to the fact that the material properties are decisively determined by the electron-electron interaction. Therefore the theory has to include the electron correlation to higher level of sophistication compared to metals. Therefore we studied NiO and transition metals via pair emission spectroscopy. Excitation via primary electrons leads to significantly increased coincidence intensity for the oxides compared to the metals [3]. We performed experiments above and below the Néel temperature and observed no temperature dependence of the coincidence spectra. This proves that electron pair emission probes the local correlation rather than long-range order [4]. We also report on first DPE experiments on these materials and compare the energy distributions obtained for the two types of excitation.

[1] J. Berakdar, Phys. Rev. B 58, 9808 (1998).

[2] B.D. Napitu and J. Berakdar, Phys. Rev. B 81, 195108 (2010).

[3] F.O. Schumann et al., Phys. Rev. B 86, 035131 (2012).

[4] F.O. Schumann et al., J. Phys.:Condens. Matter 25, 094002 (2013).

Th.04

The dual nature of 4f electrons in rare-earth intermetallics: ARPES view

D. Vyalikh (presenter) *University of Technology Dresden*

Rare-earth intermetallics with an unstable valence like Ce, Eu or Yb form a prototype of strongly correlated electron systems. The correlations arise from the interplay between almost localized 4f electrons and itinerant valence band states and result in a wealth of extraordinary phenomena. Our experiments aim to disclose details of this interaction, and reveal the fine electronic structure of such materials near the Fermi level. The particular point is the proper discrimination of (sub-) surface and bulk related phenomena. In the present contribution the following recently obtained issues for YbRh₂Si₂ and EuRh₂Si₂ will be extensively presented:

- (i) the k-resolved insight into the f-d hybridization phenomena;
- (ii) insight into the Fermi surface and manifestation of its strong 4f character. Disclosing its topology and features reflecting f-d coupling at the surface and bulk of the material;
- (iii) observation of crystal-electric field (CEF) splitting of the 4f states and their fine dispersion induced by f-d hybridization;
- (iv) clear evidence of the interplay of Dirac fermions and heavy quasi-particles.

Th.05

Correlation effects in Fe pnictides

R. Valenti (presenter) *University of Frankfurt*

In this talk I will discuss the importance of correlation effects in Fe-based superconductors. For that I will present LDA+DMFT calculations for some members of the “111”, “1111” and “122” families in comparison with ARPES and de Haas van Alphen experiments. I will also present some arguments why the related MgFeGe does not superconduct.

- [1] J. Ferber et al., Phys. Rev. Lett. 109, 236403 (2012).
- [2] J. Ferber et al., Phys. Rev. B 85, 094505 (2012).
- [3] H.O. Jeschke et al., arXiv:1305.7368.

Th.06

ARPES on iron-based superconductors: leading role of $3d_{xy,yz}$ orbitals

D. Evtushinsky (presenter) *IFW Dresden*

A short overview of the available ARPES results on iron-based superconductors will be given. Despite of the large variety of the observed Fermi surfaces [1-6], phenomenologically one can point out several common tendencies for iron high temperature superconductors—namely, band renormalization of factor of 3 [3, 6-8], often a two-gap behavior [2, 7-10], presence of electronic coupling to low-energy bosonic modes. Our recent results indicate clear correlation between the superconducting gap magnitude and orbital origin of the electronic states, with the largest gap solely for iron $3d_{xy,yz}$ orbitals. Interestingly, the electron coupling to bosonic modes was found to be stronger also for $3d_{xy,yz}$ bands. Further analysis of the electronic structures of differently doped iron arsenides consistently points to the significance of $3d_{xy,yz}$ bands, and little importance of $3d_{xy}$ and $3d_{z^2}$ bands for superconductivity in these materials.

- [1] V. B. Zabolotnyy et al., Nature (London) 457, 569 (2009).
- [2] D. V. Evtushinsky et al., New J. Phys. 11, 055069 (2009).
- [3] S. V. Borisenko et al., Phys. Rev. Lett. 105, 067002 (2010).
- [4] D. V. Evtushinsky et al., J. Phys. Soc. Jpn. 80, 023710 (2011).
- [5] S. Thirupathaiah et al., Phys. Rev. B 86, 214508 (2012).
- [6] S. V. Borisenko et al., arXiv:1204.1316.
- [7] H. Ding et al., Europhys. Lett. 83, 47001 (2008).
- [8] D. V. Evtushinsky et al., arXiv:1204.2432.
- [9] D. V. Evtushinsky et al., Phys. Rev. B 79, 054517 (2009).
- [10] D. V. Evtushinsky et al., Phys. Rev. B 87, 094501 (2013).

Th.07

Pseudogap formation above the superconducting dome in iron-pnictides

T. Shimojima (presenter) *University of Tokyo*

Several studies have been reported on the possible pseudogap formation in iron-based superconductors [1, 2]. However, whether the pseudogap phase is a generic feature of this material is still an open question. In particular, only a few angle-resolved photoemission spectroscopy studies have shown the presence of an energy gap in the momentum space in the normal state [3].

In this work, we report the momentum-resolved electronic structure of $\text{BaFe}_2(\text{As}_{1-x}\text{P}_x)_2$ by employing synchrotron radiation and laser angle-resolved photoemission spectroscopy. We observe the P-substitution evolution of pseudogap, which develops well above the magnetostructural transitions and persists above the nonmagnetic superconducting dome, showing a notable similarity with cuprates. In addition, the pseudogap formation is accompanied by inequivalent energy shifts in xz/yz orbitals of iron atoms. We will discuss the similarities and differences in pseudogap formations between iron-pnictides and cuprates [4].

[1] Y. -C. Wen et al., *Phys. Rev. Lett.* 108, 267002 (2012).

[2] S. -H. Baek et al., *Phys. Rev. B* 84, 094510 (2011).

[3] Y. -M. Xu et al., *Nat. Commun.* 2, 392 (2011).

[4] T. Shimojima et al., *Arxiv*1305.3875.

Th.08

Dynamical screening, electronic polarons, and many-body satellites in SrVO_3 : new surprises on an old compound from combined GW and dynamical mean field theory (“GW+DMFT”)

S. Biermann (presenter) *CPHT Ecole Polytechnique*

We review the recent elaboration of the description of dynamical screening effects in correlated electron materials, within dynamical mean field (DMFT) based electronic structure methods [1, 2, 3]. In this framework, the dynamical nature of screening is encoded within a frequency-dependent effective Coulomb interaction, with a pole structure corresponding to bosonic excitations (plasmons, particle-hole excitations, or more complex composite many-body excitations). Within many-body calculations, the frequency-dependence of the interactions is responsible for the appearance of satellite structures and additional low-energy mass renormalisations (“electronic polarons”) [4].

On the example of the ternary transition metal oxide SrVO_3 , we illustrate the strength of the dynamical screening effects [2]. Finally, we discuss additional nonlocal self-energy effects that substantially modify the electronic excitations in the unoccupied part of the spectra of SrVO_3 [5], described within a combination of many-body perturbation theory and DMFT, the so-called “GW+DMFT” scheme [6].

Work done in collaboration with the authors of the references below.

[1] F. Aryasetiawan et al., *Phys. Rev. B* 70, 195104 (2004)

[2] M. Casula, A. Rubtsov, and S. Biermann, *Phys. Rev. B* 85, 035115 (2012)

[3] Ph. Werner et al., *Nature Phys.* 8, 331 (2012)

[4] M. Casula, A. Rubtsov, and S. Biermann, *Phys. Rev. B* 85, 035115 (2012)

[5] J.M. Tomczak et al., *Europhys. Lett.* 100, 67001 (2012)

[6] S. Biermann, F. Aryasetiawan, and A. Georges, *Phys. Rev. Lett.* 90, 086402 (2003)

Th.09

Hidden Quasiparticles and Incoherent Photoemission Spectra in Na_2IrO_3

A. M. Oleś (presenter) *Jagellonian University and Max-Planck-Institut für Festkörperforschung*, F. Trouselet *Institute Neel, Grenoble, France*, M. Berciu *University of British Columbia*, P. Horsch *Max-Planck-Institut für Festkörperforschung*

We study two Heisenberg-Kitaev t-J-like models on a honeycomb lattice [1], focusing on the zigzag magnetic phase of Na_2IrO_3 , and investigate hole motion by exact diagonalization and variational methods. The spectral functions are quite distinct from those of cuprates and are dominated by large incoherent spectral weight at high energy, almost independent of the microscopic parameters—a universal and generic feature for zigzag magnetic correlations. We explain why quasiparticles at low energy are strongly suppressed in the experimentally relevant strong coupling regime and determine an analog of a pseudogap. We point out that the qualitative features of the predominantly incoherent spectra obtained within the two different models for the zigzag phase are similar, and they have remarkable similarity to recently reported angular resolved photoemission spectra for Na_2IrO_3 [2].

[1] F. Trouselet et al., arXiv:1302.0187 (2013).

[2] R. Comin et al., Phys. Rev. Lett. 109, 266406 (2012).

This work was supported by the Max Planck—UBC Centre for Quantum Materials, and by the Polish National Science Center (NCN) under Project No. 2012/04/A/ST3/00331.

Th.10

Emergent Fermi liquid physics within an intermediate coupling model

T. Das (presenter) *Los Alamos National Laboratory*

Understanding and modeling correlated electronic spectra has remained a constant theme of research for decades. We have relatively better modeling capabilities for systems residing either in the weakly or strongly correlated regimes. However, the intermediate coupling regime poses a challenge since both the Fermi-liquid or dynamical mean-field theories are inadequate here. Over the last few years, we have been working on developing a computational scheme for this problem. Our intermediate coupling model is based on materials-specific band structure, from which self-energy correction is computed via a self-consistent approach including full momentum dependent dynamical correlations. In this talk, I will present results for several representative compounds including actinides, cuprates and other correlated systems. A common feature of intermediate coupling scenario is that the self-energy splits the electronic structure into low-energy coherent states (emergent Fermi liquid state), and high-energy localized state (residual Mott state), yielding a coexistence of itinerant and localized states. The resulting electronic fingerprint reveals a universal “S” or waterfall shape in the dispersion, and a peak-dip-hump feature in the density of states. The results suggest a generic route for formulating the correlated Fermi-liquid physics from which a unified theory of unconventional superconductivity may emerge.

[1] T. Das et al., Phys. Rev. Lett. 108, 017001 (2012).

[2] T. Das et al., Phys. Rev. X 2, 041012 (2012).

Th.11

Recent theoretical developments in one-particle spectral function of strongly correlated materials

W. Ku (presenter) *Brookhaven National Laboratory*

Recent theoretical developments in describing ARPES spectral functions will be reviewed. First, unfolding of band structure and Fermi surfaces of first-principles calculation will be introduced, and shown to facilitate significantly the analysis of ARPES measurement [1, 2]. Second, recent breakthrough in describing spectral function of systems containing disordered impurities will be discussed. Several alarming surprises relevant to common ARPES analysis methods will be demonstrated, using Fe-based superconductors as examples [3-6]. Third, if time permitted, novel physical understanding of the quasi-particle superconducting gap of underdoped cuprates will be discussed [7, 8], explaining several puzzling ARPES observation.

[1] *Phys. Rev. Lett.* 107, 257001 (2011).

[2] *Phys. Rev. Lett.* 105, 107004 (2010).

[3] *Phys. Rev. Lett.* 109, 147003 (2012).

[4] *Phys. Rev. Lett.* 108, 207003 (2012).

[5] *Phys. Rev. Lett.* 110, 037001 (2013).

[6] *Phys. Rev. Lett.* 106, 077005 (2011).

[7] *Phys. Rev. X* 1, 011011 (2011).

[8] arXiv:1302.7317.

e-mail: weiku@bnl.gov

Th.12

Angle-resolved photoemission study of $\text{Ba}(\text{Fe}_{1-x}\text{Ru}_x)_2\text{As}_2$

R. Dhaka (presenter) *Iowa State University*, C. Liu *Iowa State University*, S. E. Hahn *Iowa State University*, R. Jiang *Iowa State University*, B. N. Harmon *Iowa State University*, A. Thaler *Iowa State University*, S. L. Bud'ko *Iowa State University*, P. C. Canfield *Iowa State University*, A. Kaminski *Iowa State University*, E. Razzoli *Paul Scherrer Institute*, M. Shi *Paul Scherrer Institute*

We have performed detailed studies of the electronic structure in $\text{Ba}(\text{Fe}_{1-x}\text{Ru}_x)_2\text{As}_2$ as a function of Ru concentration [1] and sample temperature [2], using high-resolution angle resolved photoemission spectroscopy. We find that the substitution of Ru for Fe is isoelectronic, i. e., it does not change the carrier concentration. More interestingly, there are no measured significant changes in the shape of the Fermi surface (FS) or in the Fermi velocity over a wide range of Ru substitution ($0 < x < 0.4$) [1]. This unusual behavior is in contrast with the case of Co substitution, where even small amount of Co induces large change not only in the size of the FS pockets but also in the FS topology, i. e., Lifshitz transition which is closely linked to the superconducting dome [3]. Given that the suppression of the anti-ferromagnetic and structural transition temperature is associated with the induction of the superconducting state, Ru substitution must achieve this via a mechanism that does not involve changes of the Fermi surface. We speculate that this mechanism relies on magnetic dilution that leads to the reduction of the effective Stoner enhancement. Furthermore, we reveal that the band structure of pure and Ru substituted BaFe_2As_2 changes significantly with the sample temperature. The hole and electron pockets are well nested at low temperature, which likely drives the spin density wave and resulting antiferromagnetic order. The size of the hole pocket shrinks and the electron pocket expands upon warming, i. e. the nesting is degraded at higher temperatures. These results demonstrate that the temperature dependent nesting may play an important role in driving the antiferromagnetic/paramagnetic phase transition [2].

[1] R. S. Dhaka et al., *Phys. Rev. Lett.* 107, 267002 (2011).

[2] R. S. Dhaka et al., *Phys. Rev. Lett.* 110, 067002 (2013).

[3] Chang Liu et al., *Nature Phys.* 6, 419 (2010); *Phys. Rev. B*, 84, 020509(R) (2011).

Present Address: Swiss Light Source, Paul Scherrer Institut, CH-5232 Villigen PSI, Switzerland, rajendra.dhaka@psi.ch

Th.13

The magnetic state of iron superconductors

E. Bascones (presenter) *Instituto de Ciencia de Materiales de Madrid (ICMM-CSIC)*,
M. J. Calderón *Instituto de Ciencia de Materiales de Madrid (ICMM-CSIC)*, B. Valenzuela *Instituto de Ciencia de Materiales de Madrid (ICMM-CSIC)*

A major breakthrough in superconductivity took place five years ago with the discovery of high temperature superconductivity in iron pnictides. Iron superconductors are characterized by FeAs (or FeSe) layers. The so-called undoped materials are metals which show columnar antiferromagnetism, i.e. antiferromagnetic ordering in one direction and ferromagnetic ordering in the other direction. More complex magnetic orderings appear in chalcogenides. Doping or pressure suppresses antiferromagnetism and superconductivity appears. Important effort has been dedicated to understand the strength of correlations and the origin of magnetism in these materials. Iron superconductors are multi-orbital materials. Recent calculations mostly in the normal state have emphasized that correlations are largely controlled by Hund's coupling, increase with hole doping and are orbital dependent (orbital differentiation). Magnetism has been mostly described in terms of purely itinerant or purely localized electrons. We have studied the antiferromagnetic columnar state. We find that with increasing interactions the system does not evolve trivially from the pure itinerant to the pure localized regime. Instead we find a region with strong orbital differentiation between xy and yz , which are half-filled gapped states at the Fermi level and itinerant zx , $3z^2-r^2$ and x^2-y^2 orbitals. With hole-doping the orbital differentiated region appears for smaller values of interactions. This finding suggests a model with localized and itinerant electrons. We discuss the interplay between the exchange energy of the localized electrons and the kinetic energy gain of the itinerant electrons and its role in the stabilization of magnetism and orbital ordering.

Th.14

ARPES on distinct electronic structure and high temperature superconductivity in single-layer FeSe/SrTiO₃ films

X. Zhou (presenter) *Chinese Academy of Sciences*

High resolution angle-resolved photoemission measurements have been carried out to study the electronic structure and high temperature superconductivity of the single-layer FeSe films grown on SrTiO₃ substrate [1]. Distinct Fermi surface topology and nearly isotropic superconducting gap without nodes are observed in the system [2]. Phase diagram is established and electronic indication of high temperature superconductivity at ~65K is observed in tuning the carrier concentration of the single-layer FeSe film [3]. Implications of these results on the superconductivity mechanism of the iron-based superconductors will be discussed.

[1] Q.-Y. Wang et al., *Chin. Phys. Lett.* 29, 037402 (2012).

[2] D. Liu et al., *Nat. Comm.* 3, 931 (2012).

[3] S. He et al., arXiv:1207.6823. *Nature Mater.*/DOI:10.1038/NMAT3648 (2013).

Th.15

Bandwidth renormalization in “122” iron pnictides studied by SX-ARPES

E. Razzoli (presenter) *Département de Physique and Fribourg Center for Nanomaterials, Université de Fribourg, Switzerland*, M. Shi *Swiss Light Source, Paul Scherrer Institute, Switzerland*, J. Mesot *Swiss Light Source, Paul Scherrer Institute, Switzerland*

In this contribution, we present a systematic soft x-ray angle-resolved photoemission spectroscopy (SX-ARPES) study of electron-electron correlation at low-temperature (10 K) in “122” Fe-pnictides of paramagnetic, superconducting and antiferromagnetic spin density wave (SDW) compounds, as well as the low-temperature Ru-pnictide superconductor (LaRu₂P₂).

Electronic correlations and the associated electron mass enhancements are central aspects in the discussion of superconductivity the Fe-based pnictides unconventional superconductors. Our study shows that for all the investigated compounds the three-dimensional Fermi surface can be reproduced by DFT electronic structure calculations. However, the bandwidth renormalization resulting from electron-electron correlation changes significantly in these systems.

For Fe-pnictides the bandwidth renormalization factors are consistent with the mass enhancements obtained from specific heat and/or quantum oscillation measurements, indicating the mass enhancement mainly resulting from electron-electron correlation effects. For Ru-pnictide superconductor (LaRu₂P₂), in the normal state, the bandwidth renormalization is negligible, which suggests that the mass enhancement observed in quantum oscillation experiments is due to electron-boson coupling and is limited to narrow range around the E_F [1].

[1] E. Razzoli et al., *Phys. Rev. Lett.* 108, 257005 (2012).

Th.16

ARPES and TR-ARPES studies of the electronic structure of ferropnictides high-T_c superconductors

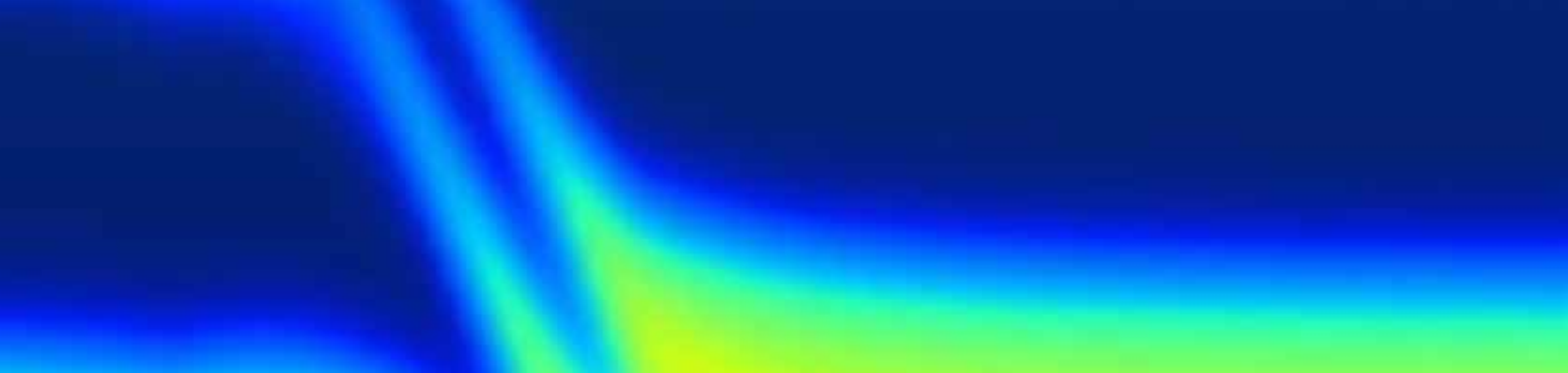
J. Fink (presenter) *IFW Dresden*, E. Rienks *HZB Berlin*, S. Thirupathiah *Universität Duisburg-Essen*, L. Rettig *FU Berlin*, I. Avigo *Universität Duisburg-Essen*, M. Wolf *FHI Berlin*, U. Bovensiepen *Universität Duisburg-Essen*

We have investigated the electronic structure of various ferropnictide high-T_c superconductors and their parent compounds. In particular we have studied the systems Ba(Fe_{1-x}Co_x)₂As₂, Ba(Fe_{1-x}yCo_xMn_y)₂As₂, and EuFe₂As_{1-x}P_x)₂. From photon energy dependent ARPES experiments, we derive the Fermiology as a function of control parameters such as doping or substitution which leads in the case of P substitution to chemical pressure. For Ba(Fe_{1-x}Co_x)₂As₂ we derive a rigid-band like change of the electronic structure with an increase of one electron per Co ion and a clear correlation between the phase diagram and the size and shape of the hole and the electron cylinders. At optimal doping the inner hole cylinders experience a Lifshitz transition to an ellipsoid around the high-symmetry Z point. At a Co concentration where superconductivity vanishes, the hole cylinders have completely disappeared. This clearly signals the importance of nesting between hole and electron pockets for the magnetic and the superconducting properties of ferropnictides. A similar correlation of the Fermiology and the phase diagram has been detected for EuFe₂(As_{1-x}P_x)₂ although there a non-rigid-band behavior has been observed. For Ba(Fe_{1-x}yCo_xMn_y)₂As₂ we have replaced in the optimally Co doped compound further Fe ions by Mn. We find again a non-rigid-band behavior, a back-doping by holes and a reduction of the superconducting transition temperature. An investigation of the mass enhancement and the scattering rates, both related to the self-energy, as a function of the Mn concentration does not show a divergence near optimally doping which would be expected in a scenario where superconductivity is mediated by a coupling of the charge carriers to quantum critical antiferromagnetic fluctuations. Using femtosecond TR-ARPES we have analyzed the response of the electronic structure of ferropnictide parent compounds to optical excitation by an infrared femtosecond laser pulse. Information on the electron-phonon coupling constant, on the excitation of coherent phonons and their coupling to the charge carriers, and the influence of the antiferromagnetic order on the relaxation processes has been obtained.

FRIDAY 02 AUGUST

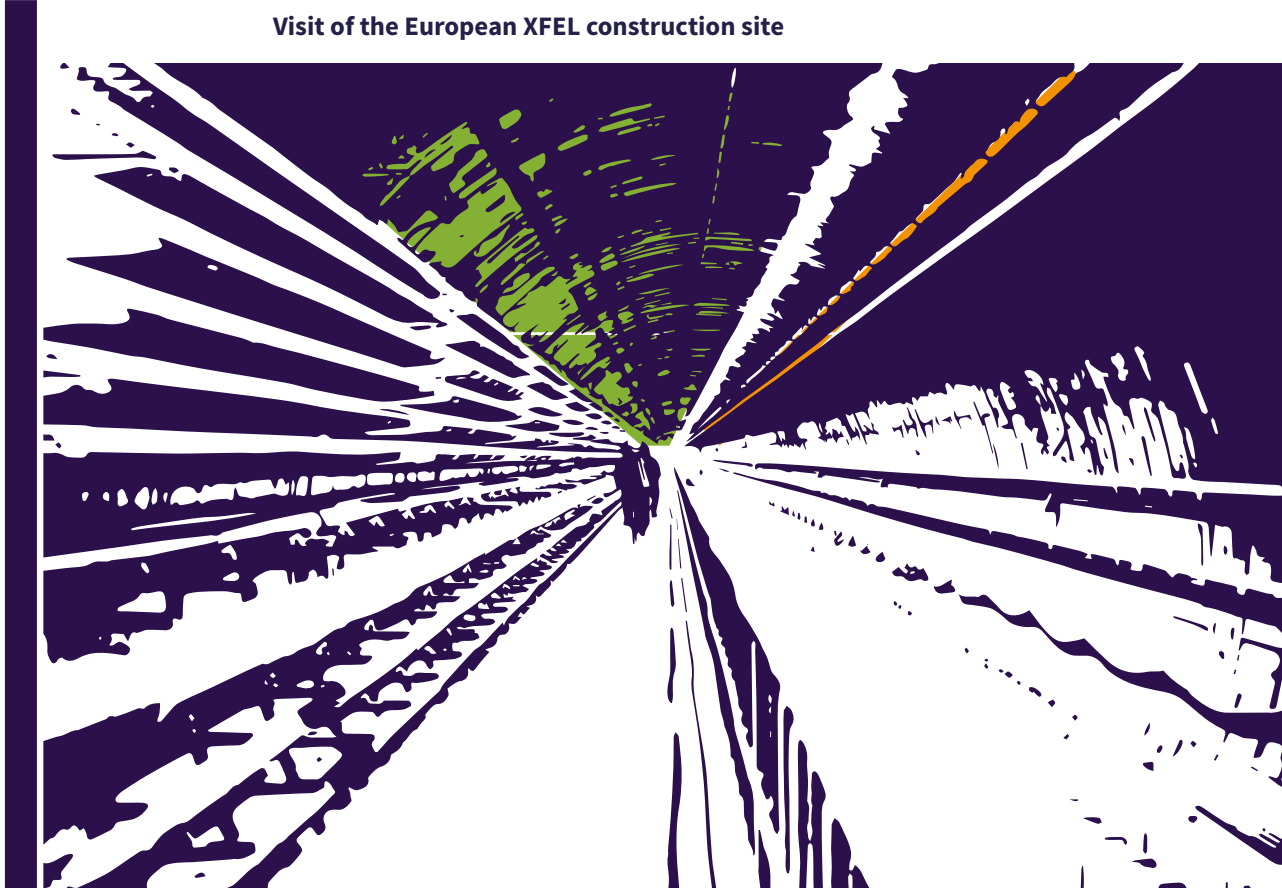
09:00	Fr.01 (invited)	Non-equilibrium optical spectroscopy: a new clue to unravel the properties of correlated materials C. Giannetti <i>Università Cattolica del Sacro Cuore</i>
09:30	Fr.02	Diffusion of doublons in a Mott insulator P. Werner <i>University of Fribourg</i>
09:55	Fr.03 (invited)	Time-resolved photoelectron spectroscopy with free-electron lasers W. Wurth <i>Universität Hamburg</i>
10:25	Fr.04	Coffee break
11:00	Fr.05 (invited)	Complementary momentum-resolved spectroscopies on a charge density wave material: photoemission and resonant inelastic x-ray scattering C. Monney <i>University of Fribourg</i>
11:30	Fr.06	Coherent optical excitation of a charge density wave phase mode in $K_{0.3}MoO_3$ J. Petersen <i>Max Planck Institute for the Structure and Dynamics of Matter and University of Oxford</i>
11:55	Fr.07 (invited)	Ultrafast magnetization dynamics and their signatures in the transient band structure M. Weinelt <i>FU Berlin</i>
12:25		CORPES¹⁵ and close-out
13:00		Lunch break

Fr



13:45

Visit of the European XFEL construction site



17:30

Fr.01

Non-equilibrium optical spectroscopy: a new clue to unravel the properties of correlated materials

C. Giannetti (presenter) *Università Cattolica del Sacro Cuore*

Here we report on the emerging non-equilibrium optical spectroscopy as a novel key to solve the puzzle of high-temperature superconductivity in copper oxides and other correlated materials.

In strongly-correlated electron materials the electronic and optical properties are significantly affected by the coupling of fermionic quasiparticles to different degrees of freedom, such as lattice vibrations and bosonic excitations of electronic origin. Broadband ultrafast spectroscopy [1, 2] is emerging as the premier technique to unravel the subtle interplay between quasiparticles and electronic or phononic collective excitations, by their different characteristic timescales and spectral responses. By investigating the femtosecond dynamics of the optical properties of prototypical copper oxides (Y-Bi2212) over the 0.5-2 eV energy range, we disentangle the electronic and phononic contributions to the generalized electron-boson Eliashberg function, showing that the spectral distribution of the electronic excitations, such as spin fluctuations and current loops, and the strength of their interaction with quasiparticles can account for the high critical temperature of the superconducting phase transition [3]. Finally, we discuss how the use of this technique can be extended to the underdoped region of the phase diagram of cuprates, in which a pseudogap in the quasiparticle density of states opens.

The microscopic modeling of the interaction of ultrashort light pulses with unconventional superconductors will be one of the key challenges of the next-years materials science, eventually leading to the full understanding of the role of the electronic correlations in controlling the dynamics on the femtosecond timescale.

[1] C. Giannetti et al., *Nat. Commun.* 2, 353 (2011).

[2] G. Coslovich et al., *Phys. Rev. Lett.* 110, 107003 (2013).

[3] S. Dal Conte et al., *Science* 335, 1600 (2012).

Fr.02

Diffusion of doublons in a Mott insulator

P. Werner (presenter) *University of Fribourg*, M. Eckstein *University of Hamburg, CFEL*

Pump-probe experiments on correlated hetero-structures [1] combine advanced material design and ultra-fast control. We use the nonequilibrium generalization of “real-space DMFT” [2, 3] to study the photo-excitation and diffusion of carriers in inhomogeneous systems. In particular, we study the diffusion from the surface of an insulating sample into the bulk, and the metallization of Mott insulating layers via the injection of doublons from neighboring layers.

[1] A. Caviglia et al., *Phys. Rev. Lett.* 108, 136801 (2012).

[2] M. Potthoff and W. Nolting, *Phys. Rev. B* 59, 2549 (1999).

[3] J. Freericks, *Phys. Rev. B* 70, 195342 (2004).

Fr.03

Time-resolved photoelectron spectroscopy with free-electron lasers

W. Wurth (presenter) *Universität Hamburg*

High-repetition rate free-electron lasers show great potential for time-resolved photoelectron spectroscopy of complex solids. They provide ultrashort pulses with unprecedented brightness and tunable wavelength covering a broad range from XUV to soft and hard x-rays. In the talk examples from experiments at FLASH, the free-electron laser at DESY in Hamburg, and prospects with sources like the European XFEL will be discussed.

Financial support from the German Ministry of Education and Research through the priority program FSP301 “FLASH” and the DFG through the collaborative research project SFB925 is gratefully acknowledged.

Fr.04

Complementary momentum-resolved spectroscopies on a charge density wave material: photoemission and resonant inelastic x-ray scattering

C. Monney (presenter) *Fritz-Haber-Institut der Max Planck Gesellschaft*

In this talk, I will compare angle-resolved photoemission spectroscopy (ARPES) and resonant inelastic x-ray scattering (RIXS) data taken on the charge density wave material TiSe_2 [1]. I will show how they provide complementary momentum-resolved information on the electronic structure of this broad band material.

While ARPES probes the occupied states after one-electron removal, RIXS provides more complicated information, which can be understood, in the case of broad band materials, as electron-hole excitations close to their Fermi level [2]. In this particular case, RIXS probes the momentum-resolved convolution of the projected occupied and unoccupied states. In this framework, I will discuss how the unoccupied band structure of a material can be accessed by combining ARPES and RIXS results.

[1] C. Monney et al., Phys. Rev. Lett. 109, 047401 (2012).

[2] L.J.P. Ament et al., Rev. Mod. Phys. 83, 705 (2011).

Fr.05

Coherent optical excitation of a charge density wave phase mode in $K_{0.3}MoO_3$

J. C. Petersen (presenter) *MPI-SD/Oxford University*, H. Liu *MPI-SD*, S. Kaiser *MPI-SD*, A. Simoncig *MPI-SD*, I. Gierz *MPI-SD*, A. Cavalieri *MPI-SD*, C. Cacho *STFC Rutherford Appleton Laboratory*, E. Turcu *STFC Rutherford Appleton Laboratory*, E. Springate *STFC Rutherford Appleton Laboratory*, S. Dhesi *Diamond Light Source*, Z. Xu *Zhejiang University*, T. Cuk *UC Berkeley*, A. Cavalleri *MPI-SD/Oxford University*

Time- and angle-resolved photoemission spectroscopy lets us directly access the evolving momentum-dependent electronic structure of strongly driven solids. Here, we study the 1D charge-density wave compound in $K_{0.3}MoO_3$ as it responds to photo-stimulation with an ultra-short laser pulse. We observe a coherent 1.7-THz-frequency modulation of the bonding band position, produced by coupling with the displacively excited amplitude mode. More surprisingly, the anti-bonding band gap oscillates at 0.8 THz, which we attribute to the generation of a coherent phase mode.

In previous ultrafast studies of electronic structure in related compounds, various gaps were melted and Raman-active amplitude modes were coherently excited [1-3]. But laser pulses do not usually excite infrared-active phase modes, which under linear response cannot be triggered by an impulse [4, 5]. We suggest that the apparent coupling in this case represents anharmonic dynamics of the strongly driven CDW order parameter.

[1] S. Hellmann et al., *Nature Commun.* 3, 1069 (2012).

[2] L. Perfetti et al., *New J. Phys.* 10, 053019 (2008).

[3] J. Petersen et al., *Phys. Rev. Lett.* 107, 177402 (2011).

[4] H.J. Zeiger et al., *Phys. Rev. B* 45, 768 (1992).

[5] R. Merlin, *Solid State Commun.* 102, 207 (1997).

Fr.06

Ultrafast magnetization dynamics and their signatures in the transient band structure

M. Weinelt (presenter) *Freie Universität Berlin*, R. Carley *Max-Born-Institute*, M. Teichmann *Freie Universität Berlin*, B. Frietsch *Freie Universität Berlin*, J. Bowlan *Freie Universität Berlin*

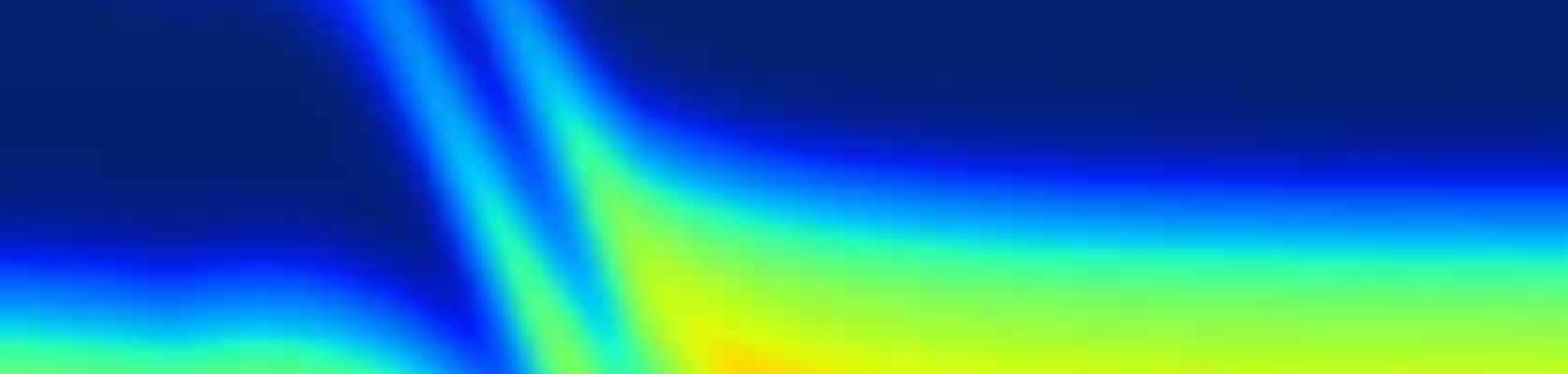
We report on an angle-resolved photoemission experiment with monochromatized high-order harmonic radiation measuring the transient band structure of Gadolinium and Terbium after femtosecond laser excitation.

Femtomagnetism is now an established and active research field in thin film and surface magnetism, which promises magnetic writing speeds three orders faster than current technology. Investigations in this area comprise the spin and magnetization dynamics in ferro- and ferrimagnetic samples initiated with a femtosecond laser pulse. In the first two picoseconds after optical excitation the electronic system and the underlying lattice and spin subsystems of the ferromagnet are not in equilibrium. It remains controversial, which microscopic processes are responsible for the change of the magnetization within a few hundred femtoseconds: scattering among electrons, phonons and magnons, and/or spin-transport?

Currently it is debated, on which timescale the band structure and spin polarization changes and if demagnetization can be described within a rigid band-structure model.

To approach these problems we perform time- and angle-resolved photoemission (TR-ARPES) with a high-order harmonics VUV source. We have studied ultrafast demagnetization for the local-moment ferromagnets Gadolinium and Terbium, prepared as epitaxial films of 10-nm thickness on a W(110) substrate. In the lanthanides equilibration of the excited state involves more than one timescale, because the optical excitation occurs in the valence band but the magnetic moment is dominated by the localized 4f electrons [1-3]. Following excitation by an intense infrared pulse ($h\nu = 1.6$ eV, fluence ~ 1 mJ/cm²), TR-ARPES with 35.6 eV photon energy allows us to directly map the transient exchange splitting of the Δ_2 -like Σ valence bands near the center of the bulk Brillouin zone [4].

Upon laser excitation the exchange splitting of the valence bands



drops with a time constant of 750 fs. While the minority valence band reacts immediately, the response of the majority counterpart is delayed by 1 ps and is only half as fast. Comparing ultrafast de- and thermal re-magnetization we conclude that the exchange splitting and the binding energy of the majority and minority spin valence bands map the true magnetization dynamics of the 5d system. Increasing the starting temperature leads to an even earlier response of the minority spin valence-band, while the slow response of the majority spin band remains unaffected. This suggests that not only superdiffusive transport but also lower sample temperatures of the system delay the demagnetization process. The temperature-dependent dynamics of the exchange splitting is in agreement with recent measurements of the Kerr-rotation [5]. In line with the latter experiment we find at 40 K a small increase of the exchange splitting within the first hundred femtoseconds after laser excitation, which indicates an initial magnetization of the sample.

Measuring in parallel the valence-band dynamics and the transient changes in 4f linear dichroism [2], we establish that at the low excitation fluence of our experiment demagnetization of the two subsystems occurs with significantly different time constants of 0.7 and 12 ps. We conclude that optical excitation drives the valence-band and 4f spin-systems for tenth of picoseconds out of magnetic equilibrium, which may constitute a key ingredients for ultrafast magnetic switching.

[1] A. Vaterlaus et al., Phys. Rev. Lett. 67, 3314 (1991).

[2] A. Melnikov et al., Phys. Rev. Lett. 100, 107202 (2008).

[3] M. Wietstruk et al., Phys. Rev. Lett. 106, 127401 (2011).

[4] R. Carley et al., Phys. Rev. Lett. 109, 057401 (2012).

[5] M. Sultan et al., Phys. Rev. B 85, 184407 (2012).

We gratefully acknowledge funding by the Deutsche Forschungsgemeinschaft through grant WE2037/4-1, the Leibniz graduate school Dynamics in New Light, the Humboldt foundation, and the Helmholtz Virtual Institute Dynamic Pathways in Multidimensional Landscapes.

POSTER SESSION 1 MONDAY, 18:50–21:00

- P1.01** Ultrafast time-resolved ARPES with XUV photon source
C. Cacho
- P1.02** Development of time- and angle-resolved photoemission spectroscopy based on NIR/MIR pump and UV/VUV/XUV probe
L Haiyun
- P1.03** The CITIUS light source
B. Ressel
- P1.04** A time-of-flight spectrometer for photoemission studies
M. Teichmann
- P1.05** Upgrade of the angle-resolved photoemission end station at NSRRC
C. M. Cheng
- P1.06** ARPES beamline at Diamond Light Source: current status
T. Kim
- P1.07** Time-resolved Auger electron spectroscopy
R. Rausch
- P1.08** Bulk electronic structure of quasicrystals studied by HAXPES
J. Nayak
- P1.09** Study of cooperative breathing-mode in molecular chains
S. Yarlagadda
- P1.10** Electronic instability in a zero-gap semiconductor: the charge-density wave in $(\text{TaSe}_4)_2\text{I}$
C. Tournier-Coletta
- P1.11** Time- and angle-resolved photoelectron spectroscopy at charge-density-wave insulators
K. Hanff
- P1.12** Electronic band structure of BaCo_2As_2 : A fully doped ferropnictide analog with reduced electronic correlations
N. Xu
- P1.13** Ultrafast magnetization enhancement in BaFe_2As_2 by coherent phonon excitation
T. Rohwer
- P1.14** Anisotropy of the superconducting gap in $\text{Ba}(\text{Fe}_{1-x}\text{Co}_x)_2\text{As}_2$ revealed by angle-resolved photoemission spectroscopy
S. Ideta
- P1.15** The ARPES study on $\text{AFe}_{17x}\text{Co}_x\text{As}$ (A=Li, Na)
Z. Ye
- P1.16** Unusual band renormalization in the simplest iron based superconductor
J. Maletz
- P1.17** Electronic structure of $\text{Fe}_{1.03}\text{Te}_{0.94}\text{S}_{0.06}$ superconductor
P. Starowicz
- P1.18** Intermediate coupling model of cuprates: a progress report
R. Markiewicz
- P1.19** Interplay between static disorder and dynamic phonon displacement in a weak correlated parent of cuprates.
D. di Sante
- P1.20** d-wave superconductors with finite range impurities of arbitrary strength
K. Scharnberg
- P1.21** The cooper pairs close to fermi surface like a source for the waterfall effect in ARPES
S. Millan
- P1.22** The signatures of superconducting correlations above the transition temperature
T. Domanski
- P1.23** The gap function from lightly to optimally doped $\text{La}_{2-x}\text{Sr}_x\text{CuO}_4$ cuprate, probed by ARPES
M. Shi
- P1.24** Spin-charge coupling in antiferromagnetic LSCO studied by the muons, neutrons, and ARPES techniques
G. Drachuck

- P1.25** Asymmetric doping dependence of L-edge RIXS spectrum in hole- and electron-doped cuprates
T. Tohyama
- P1.26** Direct observation of screening enhanced hole pairing in Spin= $\frac{1}{2}$ copper-oxide materials unravelled by high-resolution resonant inelastic X-ray scattering at FLASH
M. Rübhausen
- P1.27** Conventional superconductivity in SrPd₂Ge₂ from combined ARPES, STS and LDA studies
T. Kim
- P1.28** True bosonic coupling strength evaluated by ARPES in strongly correlated electron systems
H. Iwasawa
- P1.29** Defect states and excitations in a Mott insulator with orbital degrees of freedom: Mott-Hubbard gap versus optical and transport
A. Avella
- P1.30** Correlation and spin-orbit effects in Sr₃Ru₂O₇: a LDA+DMFT study
E. Gorelov
- P1.31** Interplay of electronic correlations and spin-orbit coupling in layered ruthenates
F. Lechermann
- P1.32** Dynamical investigation of the semiconductor-to-metal transition in LaCoO₃
M. Izquierdo
- P1.33** Metal-to-Insulator transitions in RNiO₃ thin films as seen by ultraviolet photoemission spectroscopy
E. F. Schwier
- P1.34** Investigation of the dimensional crossover of the electronic band structure in LaNiO₃ ultrathin film using in situ ARPES
Y. Hyang Keun
- P1.35** In-situ angle resolved photoemission spectroscopy of ultrathin LaNiO₃ films: Observation of orbital-lattice interaction
H. K. Yoo
- P1.36** Metal-insulator transition induced by irradiation in nanowires
G. Jia
- P1.37** Chiral OAM state in k-space measured by CD-ARPES
W. Jung
- P1.38** Synthesis and characterization of nanocrystalline ZrO₂ powders by sol-gel method
K. Park
- P1.39** Synthesis and characterization of nano-sized Eu-activated ZrO₂ phosphor powders by solution combustion method
K. Park
- P1.40** Anharmonicity due to electron-phonon coupling in magnetite
M. Hoesch
- P1.41** Interface states in LaAlO₃/SrTiO₃ heterostructures as probed by resonant inelastic x-ray scattering
F. Pfaff
- P1.42** Observation of strong spin-orbital entanglement in Sr₂RuO₄ by spin-resolved ARPES
F. Zhu
- P1.43** Na₂IrO₃ as a novel relativistic Mott insulator with a 340 meV gap
F. Zhu

POSTER SESSION 1 MONDAY, 18:50–21:00

P1.01

Ultrafast time-resolved ARPES with XUV photon source

C. Cacho (presenter) *STFC Rutherford Appleton Laboratory*, R. Chapman *STFC Rutherford Appleton Laboratory*, N. Rodrigues *STFC Rutherford Appleton Laboratory*, E. Turcu *STFC Rutherford Appleton Laboratory*, I. Gierz *Max Planck Institute for the Structure and Dynamics of Matter*, J. C. Petersen *University of Oxford*, H. Liu *Max Planck Institute for the Structure and Dynamics of Matter*, S. Kaiser *Max Planck Institute for the Structure and Dynamics of Matter*, A. Simoncig *Max Planck Institute for the Structure and Dynamics of Matter*, M. Mitrano *Max Planck Institute for the Structure and Dynamics of Matter*, A. Cavalleri *Max Planck Institute for the Structure and Dynamics of Matter*, A. Stöhr *Max Planck Institute for Solid State Research*, A. Köhler *Max Planck Institute for Solid State Research*, U. Starke *Max Planck Institute for Solid State Research*, S. Dhesi *Diamond Light Source*, A. Cavalleri *Max Planck Institute for the Structure and Dynamics of Matter*, C. Crepaldi *Elettra-Sincrotrone Trieste*, B. Ressel *Elettra-Sincrotrone Trieste*, F. Cilento *Elettra-Sincrotrone Trieste*, M. Zacchigna *Elettra-Sincrotrone Trieste*, F. Parmigiani *Elettra-Sincrotrone Trieste*, J. C. Johannsen *École Polytechnique Federale de Lausanne (EPFL)*, H. Berger *École Polytechnique Federale de Lausanne (EPFL)*, P. Bugnon *École Polytechnique Federale de Lausanne (EPFL)*, K. Kern *École Polytechnique Federale de Lausanne (EPFL)*, M. Griioni *École Polytechnique Federale de Lausanne (EPFL)*, S. Ulstrup *Aarhus University*, L. Hornekaer *Aarhus University*, F. Fromm *University of Erlangen-Nürnberg*, C. Raidel *University of Erlangen-Nürnberg*, T. Seyller *University of Erlangen-Nürnberg*, P. Hofmann *Aarhus University*, E. Springate *STFC Rutherford Appleton Laboratory*

Over decades photoemission has proven to be an extremely powerful tool to explore the electronic structure of complex materials, revealing the fundamental mechanisms behind their macroscopic properties. Complementary to high energy resolution ARPES studies [1], laser based ARPES experiments bring a wealth of innovative studies, in particular for photoinduced electronics and structural dynamics [2]. Artemis is a user facility combining an ultrafast laser system with an XUV beamline and a photoemission end-station for TR-ARPES with mid-IR pumping. High harmonic generation in gas gives access to photons in the energy region 16 eV to 80 eV with a time resolution of 30 fs [3]. The results from three types of systems (charge density wave material, topological insulator and graphene) studied at Artemis will be presented here.

Charge density waves (CDWs) underpin the electronic properties of many complex materials. In layered dichalcogenide 1T-TaS₂, the Mott gap opens as the CDW become commensurate to the lattice and yields to an insulating ground state. Performing time-resolved ARPES with XUV pulses gives access to the evolution of momentum dependent electronic structure throughout the reconstructed Brillouin zone [4]. Different features respond on distinct electronic and structural timescales, giving new information about both the static band structure and the process by which they melt after ultrafast excitation. In

the K_{0.3}MoO₃ compound, a one dimensional CDW material, the position of the bonding and anti-bonding bands oscillate with different frequencies [6]. Anharmonic dynamics processes are invoked to explain the activation of a phason mode.

Topological insulators are interesting candidates for the development of quantum computing and spintronics devices. Recent time-resolved studies on Bi₂Se₃ at low photon energy [6] explored the evolution of the effective electronic temperature (T*) and the chemical potential (μ) resulting from the photo-doping of the conduction band. Here we used the Artemis XUV source to enhance the surface sensitivity of the measurements and observed a long life hot metastable state (640 K) [7]. This state corresponds to an inhibition of the electron cooling process that is attributed to the extremely weak [8] electron-phonon scattering at the Bi₂Se₃ surface.

Finally graphene systems present promising properties for new high-speed electronics or optoelectronic devices and generate significant research efforts to understand the fundamental mechanisms. However, most of the photoemission characterisations are based on high resolution ARPES. Here we are reporting two time-resolved ARPES studies exploring the Dirac carrier dynamics. Depending on the excitation regime, a metallic or semiconductor transient state is observed close to the Fermi level. Direct interband transition leads to population inversion persisting over 130 fs [9]. Different time scales in the relaxation of the electronic temperature was observed at the Dirac point which is ascribed to optical phonon and electron-phonon-impurity scattering [10], so-called supercollisions.

[1] A. Damascelli et al., *Rev. Mod. Phys.* 76, 473 (2003).

[2] T. Rohwer et al., *Nature (London)* 471, 490 (2011).

[3] F. Frassetto et al., *Optics Express* 19, 19169 (2011).

[4] J. Petersen et al., *Phys. Rev. Lett.* 107, 177402 (2011).

[6] H.Y. Liu et al., arXiv:1206.6743 (2013).

[6] Y.H. Wang et al., *Phys. Rev. Lett.* 109, 127401 (2012).

A. Crepaldi et al., *Phys. Rev. B* 86, 206133 (2012).

[7] A. Crepaldi et al., (2013).

[8] Z.-H. Pan et al., *Phys. Rev. Lett.* 108, 187001 (2012).

[9] I. Gierz et al., (2013).

[10] J.C. Johannsen et al., (2013).

P1.02

Development of time- and angle-resolved photoemission spectroscopy based on NIR/MIR pump and UV/VUV/XUV probe

L. Haiyun (presenter) *University of Hamburg, CFEL*

Time- and angle-resolved photoemission spectroscopy (TR-ARPES) is a useful tool for directly detecting non-equilibrium electronic states and unveiling interaction between electronic structure and collective

modes. In TR-ARPES techniques, the commonly used pump and probe sources are near-infrared (800 nm) and UV (6 eV), which can only excite hot electrons and probe electronic structure limited around the center in 1st Brillouin zone (BZ). Here we report our newly developed TR-ARPES in Hamburg, which is equipped with NIR/MIR as pump and UV/VUV/XUV as probe. By applying intense pulses in THz/MIR regime, phase transitions can be vibrationally driven in strongly correlated electron systems, providing an interesting new way of research and control electronic states, for example, light-induced superconductivity. The higher photo-energies of the probe pulses are capable to fully investigate the 1st BZ, and even extend to the 2nd BZ. Further application and development of TR-ARPES are discussed.

P1.03 **The CITIUS light source**

B. Ressel (presenter) *University of Nova Gorica*, C. Grazioli *Elettra-Sincrotrone Trieste*, A. Ciavardini *Università di Roma "La Sapienza"*, D. Gauthier *Elettra-Sincrotrone Trieste*, R. Ivanov *Elettra-Sincrotrone Trieste*, C. Spezzani *Elettra-Sincrotrone Trieste*, L. Poletto *CNR-LUXOR*, P. Miotti *CNRLUXOR*, S. Gardonio *University of Nova Gorica*, M. Coreno *CNR - IMIP*, G. De Ninno *University of Nova Gorica*

A new facility for time-resolved photoemission investigations is currently under commissioning at the Elettra-Sincrotrone Trieste synchrotron light source.

The system has been realized in the framework of the "Citius Project" that has been founded by the "Italian-Slovenian Cross-border Cooperation Program 2007-2013". The facility will offer the possibility to investigate a wide variety of correlated electron materials. The experimental apparatus consists of a high power ultrafast laser system from Coherent Inc. (Legend Duo), that works at 5 kHz repetition rate and gives 3 mJ energy on 35 fs pulse duration. Ultra-short (30-50 fs) pulses are generated in the 15-70 eV spectral region, via high-harmonic generation in gas. The generated harmonics are monochromatized by a monochromator, which is equipped with three conical (time-preserving) gratings. When energy resolution is needed, a set of "classical" gratings is available. The flexibility of the monochromator makes the CITIUS beamline suitable for a very large class of pump-probe ultrafast experiments.

The laser system is equipped with an Optical Parametric Amplifier generating light in the spectral range (230-2600) nm. Both solid state and gas phase photoemission studies will be possible thanks to the availability of a flexible experimental chamber equipped with the ARToF (angle resolved time of flight) electron spectrometer, an R3000 hemispherical analyzer from VG-Scienta, a cryogenic manipulator and a surface/thin film preparation chamber. First experiments have been already performed on gas phase, cross correlating the fundamental laser frequency and the 15th harmonic generated in krypton. From the

sidebands of Kr 4p, we could estimate the time duration of EUV pulses to 40 fs.

P1.04 **A time-of-flight spectrometer for photoemission studies**

M. Teichmann (presenter) *FU Berlin*, T. Kunze *FU Berlin & SPECS GmbH*, J. Kopprasch *FU Berlin*, T. U. Kampen *SPECS GmbH*, M. Weinelt *FU Berlin*

We have developed the time-of-flight electron spectrometer THEMIS in a cooperation between FU Berlin and Specs GmbH. The spectrometer consists of an electrostatic lens system which allows for the measurement of the angular dispersion of photoemitted electrons up to an angle of 15° in both dimensions of the emission surface. Using a delayline detector, we can analyse the time and position of the arrival of electrons. By simulating the electron trajectories in the electrostatic potential, integrating the equations of motion in a self-written numerical integrator, we can deduce the emission angle and energy.

P1.05 **Upgrade of the Angle-resolved Photoemission End Station at NSRRC**

C. M. Cheng (presenter) *National Synchrotron Radiation Research Center*, C. C. Chiu *National Synchrotron Radiation Research Center*, J. Y. Yuh *National Synchrotron Radiation Research Center*, C. H. Chen *National Synchrotron Radiation Research Center*, D. J. Wang *National Synchrotron Radiation Research Center*, K. D. Tsuei *National Synchrotron Radiation Research Center*

The upgrade program of angle-resolved photoemission end station is for U9-CGM beamline in National Synchrotron Radiation Research center (NSRRC), for advanced materials research. It is motivated by critical needs in electronic structure determination relevant to two closely related research areas of prevailing interest: strongly correlated materials and naturally or artificially structured systems. An ultrahigh resolution and high-flux undulator beamline, with a cylindrical grating monochromator (CGM) and covering an energy range from 5 to 120 eV, delivers an average photon flux of 1×10^{11} photons/s with the entrance and exit slit opening at 10 μm at 360 mA storage ring current. The energy resolution was determined by measuring the absorption and photoionization spectra of gaseous samples. An energy resolving power of 110000 with a photon flux of 1×10^{10} photons/s was obtained at 16 eV and at 64 eV, with the entrance and exit slit openings at 3 and 5 μm , respectively. A analysis chamber equipped with a Scienta R4000 analyzer has only 0.42 mG residual magnetic field at measurement position, which improves the experimental condition at low photon energy. A new multi-axis cryogenic sample manipulators was developed for soft X-ray and VUV spectroscopy. It is ultrahigh vacuum

POSTER SESSION 1 MONDAY, 18:50–21:00

compatible and up to 6 axis motions. Three translational and polar angular motions are implemented by commercial stages. Azimuthal and tilting motions are driven by different gear trains and connected to stepping motors on the top flange. The angular range for azimuthal motion is about $\pm 180^\circ$. The angular range for tilting motion is from 75° to -25° . The lowest temperature of sample holder can reach 9.15 K by using liquid helium. Commissioning results will be presented to demonstrate high performance of this dedicated beamline.

P1.06 ARPES beamline at Diamond Light Source: current status

T. Kim (presenter) *Diamond Light Source*, M. Hoesch *Diamond Light Source*, P. Dudin *Diamond Light Source*, H. Wang *Diamond Light Source*, E. Longhi *Diamond Light Source*

The I05-ARPES beamline at Diamond Light Source is a facility for the analysis of the electronic structures of solids and their surfaces by high-resolution angle resolved photoemission (HR-APRES) and nano-ARPES spectro-microscopy.

5m APPLE-II quasi-periodic undulator with 140mm period delivers a high-flux soft X-rays with variable polarization (circular and linear) between 18 and 240 eV. Beamline optical scheme is based on a Plane Grating Monochromator operated in collimated light and provides high resolution ($E/\Delta E > 104$ for 20-80 eV) $< 100\mu\text{m}$ spot size on the sample. The HR-ARPES experimental station is equipped with He cryostat from Janis Research Company that should allow cooling of the samples to the temperatures below 10K.

VG Scienta 4000 electron energy analyzer provides energy resolution in order of few meV in combining with 30deg angular acceptance mode.

We report on construction, ultimate capabilities and currently achieved performance of the HR-APRES end-station at I05-ARPES beamline.

P1.07 Time-resolved Auger electron spectroscopy

R. Rausch (presenter) *University of Hamburg*, M. Potthoff *University of Hamburg*
Motivated by the recent time-resolved measurements of Auger spectra, we develop a theory of time-resolved Auger electron spectroscopy (AES) for many-body systems (Hubbard model). We use the Nakajima-Zwanzig projection formalism in Laplace space evaluated using exact states (for completely or almost completely filled bands). We discuss several setups and questions as a function of time: perturbative and non-perturbative treatment of the Auger term, screening, one-step vs. two-step process.

P1.08 Bulk electronic structure of quasicrystals studied by HAXPES

J. Nayak *UGC-DAE Consortium for Scientific Research*, M. Maniraj (presenter) *UGC-DAE Consortium for Scientific Research*, A. Rai *UGC-DAE Consortium for Scientific Research*, S. Singh *UGC-DAE Consortium for Scientific Research*, P. Rajput *European Synchrotron Radiation Facility*, J. Zegenhagen *European Synchrotron Radiation Facility*, D. L. Schlagel *Ames Laboratory U. S. DOE*, T. A. Lograsso *Ames Laboratory U. S. DOE*, A. Gloskovskii *Deutsches Elektronen-Synchrotron DESY*, K. Horn *Fritz-Haber-Institut der Max-Planck-Gesellschaft*, S. R. Barman *UGC-DAE Consortium for Scientific Research*

We use bulk sensitive hard x-ray photoelectron spectroscopy (HAXPES) to establish the existence of a pseudogap at the Fermi level (E_F) in a range of quasicrystalline solids, which explains the mechanism of formation of their intriguing aperiodic structure.[1] This observation resolves an apparent inconsistency of earlier surface sensitive valence band studies using low energy photoemission i.e. ultra-violet photoemission spectroscopy, [2] which showed a clear metallic Fermi edge, along with a small suppression of states at E_F that was identified as the signature of the pseudogap. The HAXPES valence band spectra for both icosahedral i-Al-Pd-Mn and i-Al-Cu-Fe unambiguously demonstrate the strong suppression of density of states at E_F compared to low energy photoemission. By using a detailed fitting scheme we find that, compared to i-Al-Pd-Mn, the pseudogap is fully formed in i-Al-Cu-Fe. This is in agreement with transport studies [3] that have shown that i-Al-Cu-Fe is close to a metal-insulator phase boundary. To illustrate that the suppression of the density of states is not an artifact related to the electron recoil effect, we have performed an Al 2s core level analysis, and find that there is no shift of the peak position due to recoil. Another interesting feature observed in the overall valence band of i-Al-Pd-Mn revealed by HAXPES is the shift of Pd 4d dominated peak by 0.3 eV towards higher binding energy compared to low energy photoemission. This shift is attributed to the higher bulk sensitivity of HAXPES, being related to the presence of excess Pd at the surface. A similar shift between HAXPES and low energy photoemission is also observed in the Cu 3d-dominated peak in the i-Al-Cu-Fe valence band spectrum.

[1] J. Nayak et al., *Phys. Rev. Lett.* 109, 216403 (2012).

[2] Z. M. Stadnik et al., *Phys. Rev. B* 55, 10938 (1997), G. Neuhold et al., *Phys. Rev. B* 58, 734(1998).

[3] T. Kelin et al., *Phys. Rev. Lett.* 66, 2907 (1991).

P1.09 Study of cooperative breathing-mode in molecular chains

S. Yarlagadda (presenter) *Saha Institute of Nuclear Physics*
Using a controlled analytic nonperturbative treatment that accounts for the quantum nature of the phonons, we derive a model that

generically describes the cooperative breathing-mode at strong electron-phonon interaction in one-band one-dimensional systems [1]. The effective model involves a next-nearest-neighbor hopping (that dominates over the nearest-neighbor hopping at strong coupling) and a nearest-neighbor repulsion that is significantly enhanced due to incompatibility of neighboring dilations/compressions. At non-half-filling, upon tuning the electron-phonon coupling, the system undergoes a period-doubling second-order quantum phase transition from a Luttinger liquid to a conducting commensurate charge-density-wave state: a phenomenon absent in both the Holstein model and the t-V model. Using fidelity to study the nature of the quantum phase transition, we find that the fidelity susceptibility shows a superextensive power law divergence as well as a remarkable scaling behavior; both together establish a second-order transition.

[1] R. Pankaj and S. Yalagadda *Phys. Rev. B* 86, 035453 (2012).

P1.10

Electronic instability in a zero-gap semiconductor: the charge-density wave in $(\text{TaSe}_4)_2\text{I}$

C. Tournier-Colletta (presenter) *EPFL*, L. Moreschini *ALS Berkeley*, G. Autès *EPFL*, A. Crepaldi *EPFL*, S. Moser *EPFL*, H. Berger *EPFL*, A. Walter *ALS Berkeley*, K. Kim *ALS Berkeley*, A. Bostwick *ALS Berkeley*, P. Monceau *Institut Néel*, E. Rotenberg *ALS Berkeley*, O. Yazyev *EPFL*, M. Grioni *EPFL*

We performed an extended survey of k-space by angle-resolved photoemission (ARPES) and first-principles electronic structure calculations of the paradigmatic quasi-one-dimensional compound $(\text{TaSe}_4)_2\text{I}$. We find it to be a zero-gap semiconductor in the non-distorted structure, and that finite interchain coupling is at the origin of the incommensurate modulation in the charge-density wave phase, below $T_{\text{CDW}} = 263$ K. The formation of small polarons, strongly suggested by the ARPES data, explains the puzzling semiconductor-to-semiconductor transition observed in transport at T_{CDW} .

P1.11

Time- and angle-resolved photoelectron spectroscopy at charge-density-wave insulators

K. Hanff (presenter) *University of Kiel*, S. Hellmann *University of Kiel*, T. Rohwer *University of Kiel*, M. Källäne *University of Kiel*, C. Sohrt *University of Kiel*, A. Stange *University of Kiel*, A. Carr *JILA, University of Colorado at Boulder and NIST*, M. Murnane *JILA, University of Colorado at Boulder and NIST*, H. Kapteyn *JILA, University of Colorado at Boulder and NIST*, L. Kipp *University of Kiel*, M. Bauer *University of Kiel*, K. Rossnagel *University of Kiel*

Ultra-short high-harmonic pulses enable us to study ultrafast dyna-

mics of condensed matter systems on femto- and picosecond time scales. In particular, they allow us to identify the nature and strength of interactions between various degrees of freedom in complex materials, in which typically two or more of the lattice, charge, spin and orbital degrees of freedom are strongly coupled. Our recent studies focused on the investigation of electronically driven charge-density waves, specifically pristine and rubidium intercalated 1T-TaS_2 . Here we show, that time- and angle-resolved photoelectron spectroscopy can directly measure the melting times of electronic order parameter and thus identify the dominant interaction. We are able to distinguish different time scales during the excitation and relaxation processes, which indicate the influence of electronic and lattice systems.

P1.12

Electronic band structure of BaCo_2As_2 : a fully doped ferropnictide analog with reduced electronic correlations

N. Xu (presenter) *Paul Scherrer Institut*, P. Richard *Chinese Academy of Sciences*, A. Roekeghem *Chinese Academy of Sciences*, P. Zhang *Chinese Academy of Sciences*, H. Miao *Chinese Academy of Sciences*, W. Zhang *Chinese Academy of Science*, T. Qian *Chinese Academy of Science*, M. Ferrero *Ecole Polytechnique*, A. S. Sefat *Oak Ridge National Laboratory*, S. Biermann *Ecole Polytechnique*, H. Ding *Chinese Academy of Sciences*

We report an investigation with angle-resolved photoemission spectroscopy of the Fermi surface and electronic band structure of BaCo_2As_2 . Although its quasi-nesting-free Fermi surface differs drastically from that of its Fe-pnictide cousins, we show that the BaCo_2As_2 system can be used as an approximation to the bare unoccupied band structure of the related $\text{BaFe}_{2-x}\text{Co}_x\text{As}_2$ and $\text{Ba}_{1-x}\text{K}_x\text{Fe}_2\text{As}_2$ compounds. However, our experimental results, in agreement with dynamical-mean-field-theory calculations, indicate that electronic correlations are much less important in BaCo_2As_2 than in the ferropnictides. Our findings suggest that this effect is due to the increased filling of the electronic 3d shell in the presence of significant Hund's exchange coupling.

P1.13

Ultrafast magnetization enhancement in BaFe_2As_2 by coherent phonon excitation

T. Rohwer (presenter) *Christian-Albrechts Universität zu Kiel*, L. Rettig *Universität Duisburg-Essen*, S. Hellmann *Christian-Albrechts Universität zu Kiel*, R. Cortés *Brookhaven National Laboratory*, L. Kipp *Christian-Albrechts Universität zu Kiel*, B. Kamble *Ruhr-Universität Bochum*, J. Fink *Leibniz-Institut für Festkörper- und Werkstofforschung Dresden*, K. Rossnagel *Christian-Albrechts Universität zu Kiel*, T. Wolf *Karlsruher Institut für Technologie*, I. Eremin *Ruhr-Universität Bochum*, M. Bauer *Christian-Albrechts Universität zu Kiel*, U. Bovensiepen *Universität Duisburg-Essen*

POSTER SESSION 1 MONDAY, 18:50–21:00

The interaction between electrons, lattice and magnetism is fundamental for the understanding of high temperature superconductivity in iron-pnictides.

By ultrafast time- and angle-resolved-photo-emission-spectroscopy we monitor coherent in-phase oscillations at the regions of electron and hole pockets, superimposed by a distinct momentum dependence. The observed cosine type oscillations point to new equilibrium in a transiently excited state. A tight-binding model within the Slater-Koster framework reveals the direct influence of the photoinduced A_{1g} phonon mode on the transient electronic band structure and allows the determination of the As displacement via the instantaneous Fe-As-Fe bond angle. The expansion of this model by a mean field approximation of the spin-density-wave interaction results in an enhanced average of the iron magnetic moment due to the magneto-phonon coupling.

P1.14

Anisotropy of the superconducting gap in $Ba(Fe_{1-x}Co_x)_2As_2$ revealed by angle-resolved photoemission spectroscopy

S. Ideta (presenter) *Tokyo University*, T. Yoshida *Tokyo University*, A. Fujimori *Tokyo University*, M. Hashimoto *Stanford University*, D. Lu *Stanford University*, Z. Shen *Stanford University*, M. Nakajima *Agency of Industrial Science and Technology (AIST)*, K. Kihou *Agency of Industrial Science and Technology (AIST)*, Y. Tomioka *Agency of Industrial Science and Technology (AIST)*, C. Lee *Agency of Industrial Science and Technology (AIST)*, I. Akihiro *Agency of Industrial Science and Technology (AIST)*, H. Eisaki *Agency of Industrial Science and Technology (AIST)*, S. Uchida *Tokyo University*

The existence and the direction of nodes in the superconducting order parameter give information on the momentum dependence of the pairing interaction, and an important insight into the mechanism of the superconductivity. In spite of a lot of intensive efforts on experimental and theoretical studies, a detailed knowledge of the gap structure for the iron-based superconductors (Fe-SCs) is still controversial and there are several conflicting reports: line nodes, deep gap minima, or fully isotropic gaps on the Fermi-surface (FS) sheets. Angle-resolved photoemission spectroscopy (ARPES) results of the electron-doped $BaFe_2As_2$ show nearly isotropic gaps on the hole and electron FSs [1]; however, some studies have reported signatures of the gap nodes or gap minima in the electron-doped $BaFe_2As_2$ [2-5]

In order to clarify the gap anisotropy in the electron-doped $Ba(Fe_{1-x}Co_x)_2As_2$ (Co-Ba122), the superconducting (SC) gap in Co-Ba122 has been studied by angle-resolved photoemission spectroscopy in two- and three-dimensional momentum spaces. The SC gap on the hole and electron Fermi surfaces (FSs) has been measured by several photon energies and a node or a gap minimum has been observed on

the outer hole FS near the Z point. The observation of a gap minimum and/or a node on the FSs suggests that spin fluctuations play a key role to form Cooper pairs in the overdoped Co-Ba122.

- [1] K. Terashima et al., Proc. Natl. Acad. Sci. USA 106, 7330 (2009).
- [2] J.-Ph. Reid et al., Phys. Rev. B 82, 064501 (2010).
- [3] B. Muschler et al., Phys. Rev. B 80, 180510(R) (2009).
- [4] K. Gofryk et al., Phys. Rev. B 83, 064513 (2011).
- [5] I. I. Mazin et al., Phys. Rev. B 82, 180502(R) (2010).

P1.15

The ARPES study on $AFe_{1-x}Co_xAs$ (A=Li, Na)

Z. Ye (presenter) *Fudan University*, Q. Ge *Fudan University*, Y. Zhang *Stanford University*, M. Xu *Fudan University*, J. Jiang *Fudan University*, Q. Fan *Fudan University*

With unpolar cleaved surface, and simple orbital characters of electronic structures, the 111 compounds of iron-based superconductors (represented by $AFe_{1-x}Co_xAs$ (A=Li, Na)) are ideal systems for precise angle resolved photoemission spectroscopy (ARPES) measurements. We have performed systematic ARPES studies on 111 compounds through the entire phase diagram. In this talk, I will focus on two aspects: the coexistence of spin density wave (SDW) with superconductivity, and the orbital selective correlations between nesting/scattering/Fermi surface topology and superconductivity in iron-based superconductors.

Most unconventional superconductors appear in the vicinity of a certain magnetically ordered phase. For iron-based superconductors, an SDW phase appears next to the superconducting (SC) phase, and in some cases, they even coexist, which gives a unique ground state. We revealed the distinctive electronic structure of $NaFe_{1-x}Co_xAs$ ($x = 0.0175$) in the coexisting regime. The SDW signature and the superconducting gap are observed on the same bands, illustrating the intrinsic nature of the coexistence. However, because the SDW and superconductivity are manifested in different parts of the band structure, their competition is non-exclusive. Particularly, we found that the gap distribution is anisotropic and nodeless, in contrast to the isotropic superconducting gap observed in an SDW-free $NaFe_{1-x}Co_xAs$ ($x=0.045$), which puts strong constraints on theory.

The orbital degree of freedom is responsible for many emergent properties in correlated materials. In the iron-based high temperature superconductors, the orbital degree of freedom also plays an important role. We have studied the evolution of electronic structure in $AFe_{1-x}Co_xAs$ (A=Li, Na) from optimal doping to the deeply overdoped regime, where the superconductivity is completely suppressed. We found that the superconductivity is enhanced by the Fermi surface nesting, but only when it is between d_{xz}/d_{yz} Fermi surfaces, while for the d_{xz} orbital, even nearly perfect Fermi surface nesting could not induce superconductivity. Moreover, the superconductivity is

completely suppressed just when the d_{xz}/d_{yz} hole pockets sink below Fermi energy and evolve into an electron pocket. Our results thus substantiate the critical role of the d_{xz}/d_{yz} orbitals in iron-based superconductors. Furthermore, around the zone center, we found that the d_{xz}/d_{yz} -based bands are much less sensitive to impurity scattering than the d_{xy} -based band, which explains the robust superconductivity against heavy doping in iron-based superconductors.

P1.16 Unusual band renormalization in the simplest iron based superconductor

J. Maletz (presenter) *IFW Dresden*

The electronic structure of the iron chalcogenide superconductor FeSe_{1-x} was investigated by high-resolution angle-resolved photoemission spectroscopy (ARPES). The results were compared to DFT calculations showing some significant differences between the experimental electronic structure of FeSe_{1-x} , DFT calculations and existing data on $\text{FeSe}_x\text{Te}_{1-x}$. The bands undergo a pronounced orbital dependent renormalization, different from what was observed for $\text{FeSe}_x\text{Te}_{1-x}$ and any other pnictides.

P1.17 Electronic structure of $\text{Fe}_{1.03}\text{Te}_{0.94}\text{S}_{0.06}$ superconductor

P. Starowicz (presenter) *Jagiellonian University*, H. Schwab *University of Würzburg*, J. Goraus *University of Silesia*, P. Zajdel *University of Silesia*, F. Forster *University of Würzburg*, J. Rak *Jagiellonian University*, M. Green *NIST Center for Neutron Research*, I. Vobornik *CNR-IOM, TASC Laboratory, Sincrotrone Trieste*, F. Reinert *University of Würzburg*

Band structure of superconducting $\text{Fe}_{1.03}\text{Te}_{0.94}\text{S}_{0.06}$ is studied by means of angle-resolved photoemission spectroscopy (ARPES) and ab-initio calculations. The photoemission experiment was carried out at the APE beamline of the Elettra synchrotron. Experimental data reveal spectral intensity in the regions of the Γ and M points, while no bands are found at X. In the region of the Γ point two hole pockets are observed together with a flat band located at 3-5 meV above the chemical potential (μ) with no evidence of dispersion. This heavy quasiparticle band has a dominating d_{z^2} orbital character and is located near μ in about 3% of the Brillouin zone volume. This should be understood as an evidence of Van Hove singularity. Photon energy dependent studies indicate that the outer hole pocket is two dimensional and the flat band loses intensity for the photon energy equal 30 eV or lower probably due to unfavorable photoionization cross section. Photoemission spectra collected with different geometries and polarizations allowed for the determination of orbital band characters.

Korringa-Kohn-Rostoker with coherent potential approximation (KKR-CPA) calculations were able to simulate the band structure with the input assuming fractional occupancies of Fe(2) and Te/S lattice sites. The resulting spectral functions are broadened due to disorder. When theoretical dispersions are compared to the experiment near the Γ point, no considerable band mass renormalization is observed. The calculations with the method of linearized augmented plane wave with local orbitals (LAPW+LO) were performed for stoichiometric FeTe. The resulting band structure with orbital characters is in reasonable agreement with the experimental data for two hole pockets at Γ but do not reveal the flat band with d_{z^2} character.

P1.18 Intermediate coupling model of cuprates: a progress report

R. Markiewicz (presenter) *Northeastern University*, T. Das *Los Alamos National Laboratory*, A. Bansil *Northeastern University*

In a GW model, the electronic dispersion is dressed by bosonic fluctuations (via the GW self energy), so that both electronic and bosonic features of the electronic system are treated self-consistently. This has allowed us to model the electronic features of cuprates – the dispersion renormalization, high and low energy kink features, and separation into coherent and incoherent features – as well as their bosonic features – competing spin and charge density wave and pairing fluctuations. We can now begin with the LDA bands, self-consistently dress them with GW fluctuations, and successfully describe a wide variety of spectroscopies over a wide range of doping and energy. Results will be presented for photoemission, tunneling, optical, x-ray, and neutron scattering spectroscopies, and we will show phase diagrams of competing orders and pseudogaps.

P1.19 Interplay between static disorder and dynamic phonon displacement in a weak correlated parent of cuprates.

D. Di Sante (presenter) *University of L'Aquila*, Y. Nie *Cornell University*, S. Ciuchi *University of L'Aquila*, K. Shen *Cornell University*

We study the ARPES spectra of La doped Sr_2TiO_4 , the quasi-two-dimensional $n=1$ end member of the Ruddlesden-Popper series ($\text{SrO}(\text{SrTiO}_3)_n$, where $n=\infty$ represents the well known three-dimensional perovskite SrTiO_3). The ARPES data show a single band near the Fermi level as well as a clear shoulder in the integrated spectral weight at a binding energy of 70 meV. Using a combination of Density Function Theory and model calculation for the electron self-energy that we name NCA-CPA (Non Crossing Approximation Coherent Potential Approximation) we demonstrate that all these features can be exp-

POSTER SESSION 1 MONDAY, 18:50–21:00

lained in terms of an interplay between disorder and electron-phonon interactions. In particular, the dispersion of the states below the Fermi level critically depends on the entanglement between disorder and zero-point quantum fluctuations of the phonons.

P1.20 d-wave superconductors with finite range impurities of arbitrary strength

K. Scharnberg (presenter) *University of Hamburg*, C. Rieck *University of Hamburg*

Disorder is ubiquitous in solid state physics, sometimes introduced in a controlled fashion, but often invoked to explain observations that one does not otherwise understand. The frequently used zero range potentials of arbitrary strength do not lead to scattering in two or more dimensions! Only when one ignores the divergent real part of the Green function does one find not unreasonable results for δ -function potentials. When the momentum dependence of the scattering potential is taken into account, no uncontrolled approximations are required. This generalization is of particular interest in the context of unconventional superconductors (e.g. HTCS), where the pairbreaking effect of potential scattering is expected to be mitigated when higher angular momentum scattering channels are taken into account. The predictions are, however, complicated by the fact that with increasing potential range the scattering initially increases because more scattering channels contribute. We find a whole set of reasonable parameters (potential range, potential strength) for which midgap states exists. These states are important in explaining transport properties, but one needs to check whether the parameters required are consistent with the observed T_c . The self-energies in the superconducting state have interesting frequency dependencies when the frequencies are (much) lower than the order parameter amplitude. These are reflected in the spectral functions, which are observed in ARPES. However, it is questionable whether at the presently available experimental resolution the observed linewidths can actually be attributed to static disorder. The mathematical treatment of disorder involves two steps. In the first step scattering off a single impurity is considered. This involves approximations because in a d-wave superconductor we can only take into account a rather small number of scattering channels. Furthermore, the effect of the impurity on the order parameter is neglected. The second step involves taking an average over an ensemble of impurities. This introduces the impurity concentration is another important parameter which to some extent obscures the properties of a single impurity. Some comparison will be made between different approaches to the averaging process.

P1.21

The cooper pairs close to Fermi surface like a source for the waterfall effect in ARPES

S. Millan (presenter) *UNACAR*, I. Ortiz *UNACAR*, L. Perez *IFUNAM*, C. Wang *IIM-UNAM*

The generalized Hubbard model that describing the d-wave superconducting symmetry on a square lattice within the BCS formalism [1] consider the mean field dispersion relation that contains the mean-field self-energy, the first and second neighbor mean-field hopping, and the electronic density (n) that determines the chemical potential (μ) for the superconductor state. The Fermi Surface (FS) can be calculated solving the equation $\epsilon(k) - E_F = 0$ where E_F is the Fermi energy, and for some cases $\mu = E_F$. The equation for FS can be expressed as an equation of second grade for K_y , given K_x , and the most usual solutions are ellipses and hyperbolas but the specific shapes of FS depend of Hamiltonian's parameter. The Integrand function for the superconducting gap equation shows how the states of pairs along the Fermi Surface play the most important role in the solution of the superconductor state [2], hence the system of coupled equations inherent to formalism BCS and that describes the state superconductor gives some understanding about how this state is reached. In this work has been proposed that the Waterfall effect in High T_c superconductors obtained by the ARPES technique can be explained by the distribution of Cooper pairs inside to a thin shell close to the FS, and they are concentrated in points of high crystalline symmetry. A good comparison between theory and experiment suggest that the LSCO system has a hyperbola as FS and the mean-field hopping to first and second nearest neighbor can be obtained by ARPES experimental data. Moreover, the comparison between theory and experiments for the electronic specific heat in LSCO and others systems fits very well.

[1] J.S. Millán, L.A. Pérez and C. Wang, *Physica C* 471, 735 (2011).
[2] Luis A. Pérez et al., *J. Phys. and Chem. of Solids* 69, 3369 (2008).

P1.22 The signatures of superconducting correlations above the transition temperature

T. Domanski (presenter) *M. Curie-Skłodowska University*

The angle resolved photoemission measurements on Y-Ba-Cu-O [1] and Sr-La-Cu-O [2] high T_c compounds have provided unambiguous evidence for the Bogoliubov type quasiparticle features surviving well above the superconducting state. Similar effects have been recently observed also in the ultracold fermion atom systems near the unitary limit [3].

These experimental facts indicate that short-range correlations between the preformed pairs (of whatever origin) can be gradually established upon approaching the transition temperature from above. We argue that the signatures of correlations between the preformed

pairs go hand in hand with other characteristic features of the superconducting state manifested in the spin (corresponding to magnetic degrees of freedom) and optical (probing two-body correlations in the charge sector) spectroscopies. For instance, evidence for the residual Meissner rigidity has been reported in the state-of-art measurements of magnetic response [4, 5]. Within the general framework [6-8] we shall discuss how these phenomena can be assigned to an interplay between the paired and unpaired electrons mutually interconverted by the Andreev type of scattering.

- [1] A. Kanigel et al., Phys. Rev. Lett. 101, 137002 (2008).
 [2] M. Shi et al., Eur. Phys. Lett. 88, 27008 (2009).
 [3] J.P. Gaebler et al., Nat. Phys. 6, 569 (2010).
 [4] L. Li et al., Phys. Rev. B 81, 054510 (2010).
 [5] G. Drachuck et al., Phys. Rev. B 85, 184518 (2012).
 [6] E. Altman and A. Auerbach, Phys. Rev. B 65, 104508 (2002); Y. Yildirim and W. Ku, Phys. Rev. X 1, 011011 (2011); T.M. Rice, K.-Y. Yang and F.-C. Zhang, Rep. Prog. Phys. 75, 016502 (2012).
 [7] T. Domanski and J. Ranninger, Phys. Rev. Lett. 91, 255301 (2003); T. Domanski, Phys. Rev. A 84, 023634 (2011); M. Zapalska and T. Domanski, Phys. Rev. B 84, 174520 (2011).
 [8] K.-Y. Yang et al., Phys. Rev. B 83, 214516 (2011).

P1.23

The gap function from lightly to optimally doped $\text{La}_{2-x}\text{Sr}_x\text{CuO}_4$ cuprate, probed by ARPES

M. Shi (presenter) *Paul Scherrer Institute*, E. Razzoli *Paul Scherrer Institute*, G. Drachuck *Department of Physics, Technion*, A. Keren *Department of Physics, Technion*, M. Radovic *Paul Scherrer Institute*, N. Plumb *Paul Scherrer Institute*, J. Chang *EPF Lausanne*, Y. B. Huang *Paul Scherrer Institute*, H. Ding *Chinese Academy of Sciences*, J. Mesot *Paul Scherrer Institute*

How does high-temperature superconductivity emerge on adding mobile charged carriers to an antiferromagnetic Mott insulator is a central issue for understanding the unconventional superconductivity in cuprates. In underdoped cuprate superconductors, because superconductivity is found in close proximity to magnetic and charge order, the symmetry of the gap function is of critical theoretical importance. Using angle-resolved photoemission spectroscopy (ARPES) to probe the electronic excitations of the lightly to optimally doped $\text{La}_{2-x}\text{Sr}_x\text{CuO}_4$ (LSCO), we revealed [1]: 1) the gap function of highly underdoped LSCO ($x \leq 0.08$) strongly deviates from the pure $d_{x^2-y^2}$ -form at low temperatures in both superconducting and non-superconducting phases—i.e., no node occurs on the zone diagonal and the entire underlying Fermi surface is gaped; 2) upon increasing temperature, the gap function in lightly doped LSCO ($x \leq 0.08$), evolves from a nodeless gap to $d_{x^2-y^2}$ -wave, followed by the appearance of a Fermi arc near the zone diagonal

whose length distends upon further increasing temperature; 3) in the superconducting phase of LSCO there exists a critical doping ($x \sim 0.1$) above which the momentum-dependence of the superconducting gap has a pure $d_{x^2-y^2}$ -form [2], and 4) upon entering the superconducting phase from normal state the quasiparticle peaks near k_F along the zone diagonal sharpen, reflecting that the lifetime of quasiparticles becomes considerably longer, and furthermore the quasiparticle peak width in the superconducting phase is similar in the doping range from highly underdoped to optimally doped samples. Our observations in highly underdoped LSCO could be explained by invoking either a strong fluctuating order competing with the superconducting instability, or a mixed $d_{x^2-y^2} + id_{xy}$ gap function occurring when the doping is below a quantum critical point.

- [1] E. Razzoli et al., Phys. Rev. Lett. 110, 047004 (2013).
 [2] M. Shi et al., Phys. Rev. Lett. 101, 047002 (2008).

P1.24

Spin-charge coupling in antiferromagnetic LSCO studied by the muons, neutrons, and ARPES techniques

G. Drachuck (presenter) *Technion - Israel Institute of Technology*, E. Razzoli *Paul Scherrer Institute*, G. Bazalitsky *Technion - Israel Institute of Technology*, A. Kanigel *Technion - Israel Institute of Technology*, N. Christof *Paul Scherrer Institute*, S. Ming *Paul Scherrer Institute*, A. Keren *Technion - Israel Institute of Technology*

Exploring whether a spin density wave (SDW) is responsible for the gap in high-temperature superconducting cuprates is difficult, since the region of the phase diagram where the magnetic properties are clearly exposed is different from the region where the band dispersion in the electronic excitation spectra is visible. On the one hand, long range magnetic order disappears as doping approaches 2% from below, hindering our ability to perform elastic neutron scattering (ENS). On the other hand, cuprates become insulating at low temperature as doping approaches 2% from above, thus restricting angle-resolved photoemission spectroscopy (ARPES). In fact, ARPES data for samples with doping lower than 3% are rare and missing the quasiparticle peaks in the energy distribution curves (EDCs). By preparing a series of LSCO single crystals with 0.2%-0.3% doping steps around 2%, we managed to find one to which both techniques apply. This allows us to explore the cross talk between the magnetic and electronic properties of the material. We found a diagonal (nodal) gap of 20 meV, which develops when the magnetic moment is nearly full, and does not change the position of k_F .

POSTER SESSION 1 MONDAY, 18:50–21:00

P1.25

Asymmetric doping dependence of L-edge RIXS spectrum in hole- and electron-doped cuprates

T. Tohyama (presenter) *Kyoto University*

Resonant inelastic x-ray scattering (RIXS) tuned for the L edge of a transition metal is a powerful tool to study not only charge excitations but also spin excitations in various 3d transition metal compounds.

We theoretically investigate L_3 -edge RIXS spectra for a strongly correlated single-band system, i.e., cuprates with CuO_2 plane. Based on the exact diagonalization study of the t - t' - t'' - J model and the first-collision approximation for RIXS, both spin and charge dynamics is included in RIXS spectra on the same footing. The doping-dependence of peak position qualitatively agrees with experiments but quantitatively not in hole-doped cuprates, suggesting the importance of additional effects not included in the model, that is, the three-site correlated hopping term. Including the term, we find a contrasting behavior between hole- and electron-doped cuprates in RIXS spectrum. In hole-doping, the energy of the peak position decreases with doping, while it slightly increases in electron-doping. Furthermore, we predict a possibility of observing low-energy charge dynamics coupled to local spin fluctuation in electron-doped cuprates.

P1.26

Direct observation of screening enhanced hole pairing in Spin= $\frac{1}{2}$ copper-oxide materials unravelled by high-resolution resonant inelastic X-ray scattering at FLASH

M. Rübhausen (presenter) *CFEL*, A. Ruydi *NUS*, A. Goos *CFEL*, S. Binder *CFEL*, A. Eich *UHH*, K. Botrill *UHH*, P. Abbamonte *UIUC*, D. Qui *NUS*, M. Breese *NUS*, H. Eisaki *AIST*, Y. Fujimaki *University of Tokio*, S. Uchida *University of Tokio*, M.V. Klein *UIUC*, N. Guerassimova *DESY*, R. Treusch *DESY*, J. Feldhaus *DESY*, R. Reninger *APS*

Screening of correlation energies is of great importance for electronic properties of condensed-matter many-body systems. The ratio between kinetic and potential correlation energies drives competing ground states that lead to the pairing of holes. This hole pairing can trigger either the superconducting condensate or the insulating charge density wave. However, the mechanisms behind these phenomena remain very elusive. Here, we reveal that the screening of correlation energies is key to the paired-hole state. High-resolution resonant inelastic X-ray scattering (RIXS) at the transition metal M-edges using the ultra-brilliant light source FLASH allows to probe these screening effects as well as the relevant kinetic energies by measuring the magnetic spin-excitation spectra of the hole-doped and undoped spin-ladder compounds (SLCs) $\text{Sr}_{14}\text{Cu}_{24}\text{O}_{41}$ and $\text{La}_6\text{Ca}_8\text{Cu}_{24}\text{O}_{41}$, respectively. Hole doping screens locally the correlation energy reducing it

as much as 25% compared to the undoped material. This decreases the ratio between potential and kinetic energy and triggers the local superexchange-mediated pairing of holes. Furthermore, our results demonstrate a novel method to unravel key parameters that control the pairing of charges in correlated electron systems by using RIXS at transition metal M-edges.

P1.27

Conventional superconductivity in SrPd_2Ge_2 from combined ARPES, STS and LDA studies

T. Kim (presenter) *Diamond Light Source*

Electronic structure of SrPd_2Ge_2 single crystals is studied by angle-resolved photoemission spectroscopy (ARPES), scanning tunneling spectroscopy (STS) and band-structure calculations within the local-density approximation (LDA). The STS measurements show single s-wave superconducting energy gap $\Delta(0) = 0.5$ meV. Photon-energy dependence of the observed Fermi surface reveals a strongly three-dimensional character of the corresponding electronic bands. By comparing the experimentally measured and calculated Fermi velocities a renormalization factor of 0.95 is obtained, which is much smaller than typical values reported in Fe-based superconductors. We ascribe such an unusually low band renormalization to the different orbital character of the conduction electrons and using ARPES and STS data argue that SrPd_2Ge_2 is likely to be a conventional superconductor, which makes it clearly distinct from isostructural iron pnictide superconductors of the “122” family.

P1.28

True bosonic coupling strength evaluated by ARPES in strongly correlated electron systems

H. Iwasawa (presenter) *Hiroshima University*, K. Shimada *Hiroshima University*, H. Namatame *Hiroshima University*, M. Taniguchi *Hiroshima University*, Y. Aiura *National Institute of Advanced Industrial Science and Technology*, Y. Yoshida *National Institute of Advanced Industrial Science and Technology*, I. Hase *National Institute of Advanced Industrial Science and Technology*

Information on the electron coupling effects helps in understanding the physical properties especially in the strongly correlated electron systems [1]. Such coupling effects are contained in the electron self-energy, which is experimentally accessible via angle-resolved photoemission spectroscopy (ARPES) [2]. However, the derivation of the self-energy highly depends on a so-called “bare band”. So far, the self-energy has been most often determined by assuming a phenomenological bare band such as a linear dispersion. This procedure enabled us to estimate the “effective” coupling strength but not “true” one. In this talk, we will demonstrate that such common procedure underestimates the bosonic coupling strength depending on the electron correlation effects. As an example,

we will discuss the true bosonic coupling strength in the unconventional ruthenate superconductor based on high-resolution ARPES results.

[1] H. Iwasawa et al., Phys. Rev. Lett. 105, 226406 (2010).

[2] H. Iwasawa et al., Phys. Rev. Lett. 109, 066404 (2012).

P1.29

Defect states and excitations in a Mott insulator with orbital degrees of freedom: Mott-Hubbard gap versus optical and transport

A. Avella (presenter) *Università degli Studi di Salerno*, P. Horsch *Max-Planck-Institut für Festkörperforschung*, A. M. Oleś *Jagellonian University*

We address the role played by charged defects in doped Mott insulators with active orbital degrees of freedom.

It is observed that defects feature a rather complex and rich physics, which is well captured by a degenerate Hubbard model extended by terms that describe crystal-field splittings and orbital-lattice coupling, as well as by terms generated by defects such as the Coulomb potential terms that act both on doped holes and on electrons within occupied orbitals at undoped sites. We show that the multiplet structure of the excited states generated in such systems by strong electron interactions is well described within the unrestricted Hartree-Fock approximation, once the symmetry breaking caused by the onset of magnetic and orbital order is taken into account.

Furthermore, we uncover new spectral features that arise within the Mott-Hubbard gap and in the multiplet spectrum at high energies due to the presence of defect states and strong correlations. These features reflect the action on electrons/holes of the generalized defect potential that affects charge and orbital degrees of freedom, and indirectly also spin ones. The present study elucidates the mechanism behind the Coulomb gap appearing in the band of defect states and investigates the dependence on the electron-electron interactions and the screening by the orbital polarization field.

As an illustrative example of our general approach, we present explicit calculations for the model describing three t_{2g} orbital flavors in the perovskite vanadates doped by divalent Sr or Ca ions, such as in $\text{La}_{1-x}\text{Sr}_x\text{VO}_3$ and $\text{Y}_{1-x}\text{Ca}_x\text{VO}_3$ systems. We analyze the orbital densities at vanadium ions in the vicinity of defects, and the excited defect states which determine the optical and transport gaps in doped systems [1].

[1] A. Avella et al., Phys. Rev. B 87, 045132 (2013).

P1.30

Correlation and spin-orbit effects in $\text{Sr}_3\text{Ru}_2\text{O}_7$: a LDA+DMFT study

E. Gorelov (presenter) *Forschungszentrum Jülich, IAS-3*, G. Zhang *Forschungszentrum Jülich, IAS-3*, E. Pavarini *Forschungszentrum Jülich, IAS-3*

The layered ruthenates of the Ruddlesden-Popper family $\text{Sr}_{n+1}\text{Ru}_n\text{O}_{3n+1}$ are

peculiar among strongly correlated transition-metal oxides. They exhibit a very rich phase diagram stemming from interplay between Coulomb interaction, kinetic energy, dimensionality, spin orbit and crystal field. In the present work we focus on the bilayered system $\text{Sr}_3\text{Ru}_2\text{O}_7$, which exhibits metamagnetic behavior and strong electron mass renormalizations. By means of LDA+DMFT (local-density approximation + dynamical mean-field theory) approach we study [1] magnetic properties, Fermi surface changes and electron mass renormalizations. In our LDA+DMFT scheme we use maximally-localized Wannier orbitals obtained from Linearized Augmented Plane Wave (LAPW) calculations to build a low-energy Hubbard model for the Ru d bands; we use the weak-coupling CT-quantum Monte Carlo method to solve the quantum impurity problem. We take into account the full rotationally-invariant Coulomb interaction, as well as full on-site self-energy matrix in spin-orbital space and include explicitly spin-orbit coupling.

[1] E. Gorelov, G. Zhang, and E. Pavarini, (in preparation).

P1.31

Interplay of electronic correlations and spin-orbit coupling in layered ruthenates

F. Lechermann (presenter) *University of Hamburg*, M. Behrmann *University of Hamburg*, C. Piefke *University of Hamburg*

The combination of the local-density approximation to density functional theory with explicit many-body approaches has proven to be a powerful tool to investigate the problem of strong electronic correlations on a realistic level. Notably in quasi-two-dimensional materials the interaction between the effective dimensionality and the symmetry of the underlying crystal structure with the competition between the localized and the itinerant character of electrons is indeed giving rise to highly interesting physical phenomena, especially within the family of transition-metal oxides. Here we want to focus on the intriguing interplay between rotational-invariant local Coulomb interactions and spin-orbit coupling for the case of the layered strontium ruthenates within the $\text{Sr}_{n+1}\text{Ru}_n\text{O}_{3n+1}$ Ruddlesden-Popper series. Novel results based on a generic realistic modelling of the correlated electronic structure for the $n=1,2$ members of this family of compounds will be discussed [1]. In this respect, also the intriguing metamagnetic behavior of $\text{Sr}_3\text{Ru}_2\text{O}_7$ will be addressed.

[1] M. Behrmann, C. Piefke and F. Lechermann, Phys. Rev. B 86, 045130 (2012).

P1.32

Dynamical investigation of the semiconductor-to-metal transition in LaCoO_3

M. Izquierdo *University of Hamburg*, M. Karolak *University of Hamburg*, N. Pontius *Helmholtz Zentrum Berlin*, C. Trabant *Helmholtz Zentrum Berlin*, C. Schüssler-Lan-

POSTER SESSION 1 MONDAY, 18:50–21:00

geheine *Helmholtz Zentrum Berlin*, K. Holldack *Helmholtz Zentrum Berlin*, A. Föhlisch *Helmholtz Zentrum Berlin*, K. Kummer *ESRF*, D. Prabhakaran *Clarendon Laboratory, University of Oxford*, A. T. Boothroyd *University of Oxford*, V. Efimov *Joint Institute for Nuclear Research*, M. Spiwek *DESY*, A. Belozero *Russian Academy of Sciences*, A. Poteryaev *Russian Academy of Sciences*, A. Lichtenstein *University of Hamburg*, S. Molodtsov *European XFEL*

Understanding the origin of the spin transition in LaCoO_3 is one of the longstanding aims in condensed matter physics. Besides its fundamental interest, a detailed description of this crossover will have a direct impact on the interpretation of the semiconductor-to-metal transition (SMT) and the properties of the high temperature metallic phase in this compound, which has shown to have important applications in environmental friendly energy production domains. So far, solely static experiments as a function of the temperature have been performed, although hints of dynamical effects have been preconized. In this contribution we report the results of our investigations of the SMT by means of pump-probe soft x-ray reflectivity experiments at the O K-, Co L- and La M-edges. The results have shown a dynamical excited state with participation of all the atoms in the system and relevant deviations with respect to temperature dependent data suggesting a scenario of charge and spin separation upon laser excitation. The role of extrinsic effects contributing to the high temperature phase is discussed within the framework of DFT++ calculations. From the latter, a new interpretation of the electronic correlations in this material is proposed.

P1.33 Metal-to-Insulator transitions in RNiO_3 thin films as seen by ultraviolet photoemission spectroscopy

E. F. Schwier (presenter) *Hiroshima Synchrotron Radiation Center*, Z. Vydrova *University of Fribourg*, R. Scherwitzl *University of Geneva*, M. Gibert *University of Geneva*, P. Zubko *University of Geneva*, M. G. Garnier *University of Fribourg*, J. Triscone *University of Geneva*, P. Aebi *University of Fribourg*, M. Garcia-Fernandez *Brookhaven National Laboratory*

Nickel based rare earth perovskite oxides RNiO_3 , are a model system to study temperature driven metal-to-insulator transitions (MIT). Apart from the MIT, a magnetic transition is also present in the phase diagram, where an antiferromagnetic phase with a nontrivial spin arrangement emerges at low temperatures. The driving force of the MIT as well as the nature of the antiferromagnetic ground state are still under debate and have been investigated for several decades [1, 2]. Recent advances in thin films growth [3] have stimulated research on these materials through possible applications as temperature dependent switches in nano-electronics. Due to the absence of sufficiently large single crystals, epitaxial thin films are the closest system

available to study the intrinsic properties of nickelates. In addition, thin films can be grown sufficiently thin in order to study the effect of epitaxial strain on their properties [4] as well as its role in the interplay between the electronic, magnetic and geometric degrees of freedom in general.

Here we present results from temperature dependent angle-integrated ultraviolet photoemission measurements on RNiO_3 ($R=\text{Sm}, \text{Nd}$) thin films across the MI and magnetic transition. These results will be discussed in the context of a doped Mott-Hubbard insulator model and a case for a possible coupling between the electronic and magnetic structure in the system will be made.

- [1] M. Medarde, *J. of Phys.: Cond. Matt.* 9, 1679 (1997).
- [2] G. Catalan, R. Bowman, and J. Gregg, *Phys. Rev. B* 62, 7892 (2000).
- [3] A. Tiwari, C. Jin, and J. Narayan, *App. Phys. Lett.* 80, 4039 (2002).
- [4] R. Scherwitzl et al., *Adv. Mater.* 22, 5517 (2010).

P1.34 Investigation of the dimensional crossover of the electronic band structure in LaNiO_3 ultrathin film using in situ ARPES

Y. Hyang Keun (presenter) *CFI-CES, IBS & Seoul National University*, S. I. Hyun, Y. J. Chang, L. Moreschini, D. W. Jeong, C. H. Sohn, Y. S. Kim, A. Bostwick, E. Rotenberg, J. H. Shim, T. W. Noh

Recently, two-dimensional (2D) LaNiO_3 (LNO) system has attracted increasing attention due to realization of the electronic band structure analogous to that of the high- T_c cuprate superconductors. Bulk RNiO_3 (R : rare earth) has d^7 electrons with fully occupied t_{2g} and partially filled e_g electrons. Recent theoretical calculations predicted the orbital reconstruction for single $d_{x^2-y^2}$ band structure in the 2D LaNiO_3 system, similar to that of high- T_c cuprate superconductors. To confirm this interesting prediction, the orbital characteristics in 2D LaNiO_3 system has been investigated using synchrotron-based x-ray measurements, such as soft x-ray reflectivity, x-ray absorption spectroscopy and so on. However, fundamental understanding of the electronic reconstruction related to orbital characteristics in 2D LNO system has been still elusive due to absence of direct electronic structure measurements using angle-resolved photoemission spectroscopy (ARPES).

We investigated the electronic structure of LaNiO_3 ultrathin films using in-situ ARPES system located at beam line 7.0.1 of the Advanced Light Source. (1) At first, we investigated three-dimensional (3D) electronic band structure of LaNiO_3 thick film deposited on SrTiO_3 substrate. The measured 3D electronic band structure can be explained by the DMFT calculations (not by the LDA calculations), indicating the importance of the correlation effects. (2) Then, we also prepared LaNiO_3 ultrathin films with thickness between 1 and 5 unit cells (UC) We observed that the dimensional crossover of the electronic structure occurs around

3 UC of LaNiO₃ film. Contrary to earlier theoretical works, our LaNiO₃ ultrathin film has a Fermi surface down to 1 UC. We also found that the quasi particle peak at Fermi level was suppressed in 2D LaNiO₃ ultrathin films. This could be understood by disorder effects, such as Anderson localization or percolation of insulating channels, in the insulating state of the 2D LNO ultrathin films. Further details will be discussed in presentation.

P1.35 **In-situ angle resolved photoemission spectroscopy of ultrathin LaNiO₃ films: Observation of orbital-lattice interaction**

H. K. Yoo *Seoul National University*, C. H. Sohn (presenter) *Seoul National University*

We reported the electronic band structure of ultrathin LaNiO₃ films using in-situ angle resolved photoemission spectroscopy (ARPES). Every LaNiO₃ film was grown by pulsed laser deposition method and transferred to ARPES chamber without breaking vacuum. We controlled the strain for LaNiO₃ films using various substrates such as LaAlO₃, NdGaO₃ and SrTiO₃. Our APRES data clearly demonstrate that electronic band structure changes systematically corresponding to the strain of the films. Comparing DMFT calculations, we found that the energy of $3z^2-r^2$ (x^2-y^2) orbitals of tensile strain case is lower (higher) than that of compressive strain case, which supports the present theoretical prediction.

P1.36 **Metal-insulator transition induced by irradiation in nanowires**

G. Jia (presenter) *USC*

Ga-doped ZnO nanowires have been synthesized by pulsed laser chemical vapor deposition method. The crystal structure and photoluminescence spectra indicate that the dopant atoms are well integrated into the ZnO wurtzite lattice. The electrical transport properties are systematically investigated on nanowire configured as a field-effect transistor, demonstrating for the first time the effects of light illumination on the charge conduction under temperature variation in doped ZnO nanowire system. Among the experimental highlights, a pronounced semiconductor-to-metal transition is observed under UV band-to-band excitation, as a consequence of the reduction of electron mobility arising from the drastically enhanced Coulomb interactions. Another feature is the presence of two reproducible resistance valleys at 220 K and 320 K upon UV irradiation. This phenomenon originates from the impurity band, arising from the native defects as well as the extrinsic Ga dopants, which serve as trapping and detrapping centers for photogene-

rated electrons. This work demonstrates that due to the dimensional confinement and enhanced defect states in quasi-one-dimensional structures, the localized impurity states can significantly influence charge transport.

P1.37 **Chiral OAM state in k-space measured by CD-ARPES**

W. Jung (presenter) *Yonsei University*, C. Kim *Yonsei University*

We measured electronic structures of perovskite oxide materials Sr₂MO₄ (M=Rh, Ru) with angle-resolved photoemission spectroscopy (ARPES) using circular dichroism (CD) method to investigate orbital angular momentum (OAM) characters. We observe large CD which shows complicated orbital structures of Sr₂MO₄. For Sr₂RuO₄, β and γ pockets which are hole pockets near the point show a $\sin 4\theta$ symmetry while α electron pocket near the X-point shows a $\sin 2\theta$ symmetry. In Sr₂RhO₄, α pockets which are hole pockets near the point show a $\sin \theta$ symmetry while β electron pocket near the X-point shows a $\sin 2\theta$ symmetry. In our view, the CD modulations of the three bands come from. This complex OAM ordering is an evidence of a time reversal symmetry (TRS) breaking and hidden magnetic order which is in Sr₂MO₄ system. Also, these are clue to investigate the problems which is including p-wave superconductivity and incommensurate magnetic excitation.

P1.38 **Synthesis and characterization of nanocrystalline ZrO₂ powders by sol-gel method**

K. Park (presenter) *Sejong University*, A. Hakeem *Sejong University*

ZrO₂ nano-sized powders were synthesized via the sol-gel method, using organic precursors such as citric acid, ethylene glycol, and glycerol. This sol-gel method is suitable for the fabrication of nano-sized metal oxides starting from a colloidal solution. The organic entity used in this study played an important role in the morphology and crystallite size of the nanopowders. The X-ray diffraction (XRD) measurement was carried out to determine the crystal structure and phases purity. The powder size of the synthesized ZrO₂ was in the range of 10 to 95 nm. Fourier transform infrared (FT-IR) spectroscopy was used to predict chemical bonding. The morphology and size of the synthesized powders were investigated by field emission scanning electron microscope (FE-SEM) and TEM. The photoluminescence properties (excitation and emission) of the synthesized nanopowders were analyzed by photoluminescence spectroscopy. It was found that powder characteristics, i.e., size, morphology, phase purity, and optical properties, depended strongly on the process conditions, including choice of organic precursors, pH during hydrolysis, and thermal treatment.

POSTER SESSION 1 MONDAY, 18:50–21:00

P1.39

Synthesis and characterization of nano-sized Eu-activated ZrO₂ phosphor powders by solution combustion method

K. Park (presenter) *Sejong University*, S. Yoon *Sejong University*, A. Hakeem *Sejong University*

High-quality Eu³⁺-doped ZrO₂ nano-sized powders, i.e. smooth surface and narrow size distribution, were synthesized via the solution combustion method. The solution combustion method is widely considered as a favorable route for synthesizing pure, nano-sized powders. In this study, we investigated the microstructure and optical properties of Eu³⁺-doped ZrO₂ nanopowders, depending on Eu³⁺ content. The X-ray diffraction (XRD) measurement was carried out to determine the crystal structure and phases purity. The powder size of the synthesized ZrO₂ nanopowders was in the range of 30 to 200 nm. The size of the synthesized ZrO₂ nanopowders was controlled by changing the process conditions. Fourier transform infrared (FT-IR) spectroscopy was used to determine chemical bonding. The morphology and size of the synthesized powders were investigated by field emission scanning electron microscope (FE-SEM) and TEM. The photoluminescence properties (excitation and emission) of the ZrO₂ nanopowders were analyzed with a spectrofluorometer. The photoluminescence properties depended strongly on the process conditions, such as the ratio of the nitrate to combustion fuel and annealing temperature.

P1.40

Anharmonicity due to electron-phonon coupling in magnetite

M. Hoesch (presenter) *Diamond Light Source*

We present the results of inelastic x-ray scattering for magnetite and analyze the energies and widths of the phonon modes with different symmetries in a broad range of temperature $125 < T < 293$ K. The phonon modes with X4 and 5 symmetries broaden in a nonlinear way with decreasing T when the Verwey transition is approached. It is found that the maxima of phonon widths occur away from high-symmetry points which points at the incommensurate character of critical fluctuations. Strong phonon anharmonicity induced by electron-phonon coupling is discovered by a combination of these experimental results with ab initio calculations which take into account local Coulomb interactions at Fe ions. It (i) explains observed anomalous phonon broadening, and (ii) demonstrates that the Verwey transition is a cooperative phenomenon which involves a wide spectrum of phonons coupled to the electron charge fluctuations condensing in the low-symmetry phase.

P1.41

Interface states in LaAlO₃/SrTiO₃ heterostructures as probed by resonant inelastic x-ray scattering

F. Pfaff (presenter) *University of Würzburg*, H. Fujiwara *Osaka University*, Y. Nishitani *Konan University*, A. Yamasaki *Konan University*, Y. Harada *University of Tokyo*, A. Sekiyama *Osaka University*, S. Suga *Osaka University*, M. Sing *University of Würzburg*, R. Claessen *University of Würzburg*

The interface between the two band insulators LaAlO₃ (LAO) and SrTiO₃ (STO) hosts a two-dimensional electron system of itinerant charge carriers if the LAO overlayer thickness exceeds 3 monolayers. Interface ferromagnetism coexisting with superconductivity has been found and attributed to local moments. Recently, two peaks in resonant inelastic x-ray scattering (RIXS) indeed have been correlated with delocalized and localized charge carriers [1]. To shed light on the coexistence of the two types of Ti 3d carriers we performed RIXS on LAO/STO heterostructures with different overlayer thicknesses and different concentrations of oxygen vacancies. Already for the heterostructure with a film thickness of 3 monolayers, which is insulating, we observe a finite charge carrier concentration. This is in line with the finding of a critical thickness for ferromagnetism in LAO/STO heterostructures by Kalisky et al. [2]. Furthermore, while there is an increase of the total charge seen in RIXS with increasing film thickness for samples showing the critical thickness behavior in conductivity, surprisingly, the spectra remain essentially unchanged for samples with fixed thickness that have been intentionally doped with oxygen vacancies. At variance with these findings, an increase of the total charge can be observed in the Ti 2p core level spectra for different film thicknesses as well as oxygen vacancy concentrations in photoemission experiments. We discuss this with respect to a possible non equilibrium situation due to the generation of electron-hole pairs during irradiation.

[1] Ke-Jin Zhou et al., *Phys. Rev. B* 83, 201402(R) (2011).

[2] B. Kalisky et al., *Nat. Comm.* 3, 922 (2012).

P1.42

Observation of strong spin-orbital entanglement in Sr_2RuO_4 by spin-resolved ARPES

C. N. Veenstra *University of British Columbia*, Z. Zhu (presenter) *University of British Columbia*, M. Raichle *University of British Columbia*, B. M. Ludbrook *University of British Columbia*, A. Nicolaou *University of British Columbia*, B. Slomski *Universität Zürich-Irchel*, G. Landolt *Universität Zürich-Irchel*, S. Kittaka *Kyoto University*, Y. Maeno *Kyoto University*, J. H. Dil *Universität Zürich-Irchel*, I. S. Elfimov *University of British Columbia*, M. W. Haverkort *University of British Columbia*, A. Damascelli *University of British Columbia*

After a flurry of experimental activity, Sr_2RuO_4 has become a hallmark candidate for spin-triplet chiral p-wave superconductivity, the electronic analogue of superfluid ^3He . However, despite the apparent existence of such a pairing, some later experiments do not fully support this conclusion, as they cannot be explained within a theoretical model using spin-triplet superconductivity alone. A resolution might come from the inclusion of spin-orbit coupling, which has been conjectured to play a key role in the low energy electronic structure [1]. Using circularly polarized light combined with spin- and angle-resolved photoemission spectroscopy, we directly measure the value of the effective spin-orbit coupling to be 130 meV [2]. This is even larger than theoretically predicted and comparable to the energy splitting of the d_{xy} and $d_{xz,yz}$ orbitals around the Fermi surface, resulting in a strongly momentum-dependent entanglement of spin and orbital character. As a consequence, the classification of the Cooper pairs in terms of singlets or triplets fundamentally breaks down, necessitating a description of the unconventional superconducting state of Sr_2RuO_4 beyond these pure spin eigenstates [2].

[1] M.W. Haverkort et al., Phys. Rev. Lett. 101, 026406 (2008).

[2] C. N. Veenstra et al., arXiv:1303.5444 (2013).

P1.43

Na_2IrO_3 as a novel relativistic Mott insulator with a 340 meV gap

R. Comin *University of British Columbia*, G. Levy *University of British Columbia*, B. Ludbrook *University of British Columbia*, Z. Zhu (presenter) *University of British Columbia*, C. N. Veenstra *University of British Columbia*, J. A. Rosen *University of British Columbia*, Y. Singh *Indian Institute of Science Education and Research (IISER)*, P. Gegenwart *Georg-August-Universität Göttingen*, D. Stricker *Université de Genève*, J. N. Hancock *Université de Genève*, D. van der Marel *Université de Genève*, I. S. Elfimov *University of British Columbia*, A. Damascelli *University of British Columbia*

We have studied Na_2IrO_3 by ARPES, optics, and band structure calculations in the local-density approximation (LDA). The weak dispersion of the Ir 5d- t_{2g} manifold highlights the importance of structural distortions and spin-orbit coupling (SO) in driving the system closer to a Mott transition. We detected an insulating gap $\Delta_{\text{gap}} = 340$ meV which, at variance with a Slater-type description, is already open at 300 K and does not show significant temperature dependence even across $T_N=15$ K. An LDA analysis with the inclusion of SO and Coulomb repulsion U revealed that, while the prodromes of an underlying insulating state are already found in LDA+SO, the correct gap magnitude can only be reproduced by LDA+SO+ U , with $U=3$ eV. This establishes Na_2IrO_3 as a novel type of Mott-like correlated insulator in which Coulomb and relativistic effects have to be treated on an equal footing [1].

[1] R. Comin et al., Phys. Rev. Lett. 109, 266406 (2013).

POSTER SESSION 2 TUESDAY, 18:50–21:00

- P2.01** Dynamical mean-field approach to core-level spectroscopy for 3d systems
A. Hariki
- P2.02** Non-equilibrium self-energy-functional theory and conserving approximations
F. Hofmann
- P2.03** Non-local correlations in real time: nonequilibrium dynamical cluster approximation
N. Tsuji
- P2.04** Electron-phonon coupling in the transition-metal diborides
S. Sichkar
- P2.05** Solution of the periodic anderson model by means of a continued fraction algorithm
A. Chikina
- P2.06** Variational lattice approach for correlated systems
A. Lichtenstein
- P2.07** The 1/Z method for determining the quasi-particle excitation spectrum of any arbitrary quantum lattice systems
P. Naves
- P2.08** ARPES study on the electronic structures of doped SmB_6
C. H. Min
- P2.09** Momentum-Resolved Temperature-Dependent Electronic Structure of SmB_6
J. Denlinger
- P2.10** d-f hybridization at the origin of metallic behavior in SmB_6
E. Fratzeskakis
- P2.11** Low-energy photoemission spectroscopy investigation of the Yb electronic structure
L. Petaccia
- P2.12** Yb Valence Change in $\text{Ce}_{1-x}\text{Yb}_x\text{CoIn}_5$ from spectroscopy and bulk properties
L. Dudy
- P2.13** Different localisation regimes of the Cerium 4f electron in epitaxial Kondo surface alloys
H. Schwab
- P2.14** High-resolution angle-resolved photoemission study of electronic structure and charge-density wave formation in HoTe_3
G. Liu
- P2.15** Formation of the coherent heavy fermion liquid at the “hidden order” transition in URu_2Si_2
J. Geck
- P2.16** Model calculations based on electron-hole correlations to investigate photoemission data of TlSe_2
G. Monney
- P2.17** Electronic structure and photo emission of topological insulators: effects of correlations, doping and alloying
J. Minar
- P2.18** Tailoring the electronic texture of a topological insulator via its surface orientation
L. Barreto
- P2.19** Influence of orbital mixing on the spin structure of Rashba systems and topological insulators
H. Dil
- P2.20** Non 100% spin polarization in the ensemble of photoelectrons from topological insulator thin films
L. Plucinski
- P2.21** A tunable topological insulator in TlBiSe_2 with manipulating chemical composition
K. Kuroda
- P2.22** Spin polarized surface states in topological insulator $\text{Bi}_2\text{Te}_2\text{Se}$ and $\text{Bi}_2\text{Se}_2\text{Te}$
K. Miyamoto
- P2.23** Time-resolved ARPES investigation of the effective Fermi-Dirac distribution of Bi_2Se_3
A. Crepaldi

- P2.24** Layer-by-layer entangled spin-orbital texture of the topological surface state in Bi_2Se_3
Z. Zhu (see [Tu.12](#))
- P2.25** 2PPE measurement on $\text{Sb}_2\text{Te}_2\text{S}$ with an angle-resolving time-of-flight spectrometer
T. Kunze
- P2.26** Lifetime broadening of topological surface states with and without deposited magnetic moments
M. Scholz
- P2.27** Bi thin films on $\text{InAs}(111)$: a potential topological insulator
K. Hricovini
- P2.28** The effects of band bending on the topological insulator $\text{Bi}_2\text{Se}_{3-x}\text{Te}_x$
N. de Jong
- P2.29** Switch of coupled spin-orbital texture in topological insulators
Y. Cao
- P2.30** Creation of helical Dirac fermions by interfacing two gapped systems of ordinary fermions
M. Yao
- P2.31** Graphene sublattice symmetry and isospin determined by circular dichroism in ARPES
C. Ast
- P2.32** Electron-phonon coupling at doped metal-graphene interfaces studied by ARPES
A. Grueneis
- P2.33** Exploring unoccupied electronic structure and symmetry of valence bands of graphite using ARPES
S. K. Mahatha
- P2.34** Can graphene be turned into a topological insulator?
C. Straßer
- P2.35** Many-body interactions in the sigma band of graphene
F. Mazzola
- P2.36** Snapshots of non-equilibrium Dirac carrier distributions in graphene
I. Gierz
- P2.37** Hot carrier relaxation on the Dirac cone in quasi free-standing graphene probed by time- and angle-resolved photoemission
J. C. Johannsen
- P2.38** Correlation effects in the spin resolved bandstructure of cobalt measured by spin polarized momentum microscopy
C. Tusche
- P2.39** Electronic and magnetic properties of isolated atoms on surfaces
S. Gardonio
- P2.40** Quantum well states in Ag thin films on $\text{MoS}_2(0001)$ surface
S. K. Mahatha
- P2.41** Why does adding transition metal to Pt increase the surface reactivity
Y. S. Kim
- P2.42** High-resolution ARPES study of the electron self-energy and coupling parameters in palladium
K. Shimada
- P2.43** From surface to interface: A study of low-dimensional electron cases on SrTiO_3 and in $\text{LaAlO}_3/\text{SrTiO}_3$
N. Plumb
- P2.44** Momentum resolved inverse photoemission spectroscopy studies on $\text{Ni}_2\text{MnGa}(100)$ and $\text{Mn}_2\text{NiGa}(100)$ magnetic shape memory alloys
M. Maniraj

POSTER SESSION 2 TUESDAY, 18:50–21:00

P2.01

Dynamical mean-field approach to core-level spectroscopy for 3d systems

A. Hariki (presenter) *Osaka Prefecture University*, T. Uozumi *Osaka Prefecture University*

Core-level spectroscopy is a powerful tool to investigate electronic structures of strongly correlated systems, such as 3d transition metal oxides. Recent experimental progresses, especially in energy resolution and bulk sensitivity owing to high energy X-ray sources, have enabled us to access fine spectral features characterizing the electronic properties of compounds. For example, in the $2p_{3/2}$ main line (ML) of 2p core-level X-ray photoemission spectroscopy (XPS), a double-peak structure was found for NiO and various features were found for cuprates, which are considered to be connected with an insulating property of NiO and high- T_c superconductivity. However, a conventional theoretical framework for spectral analyses, based on a single impurity model, cannot explain such features because of a lack of non-local screening (NLS) effects in the XPS final state. Thus, an extended framework is required to derive information on electronic structures from such fine spectral features.

Recently, we proposed a new framework based on a dynamical mean-field theory (DMFT) [1, 2]. The DMFT is widely accepted as an efficient framework to treat electronic structures of strongly correlated systems. However, applications to core-level spectroscopy carried out so far has been restricted in somewhat simple cases, i.e., the paramagnetic phases of a single-band Hubbard model with unrealistic density of states. In our framework, we combine a single impurity Anderson model (SIAM) with the LCAO band calculation under the DMFT in order to consider the realistic crystal structure. This is the first attempt applying such a DMFT-based framework in the core-level XPS study. As an impurity solver, we adopt a configuration interaction method which has several advantages to discuss multi-orbital systems on the basis of spectral functions, such as partial density of states (PDOS). We show that the $2p_{3/2}$ ML of NiO is strongly affected by the antiferromagnetic ordering in addition to the NLS accompanied by a Zhang-Rice doublet formation. As for cuprates, rich varieties in the $2p_{3/2}$ ML structure reflect the band reconstruction induced by the carrier doping and the NLS from the Zhang-Rice singlet band. We demonstrate the close connection between core-level spectra and PDOS thorough analysis of the optimized hybridization function of the SIAM obtained in our framework. Moreover, we report and discuss the results for valence band photoemission spectroscopy.

[1] A. Hariki, Y. Ichinozuka, and T. Uozumi, *J. Phys. Soc. Jpn.* 82, 023709 (2013). ; [2] A. Hariki, Y. Ichinozuka, and T. Uozumi, *J. Phys. Soc. Jpn.* 82 (2013), in Press.

P2.02

Non-equilibrium self-energy-functional theory and conserving approximations

F. Hofmann (presenter) *University of Hamburg*, M. Eckstein *University of Hamburg, CFEL*, M. Potthoff *University of Hamburg*

The self-energy-functional theory (SFT) [1] provides a general framework for the systematic construction of non-perturbative and thermodynamically consistent approximations in order to study strongly correlated systems in the thermodynamical limit in and out of equilibrium.

On the space of non-equilibrium self-energies a functional can be constructed which is stationary at the physical self-energy and equals the physical grand canonical potential when evaluated at the latter. Without approximating the (formally unknown) functional, the variational principle can be evaluated by restricting the self-energies to a subspace of (numerically) solvable reference systems.

By choosing appropriate classes of reference systems, non-equilibrium generalizations of the variational-cluster-approach (VCA) and of the dynamical-mean-field-theory (DMFT) can be derived from SFT as well as different variants. SFT allows for studying phases and phase transitions as for example the Mott metal-insulator transition, magnetic phase transitions or the transition from antiferromagnetic to the superconducting phase in Hubbard-like models, as well as short-time dynamics.

Here it is shown for the time-dependent generalization of the approach that the formalism respects macroscopic conservation laws, namely conservation of total particle number, spin and total energy [2]. Therewith it is generally possible to construct conserving approximations that are non-perturbative.

[1] M. Potthoff, *AIP Conf. Proc.* 1419, 199 (2011).

[2] to be published.

P2.03

Non-local correlations in real time: nonequilibrium dynamical cluster approximation

N. Tsuji (presenter) *University of Tokyo*, P. Barmettler *University of Geneva*, P. Werner *University of Fribourg*, H. Aoki *University of Tokyo*

Non-local correlations and fluctuations are believed to play an important role in low dimensional correlated electron systems, e.g. in d-wave superconductivity and the pseudogap phenomenon in high- T_c cuprates. Recent progress of time-resolved angle-resolved photoemission spectroscopy (ARPES) starts to unveil their momentum-dependent real-time dynamics, which will shed a new light on the study of correlated electronic structures.

Motivated by these, here we attempt a new theoretical approach,

namely a nonequilibrium generalization of the dynamical cluster approximation (DCA). It is an extension of the established nonequilibrium dynamical mean-field theory, taking account of the momentum dependence of the self-energy. We apply the nonequilibrium DCA to the one-dimensional Hubbard model, and study the relaxation and thermalization dynamics after an interaction quench. We benchmark the validity of the method by comparing the results with the time-dependent density matrix renormalization group. We show how non-local correlations are important in understanding real-time dynamics even in highly excited systems.

P2.04

Electron-phonon coupling in the transition-metal diborides

S. Sichkar (presenter) *Institute of Metal Physics*

The electronic structure, optical and x-ray absorption spectra, angle dependence of the cyclotron masses and extremal cross sections of the Fermi surface, phonon spectra, electron-phonon Eliashberg and transport spectral functions, temperature dependence of electrical resistivity of the MB_2 ($M=Ti$ and Zr) diborides were investigated from first principles using the fully relativistic and full potential linear muffin-tin orbital methods. The calculations of the dynamic matrix were carried out within the framework of the linear response theory.

Calculated phonon spectra and phonon DOSs for both ZrB_2 and TiB_2 are in good agreement with experimental results as well as previous calculations. The Eliashberg function of electron-phonon interaction in ZrB_2 is in good agreement with the experimentally measured point contact spectral function for both the position and the shape of the major peaks. There are no regions with high electron-phonon interaction or phonon dispersion curves with soft modes in either ZrB_2 or TiB_2 . This is in agreement with the fact that no trace of superconductivity was found in these borides. The averaged electron-phonon interaction constant was found to be rather small $\lambda=0.14$ and 0.15 for ZrB_2 and TiB_2 , respectively.

The temperature dependence of the electrical resistivity in ZrB_2 and TiB_2 in the lowest-order variational approximation of the Boltzmann equation was calculated. It was found rather small anisotropical behavior of the electrical resistivity in ZrB_2 to be in good agreement with experimental observation. The anisotropy of electrical resistivity in TiB_2 is larger than it is in ZrB_2 .

P2.05

Solution of the Periodic Anderson Model by means of a continued fraction algorithm.

A. Chikina (presenter) *TU Dresden*, K. Matho *CNRS Grenoble*, M. Höppner *TU Dresden/MPI-FKF Stuttgart*, S. Danzenbächer *TU Dresden*, D. Vyalikh *TU Dresden*,

C. Laubschat *TU Dresden*

The semi-phenomenological continued fraction method, previously applied to the Hubbard model [1], was adapted to the Periodic Anderson Model (PAM) with momentum independent hybridization. The method applies to the various paramagnetic phases that can be modelled with the PAM by varying the filling [2]: the Kondo regime including the Kondo insulator, the charge transfer regime including the Mott insulator. The partial fillings are determined self-consistently. We have developed a numerical code with a local self energy, allowing to compare our results with the ones derived by the Dynamical Mean Field Theory (DMFT) [1]. The scenario previously applied to $CeFePO$ in comparison to ARPES [3] will be discussed in detail. We show that realistic kinetic energy input (one body part of PAM) has important feedback on the quasi particle density spectrum, notably through the appearance of renormalized van Hove singularities. The rapidity in terms of computer time, the ease of changing model parameters and generating ARPES intensity plots including matrix element effects, makes the new code a useful strategic tool being midway between microscopic theory and experiment.

[1] R. Hayn, P. Lombardo, and K. Matho, *Phys. Rev. B* 74, 205124 (2006).

[2] A. Amaricci et al., *Phys. Rev. B* 85, 235110 (2012).

[3] M. G. Holder et al., *Phys. Rev. Lett.* 104, 096402 (2010).

P2.06

Variational lattice approach for correlated systems

A. Lichtenstein (presenter) *University of Hamburg*, A. Wilhelm *University of Hamburg*, H. Hafermann *CEA/Saclay*

We introduce an efficient strategy to treat long ranged correlations in fermionic lattices, the so called variational lattice approach (VLA). The VLA combines the recently developed dual fermion approach for k -dependent problems and the exact diagonalization technique. We present first benchmark results. The phase diagram of the half-filled paramagnetic Mott-Hubbard transition is discussed and results are compared to CDMFT and DCA calculations.

P2.07

The 1/Z method for determining the quasi-particle excitation spectrum of any arbitrary quantum lattice systems

P. Navez (presenter) *Universitaet Duisburg Essen*, K. Krutitsky *Universitaet Duisburg Essen*, F. Queisser *University of Vancouver*, R. Schutzhold *Universitaet Duisburg Essen*

Quantum lattice systems such as Bose and Fermi Hubbard gases or spin Heisenberg magnets can all generally be investigated using the 1/Z expansion method where Z is the coordination number. In the lea-

POSTER SESSION 2 TUESDAY, 18:50–21:00

ding order, this method reproduces well the excitation spectra found in the literature. In the next order in $1/Z$, using the variable separation technique for the two-sites reduced correlated density matrix, we find that these excitations can be virtually produced in pairs in order to generate quantum fluctuations. We illustrate the potential use of these general concepts in many cases such as virtual particle-hole pairs in the Hubbard models that lowers the ground state energy in the Mott phase or two virtual magnons of opposite spins in Heisenberg models that tends to reduce antiferromagnetism.

P2.08

ARPES study on the electronic structures of doped SmB_6

C. H. Min (presenter) *University of Würzburg*

SmB_6 displays a promising transport behavior as a 3-dimensional topological Kondo insulator. However, the surface states on SmB_6 not only have been barely addressed by angle-resolved photoemission spectroscopy, but also should be classified as topological surface states or non-topological surface states. Especially, the influences of both (1) the non-magnetic ion substitution in SmB_6 and (2) the magnetic moments on its topological surface states have not been investigated. Here, we would like to show the electronic structures of electron-doped SmB_6 obtained from ARPES below 10 K. The electron doping may help us to observe the large area of Dirac cones and to reduce magnetic moments on its surface and bulk.

P2.09

Momentum-resolved temperature-dependent electronic structure of SmB_6

J. Denlinger (presenter) *Lawrence Berkeley National Laboratory*, J. W. Allen *University of Michigan*, J. W. Kim *POSTECH*, J. H. Shim *POSTECH*, B. I. Min *POSTECH*, J. S. Kang *Catholic University of Korea*, Z. Fisk *University of California, Irvine*

The rare earth hexaboride SmB_6 has been a paradigm mixed-valent insulator for over 40 years. Recent renewed interest in SmB_6 comes from the prediction of the existence of topological surface states due to the inversion of f and d-bands at the X-point [1], and from transport measurements giving evidence for surface conductivity at low temperatures [2, 3]. The existence of such surface states would provide an explanation for a long time puzzle of possible “in-gap” states causing a finite resistivity saturation below 4K. In order to test this new model, a global momentum space view of the Sm 4f band dispersions and hybridization with Sm 5d states close to the Fermi level (E_F) has been probed using angle-resolved photoemission. Large dispersions of the Sm 4f and bulk Sm 5d electron bands near E_F have been observed. Momentum-resolved temperature-dependent spectra reveal a distinct movement of states through E_F consistent with the bulk conductivity

transition from insulator to bad metal. Also, temperature-dependence of Sm 5d states and Sm 4f states are shown to be correlated to each other and to be consistent with bulk valence changes and transport properties. Key points of discrepancy between the observed single Sm 4f band and theoretical crystal field-split sub-bands are highlighted. Prospects for being able to observe the recently predicted topological surface states is also discussed.

[1] Dzero et al., *Phys. Rev. Lett.* 104, 106408 (2010).

[2] S. Wolgast et al., arXiv:1211.5204 (2012).

[3] J. Botimer et al., arXiv:1211.6769 (2012)

P2.10

d-f hybridization at the origin of metallic behavior in SmB_6

E. Frantzeskakis (presenter) *University of Amsterdam*

Topological insulators is a novel class of quantum matter with a strong potential for spintronics applications and “Majorana-hunting” devices. A considerable scientific effort targets at suppressing their bulk conductivity which masks the transport properties of the topological surface states [1]. The mixed-valence compound SmB_6 has been proposed as a paradigm of a “real” topological bulk insulator as theoretical studies have suggested topologically-protected states within a Kondo-derived electronic gap [2].

We have performed high resolution Angle-Resolved Photoelectron Spectroscopy measurements on the (100) surface of SmB_6 . Well-resolved electronic states are straddling the Fermi level at variance with bulk calculations. We present evidence that these states are a direct result of the d-f hybridization at the origin of a Kondo band gap. Our results can give insight to the long withstanding question about the origin of the low-temperature residual resistivity of SmB_6 .

[1] M. Z. Hasan and C.L. Kane, *Rev. Mod. Phys.* 82, 3045 (2010).

[2] F. Lu et al., *Phys. Rev. Lett.* 110, 096401 (2013).

P2.11

Low-energy photoemission spectroscopy investigation of the Yb electronic structure

L. Petaccia (presenter) *Elettra-Sincrotrone Trieste*, F. Offi *CNISM and Università Roma Tre*, P. Vilmercati *Elettra-Sincrotrone Trieste*, S. Gorovikov *Elettra-Sincrotrone Trieste*, A. Ruocco *CNISM and Università Roma Tre*, M. I. Trioni *CNR-ISTM*, A. Rizzo *CNISM and Università Roma Tre*, A. Goldoni *Elettra-Sincrotrone Trieste*, G. Stefani *CNISM and Università Roma Tre*, G. Panaccione *CNR-IOM*, S. Iacobucci *CNR-IFN*

The peculiar electronic structure of rare-earth elements and compounds is mostly defined by the partially filled 4f band. Of particular interest is the investigation of the valence states, which is linked to the degree of hybridization of f electrons with delocalized s-d bands. In the simple case of Yb, the 4f states are fully occupied with a Fermi

level of 6s character and a 2+ valency. However, the occupation of the Yb valence band has been the subject of several investigations over the years, intended in particular to separate the contribution of 5d states. Early experimental photoelectron emission (PES) spectra at very low excitation energy ($h\nu < 10$ eV) have reported a spectral modulation in the region close to the Fermi level that was attributed to the emission from a 5d band. The poor energy resolution did not allow however a detailed investigation of such spectral features. In recent years this low-energy photoemission spectroscopy (LEPES) encountered a renewed interest, under the stimulus of the extremely high-energy resolution obtainable with laser excited LEPES and given the expectation of a large increase of the bulk sensitivity at these low energies. We monitored the 4f spectral intensity in polycrystalline Yb films in the LEPES regime, between 5.5 and 21 eV photon energy, at the BaDElPh beamline of the ELETTRA synchrotron. We observe a moderate increase of the electron attenuation length and, thus, of the information depth at the lowest energies. For $h\nu < 11$ eV a prominent peak at the Fermi level is observed. The analysis of its intensity variation versus photon energy and the comparison of the experimental spectra with ab-initio density of states (DOS) calculations allow to attribute this structure to a p band crossing the Fermi level, enhanced at selected photon energies due to the influence of the empty DOS, probably amplified by a photoionization cross section effect and by the general increase of the photoelectron yield at low photon energy. In this respect LEPES may thus be considered as a probe of the joint DOS.

P2.12 Yb valence change in $\text{Ce}_{1-x}\text{Yb}_x\text{CoIn}_5$ from spectroscopy and bulk properties

L. Dudy (presenter) *University of Würzburg*, J. Denlinger *Advanced Light Source*, L. Shu *Fudan University*, M. Janoschek *Los Alamos National Laboratory*, J. W. Allen *University of Michigan*, B. M. Maple *University of California*

The electronic structure of $\text{Ce}_{1-x}\text{Yb}_x\text{CoIn}_5$ has been studied by a combination of photoemission, x-ray absorption and bulk property measurements. Previous findings of a Ce valence near 3+ for all x and of an Yb valence near 2.3+ for $x < 0.3$ were confirmed. One new result of this study is that the Yb valence for $x < 0.2$ increases rapidly with decreasing x from 2.3 toward 3+, which correlates well with de Haas van Alphen results showing a change of Fermi surface around $x = 0.2$. Another new result is the direct observation by angle resolved photoemission Fermi surface maps of about 50% cross sectional area reductions of the α and β sheets for $x = 1$ compared to $x = 0$, and a smaller, essentially proportionate, size change of the α sheet for $x = 0.2$. These changes are found to be in good general agreement with expectations from simple electron counting. The implications of these results for the unusual

robustness of superconductivity and Kondo coherence with increasing x in this alloy system are discussed.

P2.13 Different localisation regimes of the Cerium 4f electron in epitaxial Kondo surface alloys

H. Schwab (presenter) *Universität Würzburg*, M. Mulazzi *Universität Würzburg*, F. Reinert *Universität Würzburg*

Strong correlations in two dimensions produce surface-specific effects due to the reduced coordination and the presence of unsaturated chemical bonds, like lower Kondo temperature and different valences that have specific temperature dependences. In this contribution, I will show how these phenomena can be experimentally observed on thin two-dimensional lattices of Cerium atoms alloyed with transition metals, whose preparation is extremely reproducible and very well characterised [1].

X-ray Photoelectron Spectroscopy on the Cerium 3d core levels is a well-established method to investigate the relevant energy scales of Cerium-based compounds. When the interactions between the 4f sites is small, an interpretation based on the single-impurity Anderson model is possible and fitting the data using the theory of Gunnarsson and Schönhammer [2] gives an estimate of the physical parameters. Using this approach, we determined the degree of localisation, the hybridisation and the on-site Coulomb energy for three compounds: $\text{CeAg}_x/\text{Ag}(111)$, $\text{CePt}_x/\text{Pt}(111)$ and $\text{CePd}_x/\text{Pd}(111)$. The occupation number of the 4f sites varies from the very localised atomic limit to the mixed-valence and the degree and the change in the hybridisation between the 4f and conduction electrons determines variations of the Kondo temperature by about two orders of magnitude.

With this information and with the detailed surface characterisation, it is possible to study the band structure of these Kondo lattices in different regimes with high resolution ARPES at low temperatures and open the way to the direct tunability of the Kondo temperature by the preparation of ternary films of 2D Kondo lattices.

[1] M. Klein et al., *Phys. Rev. Lett.* 106, 186407 (2011), H. Schwab et al., *Phys. Rev. B* 85, 125130 (2012).

[2] O. Gunnarsson et al., *Phys. Rev. B* 28, 4315 (1983).

P2.14 High-resolution angle-resolved photoemission study of electronic structure and charge-density wave formation in HoTe_3

G. Liu (presenter) *Chinese Academy of Sciences*

We performed High-resolution angle-resolved photoemission spectroscopy (ARPES) measurement on a single crystal of HoTe_3 , a quasi-two-dimensional rare-earth-element tritelluride charge-density-wa-

POSTER SESSION 2 TUESDAY, 18:50–21:00

ve (CDW) compound. The main features of the electronic structure in this compound is established by employing a quasi-CW laser (7 eV) and a helium discharging lamp (21.22 eV) as excitation light sources. It reveals many bands backfolded according to the CDW periodicity and two incommensurate CDW gaps created by perpendicular Fermi surface (FS) nesting vectors. The larger gap is found to open in well nested regions of the FSs, whereas other FS sections with poor nesting remain ungapped. In particular, some peculiar features are identified by using our ultra-high resolution and bulk sensitive laser.

P2.15

Formation of the coherent heavy fermion liquid at the “hidden order” transition in URu₂Si₂

J. Geck (presenter) *IFW Dresden*, S. Chatterjee *Cornell University*, J. Trinckauf *IFW Dresden*, D. Shai *Cornell University*, J. Harter *Cornell University*, T. Williams *McMaster University*, G. Luke *McMaster University*, K. Shen *Cornell University*

The interactions between localized and delocalized electrons in the so-called heavy fermion materials result in fascinating and unexpected quantum phenomena, which continue to challenge condensed matter researchers. One of the most prominent examples is the enigmatic “hidden order” (HO) state in URu₂Si₂, which is characterized by a large loss of entropy at 17.5 Kelvin. We present a high-resolution angle-resolved photoemission study of the heavy-fermion superconductor URu₂Si₂. Detailed measurements as a function of both photon energy and temperature allow us to disentangle a variety of spectral features, revealing the evolution of the low-energy electronic structure across the hidden order transition. Already above this transition we clearly observe incoherent heavy fermion states below the Fermi level that do not hybridize significantly with the conduction bands. Upon entering the hidden order phase, these incoherent states begin to hybridize with the conduction band and rapidly transform into a coherent heavy fermion liquid. This evolution is in stark contrast with the gradual crossover expected in Kondo lattice systems, which we attribute to the coupling of the heavy fermion states to the hidden order parameter.

P2.16

Model calculations based on electron-hole correlations to investigate photoemission data of TiSe₂

G. Monney (presenter) *University of Fribourg*, C. Monney *Fritz Haber Institute*, B. Hildebrand *University of Fribourg*, P. Aebi *University of Fribourg*, H. Beck *University of Fribourg*

TiSe₂ is a correlated material with a very small (positive or negative) indirect gap and it is unclear whether the ground state is a semi-con-

ductor or a semimetal. Below T=200K, its phase transition towards a commensurate charge density wave (CDW) is observable in photoemission. Above the transition temperature, typical spectral features of the CDW are already observed and we developed a theoretical model accounting for CDW fluctuations to explain them. This model of interacting electrons and holes allows to investigate the differences between a bare semi-metal and a semi-conductor. The question of the origin of the charge density wave (driven by electron correlations or by the lattice via phonon softening) is also discussed.

P2.17

Electronic structure and photoemission of topological insulators: effects of correlations, doping and alloying

J. Minar (presenter) *LMU Munich*, J. Braun *LMU Munich*, J. Sánchez-Barriga *HZB Berlin*, O. Rader *HZB Berlin*, H. Ebert *LMU Munich*

We discuss calculated spectral features of Bi₂Te₃, Bi₂Se₃, Sb₂Te₃ and Bi₂(Te_{1-x}Se_x)₃ and compare with corresponding experimental data. The effect of electronic correlations on the topological surface state (TSS) will be shown for Mn doped Bi₂Se₃ by means of the KKR+DMFT method. Here we will concentrate in particular on the formation of the local magnetic moment and its effect on the TSS. In order to simulate the spectral features above the Curie temperature we will perform disorder local moment (DLM) calculations in combination with the KKR+DMFT method. Furthermore, the dependence of the circular dichroism in the angular distribution (CDAD) on the photon energy is identified as a final state effect. To discuss these results in more detail, a complete calculation of the spin-polarization vector including the component perpendicular to the surface is presented. In addition, the behavior of Rashba split surface resonances which had been observed at higher binding energies is analyzed. Last but not least the unoccupied bulk and surface states of these materials are investigated by use of our one-step photoemission theory. The calculations have been performed in the framework of the fully relativistic version of the one-step model that is part of the Munich SPR-KKR program package. To guarantee for a quantitative description of the surface-sensitive spectral features special attention is paid to the image-potential behavior of the surface barrier, which is included as an additional layer in the photoemission formalism.

P2.18

Tailoring the electronic texture of a topological insulator via its surface orientation

L. Barreto (presenter) *Aarhus University*, W. Simoes e Silva *Aarhus University*, M. Stensgaard *Aarhus University*, S. Ulstrup *Aarhus University*, M. Bianchi *Aarhus University*, X. Zhu *Aarhus University*, M. Dendzik *Aarhus University*, P. Hofmann

Aarhus University

Topological insulators are characterised by an insulating bulk band structure, but topological considerations require their surfaces to support gap-less, metallic states. Meanwhile, many examples of such materials have been predicted and found experimentally, but experimental effort has concentrated on the closed-packed (111) surface of these materials. Thus, the theoretical picture of an insulating bulk embedded in a metallic surface from all sides of a crystal still needs to be confirmed.

Here we present angle-resolved photoemission spectroscopy results from the (110) surface of the topological insulator $\text{Bi}_{1-x}\text{Sb}_x$ ($x \approx 0.15$). As expected, this surface also supports metallic states but the change in surface orientation drastically modifies the band topology, leading to three Dirac cones instead of one. This illustrates the possibility to tailor the basic topological properties of the surface via its crystallographic direction. Here it introduces a valley degree of freedom not previously achieved for topological insulator systems.

P2.19

Influence of orbital mixing on the spin structure of Rashba systems and topological insulators

J. H. Dil (presenter) *Swiss Light Source*, B. Slomski *Swiss Light Source*, G. Landolt *University of Zurich*, S. Muff *University of Zurich*, J. Osterwalder *University of Zurich*

In recent years the study of the spin-resolved band structure by means of spin- and angle-resolved photoemission (S-ARPES) has experienced a significant boost. A main reason for this has been the prediction and discovery of 3D topological insulators, which are best characterized by their peculiar spin structure. Simultaneously many new systems with a sizable Rashba-type spin splitting have been found, with spin structures that in some cases significantly deviate from what is expected from the simple Rashba model. With few exceptions the S-ARPES measurements on both types of systems have been interpreted in the light of pure spin states, which is given the large influence of spin-orbit interaction (SOI) a rough assumption. Under the influence of SOI any change in the orbital character of a state will have a direct consequence for its spin structure. Furthermore it has been assumed that if hybridization of spin states has to be taken into account, only states with parallel spin can interact and others will not be influenced. Here it will be shown that depending on the exact orbital symmetry also the interaction between states with orthogonal spin has to be considered. Our S-ARPES measurements indicate that this leads to a significant reduction of the Rashba-type spin splitting and a reduced degree of measured spin polarization. Experimental results obtained for Pb quantum well states show that ultimately this orbital mixing leads to a reversal of the spin helicity.

Although for topological insulators typically only a single spin polarized band has to be considered in a given momentum and energy range, the influence of orbital mixing is also observed for these systems. The most astonishing realization of this is the reversal of the measured spin helicity of the topological surface state as a function of light polarization. It will be shown how such measurements can be used to determine the orbital composition.

P2.20

Non 100% spin polarization in the ensemble of photoelectrons from topological insulator thin films

L. Plucinski (presenter) *FZ Jülich*, A. Herdt *FZ Jülich*, G. Bihlmayer *FZ Jülich*, G. Mussler *FZ Jülich*, S. Döring *Universität Duisburg-Essen*, D. Grützmacher *FZ Jülich*, S. Blügel *FZ Jülich*, C. M. Schneider *FZ Jülich*

Spin polarized photoemission spectra from surfaces of Bi_2Te_3 [1] and Sb_2Te_3 [2] topological insulator (TI) thin films [3] prepared by the optimized procedure under the UHV [4] show up to 45% in-plane spin polarization in the Dirac cone near the Fermi level. This is consistent with the dedicated ab initio theoretical results, which find spin polarization in the order of 40-50% when averaged over the surface quintuple layer with the exponential depth profile related to the scattering mean free path of the VUV photoelectrons. Furthermore a non-zero out-of-plane spin polarization component is found in the Bi_2Te_3 hexagram Fermi surface [1].

We will discuss the spin-orbit entanglement mechanism behind the non-100% spin polarization in topologically protected surface states, and propose possible surface engineering solutions to increase the spin polarization of the Dirac cone in films grown by the MBE. Furthermore we will compare analytical band structure models with the DFT-based slab calculations.

First results on Fe desposition on the thin film of Sb_2Te_3 will also be presented and in the outlook we will provide ideas for future spectroscopic research directions on TI thin films.

[1] A. Herdt et al., *Phys. Rev. B* 87, 035127 (2013).

[2] L. Plucinski et al., *J. Appl. Phys.* 113, 053706 (2013).

[3] J. Krumrain et al., *J. Cryst. Growth* 324, 115 (2011).

[4] L. Plucinski et al., *Appl. Phys. Lett.* 98, 222503 (2011).

P2.21

A tunable topological insulator in TlBiSe_2 with manipulating chemical composition

K. Kuroda (presenter) *Hiroshima University*, K. Shirai *Hiroshima University*, K. Miyamoto *Hiroshima Synchrotron Radiation Center*, T. Okuda *Hiroshima Synchrotron Radiation Center*, S. Uueda *NIMS*, M. Arita *Hiroshima Synchrotron Radiation Center*, K. Shimada *Hiroshima Synchrotron Radiation Center*, H. Namatame *Hiro-*

POSTER SESSION 2 TUESDAY, 18:50–21:00

Hiroshima Synchrotron Radiation Center, M. Taniguchi Hiroshima Synchrotron Radiation Center, Y. Ueda Kure National College of Technology, A. Kimura Hiroshima University

Topological insulators (TIs) with a Dirac cone-like surface state forming a helical spin texture are known as a fertile ground to realize new exotic physical phenomena [1, 2], however, realizations of these phenomena still missing owing to mostly a lack of bulk insulating property and in-gap Dirac point (DP) feature. The lack of topological nature near the DP could be a serious problem for spintronic applications. Therefore, the realization of bulk insulating property and in-gap DP is a crucial key and center of current task [3-5]. Recently, ternary chalcogenide TlBiSe_2 was discovered to be one of the most promising TIs, which features in-gap Dirac point. This feature has never been achieved in mostly studied TI such as Bi_2Se_3 [6].

Here, we report a first demonstration of a tunable topological insulator into the bulk insulating phase in TlBiSe_2 synthesized with site-defect restraining condition. Our spin-ARPES measurement with variable light polarizations has revealed clear spin polarization with helicity reversal with respect to the DP. This functional DP has eventually controlled close to the Fermi energy with bulk insulating phase. This result gives us a great ground for the realization of exotic phenomena as well as ambipolar gate control for spin current in future devices.

- [1] M. Z. Hasan and C. L. Kane, *Rev. Mod. Phys.* 82, 3045 (2010).
- [2] X.-L. Qi and S.-C. Zhang, *Rev. Mod. Phys.* 83, 1057 (2011).
- [3] J. G. Analytis et al., *Phys. Rev. B* 81, 205407 (2010).
- [4] K. Eto et al., *Phys. Rev. B* 81, 195309 (2010).
- [5] Shunghun Kim et al., *Phys. Rev. Lett.* 107, 056803 (2011).
- [6] K. Kuroda et al., *Phys. Rev. Lett.* 105, 146801 (2010).

P2.22

Spin polarized surface states in topological insulator $\text{Bi}_2\text{Te}_2\text{Se}$ and $\text{Bi}_2\text{Se}_2\text{Te}$

K. Miyamoto (presenter) *Hiroshima Synchrotron Radiation Center*, T. Okuda *Hiroshima Synchrotron Radiation Center*, A. Kimura *Hiroshima University*, K. Kuroda *Hiroshima University*, H. Namatame *Hiroshima Synchrotron Radiation Center*, M. Taniguchi *Hiroshima Synchrotron Radiation Center*, S. Ereemeev *Tomsk State University*, T. Menshchikova *Tomsk State University*, E. Chulkov *Donostia International Physics Center (DIPC)*, K. Kokh *Russian Academy of Sciences*, O. Tereshchenko *Novosibirsk State University*

Topological insulators have attracted a great deal of attention as key material for spintronics technology. Among the established TIs, Bi_2X_3 (X=Se, Te) has been mostly studied because of their relatively large energy gap and the simplest topological surface state (TSS) with helical spin texture. However, an absence of the topological natures (helical spin texture and peculiar Landau level) of TSS below Dirac point (ED) has been shown by spin- and angle-resolved photoemission spectroscopy (S-ARPES) and scanning tunneling spectroscopy under

perpendicular magnetic field. It could be a disadvantage for extending its spintronic applications. Recently, one of the ternary tetradymite compounds, $\text{Bi}_2\text{Te}_2\text{Se}$ was shown to be a TI by the ARPES measurement. Importantly, a highly bulk resistive feature in this compound has successfully led to the observation of its surface-derived quantum oscillations in the magnetotransport experiment. We have unambiguously clarified the spin feature of TSS in $\text{Bi}_2\text{Te}_2\text{Se}$ and $\text{Bi}_2\text{Se}_2\text{Te}$ for the first time by our novel S-ARPES. The markedly high spin polarization of topological surface states has been found to be 77% and is persistent in the wide energy range across ED in those compounds. The finding promises to extend the variety of spintronic applications.

P2.23

Time-resolved ARPES investigation of the effective Fermi-Dirac distribution of Bi_2Se_3

A. Crepaldi (presenter) *Elettra-Sincrotrone Trieste*, F. Cilento *Elettra-Sincrotrone Trieste*, B. Ressel *Elettra-Sincrotrone Trieste*, M. Zacchigna *IOM-CNR Laboratorio TASC*, C. Cacho *STFC Rutherford Appleton Laboratory*, E. Turcu *STFC Rutherford Appleton Laboratory*, E. Springate *STFC Rutherford Appleton Laboratory*, K. Kern *Max-Planck-Institut für Festkörperforschung*, M. Grioni *Ecole Polytechnique Federale de Lausanne (EPFL)*, F. Parmigiani *Universita degli Studi di Trieste Italy*, H. Berger *Ecole Polytechnique Federale de Lausanne (EPFL)*, P. Bugnon *Ecole Polytechnique Federale de Lausanne (EPFL)*

Topological insulators constitute a new quantum phase of matter, theoretically proposed [1] and experimentally identified by means of STM/STS [2] and ARPES [3], namely with spin resolution [4]. The topological protection granted by the inverted band gap, along with the spin polarization of the surface state, makes this family of compound extremely appealing for application in spintronics devices. This motivated thorough investigations of the surface transport properties [5], which are partially hindered by the bulk conduction band.

The absence of back-scattering [2] makes more and more important the role of phonons as a mechanism to mediate electron scattering. Recently, a surprisingly small electron-phonon coupling has been reported by static ARPES at the surface of Bi_2Se_3 [6].

We present here our detailed time resolved ARPES (tr-ARPES) investigation of the out-of-equilibrium electronic properties of Bi_2Se_3 . Tr-ARPES represents a unique experimental tool to access the electronic coupling to the various phonon modes, by investigating the relaxation of the effective Fermi-Dirac distribution [7]. Recently, several TR-ARPES studies reported a long lasting out-of-equilibrium signal in the Dirac cone [8, 9], whose characteristic relaxation time provides a direct insight in the scattering mechanism between the bulk conduction band and the Dirac particle [7, 10].

For the first time here we report also a TR-ARPES study of Bi_2Se_3 with the use of extreme UV light, as generated by high harmonics of the Ti-

Sa laser. The higher kinetic energies, ten times larger than in standard laser-based setup, provides us enhanced surface sensitivity, paving the way for the direct access to the electronic scattering mechanism at the surface of topological insulators.

- [1] L. Fu et al., Phys. Rev. Lett. 98, 106803 (2007).
- [2] P. Roushan et al., Nature (London) 460, 1106 (2009).
- [3] D. Hsieh et al., Nature (London) 452, 970 (2008).
- [4] D. Hsieh et al., Nature (London) 460, 1101 (2009)
- [5] Y. Zhang et al., Nature Phys. 6, 584 (2010).
- [6] Z.-H. Pan et al., Phys. Rev. Lett. 108, 187001 (2012).
- [7] A. Crepaldi et al., Phys. Rev. B, 86, 205133 (2012).
- [8] J. A. Sobota et al., Phys. Rev. Lett. 108, 117403 (2012).
- [9] M. Hajlaoui et al., NanoLett. 12, 3532 (2012).
- [10] Y. H. Wang et al., Phys. Rev. Lett. 109, 127401 (2012).

P2.25

2PPE measurement on $\text{Sb}_2\text{Te}_2\text{S}$ with an angle-resolving time-of-flight spectrometer

T. Kunze (presenter) *FU Berlin & SPECS GmbH*, D. Lawrenz *FU Berlin*, M. Teichmann *FU Berlin*, T. U. Kampen *SPECS GmbH*, M. Weinelt *FU Berlin*

We present two-photon photoemission measurements on the p-doped topological insulator $\text{Sb}_2\text{Te}_2\text{S}$. The Dirac cone of this system lies above the Fermi energy and is therefore only accessible using two-photon photoemission.

We detect the photoemitted electrons with an angle-resolving time-of-flight spectrometer. This instrument allows us to measure the kinetic energy E as a function of k_x and k_y without rotating the sample. Our laser system with two OPAs gives us the opportunity to choose the energy of the infrared and ultraviolet pulse independently. This allows us to create a resonant population and efficient probing of the Dirac cone.

The population dynamics of $\text{Sb}_2\text{Te}_2\text{S}$ have been analyzed. We determined the lifetime of the first and second image-potential states. The Dirac cone is populated by indirect filling via the conduction band. The relaxation of the Dirac cone happens on a much larger picosecond timescale.

P2.26

Lifetime broadening of topological surface states with and without deposited magnetic moments

M. Scholz (presenter) *University of Würzburg and Helmholtz Zentrum Berlin*, J. Sánchez-Barriga *Helmholtz-Zentrum Berlin*, D. Marchenko *Helmholtz-Zentrum Berlin*, A. Varykhalov *Helmholtz-Zentrum Berlin*, E. Rienks *Helmholtz-Zentrum Berlin*, L. Yashina *Moscow State University*, A. Volykhov *Moscow State University*, O. Rader *Helmholtz-Zentrum Berlin*

The lifetime broadening of the angle-resolved photoemission signal from the surface states of Bi_2Se_3 and Bi_2Te_3 is studied. It is revealed that hexagonal warping in Bi_2Te_3 introduces an anisotropy for electrons propagating along GK and GM. Moreover, we show that the electron-phonon coupling strength is substantial and in good agreement with theoretical predictions. The small Fermi surface is believed to limit the number of phonon modes for electron scattering. In line with this, the imaginary part of the self-energy from the surface state electrons declines with higher binding energies. In addition, we find that Fe surface impurities have a much stronger influence on the lifetimes as compared to Ag. This is independent of the sign of the doping which is p-type when Fe is deposited at low temperature.

P2.27

Bi thin films on $\text{InAs}(111)$: a potential topological insulator

K. Hricovini (presenter) *Université de Cergy-Pontoise*, C. Richter *Université de Cergy-Pontoise*, O. Heckmann *Université de Cergy-Pontoise*, W. Wang *Linköping University*, H. Ebert *LMU München*, J. Minar *LMU München*, J. Braun *LMU München*, M. Leandersson *Lund University*, J. Sadowski *Lund University*, B. Thiagarajan *Lund University*, J. M. Mariot *Université Pierre et Marie Curie*, J. Kanski *Chalmers University of Technology*

The growth of thin films can open a new route in the search for technologically interesting topological insulators (TI). The lattice distortion, a parameter that can be controlled in thin films, plays an essential role for the band inversion, which appears to be a key ingredient for topologically non-trivial materials [1].

A single, free standing $\text{Bi}(111)$ bi-layer has been predicted by calculations to be a TI [2]. Another theoretical study [3] indicates more complex behaviour of $\text{Bi}(111)$ films. This clearly indicates that the electronic properties of Bi thin films are far from being understood. In fact, it appears that all the $\text{Bi}(111)$ ultrathin films are characterized by a nontrivial Z2 number independent of the film thickness. This is a special interesting class of films having an intermediate inter-bi-layer coupling strength that may have a significant influence on the topological properties [3]. It should be noted that the substrate may have additional effects on the electronic structure and hence on the topological properties of Bi films, which is of interest for future studies.

We have deposited Bi thin layers on both $\text{InAs}(111)$ -A and -B surfaces. As these $\text{InAs}(111)$ surfaces have different termination (A is In terminated; B is As terminated), the reactivity of Bi thin layers is expected to be different. Bi growth is epitaxial on the $\text{InAs}(111)$ -A surface, and a Bi monocrystal of very high quality is obtained after depositing several bi-layers. Annealing results in removing the Bi film, except 1 ML that remains on both faces of the substrate.

The electronic structure in the vicinity of the Fermi level is strongly

POSTER SESSION 2 TUESDAY, 18:50–21:00

face-dependent. On face A, the surface metallic state existing on the Bi crystal is conserved and a new surface state appears in the close vicinity of the point. The dispersion of this new surface state seems to collapse in a Dirac point at $k = 0$. The situation on InAs(111)-B is completely different. The surface state of the bare Bi monocrystal disappears and is replaced by a new state with a clear parabolic dispersion. The spectral intensity of this state is extremely high, comparable to the emission of bulk band states. It appears that this surface state is a result of an “amplification” of the accumulation layer observed not only on the InAs(111) surface [4] but, more generally, on various InAs surfaces [5]. The amplification of the state is due to downward band bending, Bi being a donor on InAs surfaces. Here, the situation is equivalent to a ladder of two-dimensional electron gas states within the surface quantum well observed by King et al. [6].

We performed as well spin-resolved photoemission on the Bi/In-As(111)-B surface state and we measured a spin polarization. The bands show a weak splitting due a Rashba-type spin-orbit coupling. The splitting is very small (a few meV), similar to what was measured on ultrathin Pb quantum wells [7].

[1] Z. Zhu et al., Phys. Rev. B 85, 235401 (2012).

[2] M. Wada et al., Phys. Rev. B 83, 121310(R) (2011).

[3] Z. Liu et al., Phys. Rev. Lett. 107, 136805 (2011).

[4] K. Szamota-Leandersson et al., Surf. Sci., 605, 12 (2011).

[5] L.Ö. Olsson et al., Phys. Rev. Lett. 76, 3626 (1996).

[6] P.D.C. King et al., Phys. Rev. Lett. 107, 096802 (2011).

[7] J.H. Dil et al., Phys. Rev. Lett. 10, 266802 (2008).

P2.28

The effects of band bending on the topological insulator $\text{Bi}_2\text{Se}_{3-x}\text{Te}_x$

N. de Jong (presenter) *IoP UvA*

Topological insulators (TIs) have become a large area of interest in the hard condensed matter community. Ideal 3D topological insulators have an insulating bulk with topologically protected surface states crossing the Fermi level. These states are promising candidates for applications in spintronic devices and for the “hunt” of Majorana fermions [1]. Research effort has been concentrated on TI compounds of the $\text{Bi}_2\text{Se}_{3-x}\text{Te}_x$ family. Single crystals from this family show a typical semiconducting character because of added carriers by impurities. Such semiconducting character is at the origin of surface band bending which may result into the formation of spin-split 2D quantum well states [2]. However, there is no information of how bending influences the topological surface states under surface illumination typical for ARPES experiments.

Here we present ARPES measurements on different compositions from the $\text{Bi}_{2-y}\text{Sb}_y\text{Se}_{3-x}\text{Te}_x$ family with a view to the effect of illumination,

residual pressure and temperature on the sign and magnitude of the surface band bending. We conclude that there is a direct competition between the illumination flux and the residual pressure with respect to the energy position of the surface and bulk bands. The surface photovoltage effect tends to counterbalance the initial band bending. We investigate the spatial and temporal scales of the illumination effect and stress its importance even with moderate synchrotron radiation illumination.

[1] M. Z. Hasan and C.L. Kane, Rev. Mod. Phys. 82, 3045 (2010).

[2] P. D. C. King et al. Phys. Rev. Lett. 107, 096802 (2011).

P2.29

Switch of coupled spin-orbital texture in topological insulators

Y. Cao (presenter) *University of Colorado*, J. Waugh *University of Colorado*, X. W.

Zhang *National Renewable Energy Laboratory*, J. W. Luo *National Renewable Energy*

Laboratory, Q. Wang *University of Colorado*, T. Reber *University of Colorado*, S.

Parham *University of Colorado*, N. Plumb *Swiss Light Source*, G. Landolt *University*

of Zurich, J. H. Dil *University of Zurich*, S. K. Mo *Advanced Light Source*, Z. Xu *Brook-*

haven National Laboratory, A. Yang *Brookhaven National Laboratory*, J. Schneeloch

Brookhaven National Laboratory, G. D. Gu *Brookhaven National Laboratory*, M.

Brahlek *Rutgers University*, N. Bansal *Rutgers University*, S. Oh *Rutgers University*,

A. Zunger *University of Colorado*, D. Dessau *University of Colorado*

A hand-waving picture of the Dirac state employs a chiral spin texture. However, due to the strong spin-orbit coupling inherent in the topological insulators, spin is not a good quantum number of the Dirac state. Instead we would like to map the orbital components of the Dirac wavefunction and explore how spin and orbital degrees of freedom couple and contribute to the total angular momentum J , which is a candidate of a conserved quantity. Here we present results from orbital-selective and spin-resolved ARPES experiments and first-principles calculations that map the complete wavefunction of the topological state. Our results show the topological wavefunction has a coupled spin-orbital texture – a superposition of orbital wavefunctions coupled with the corresponding spin textures. The in-plane orbital wavefunction is asymmetric relative to the Dirac Point (DP), switching from being predominantly tangential to the k -space constant energy surfaces above the DP, to being predominantly radial to them below the DP. The orbital texture switch occurs exactly at the DP and therefore is intrinsic to the topological physics, which is absent in the known descriptions of the topological Dirac state. Also, the in-plane orbital wavefunction above the Dirac point couples to a “backwards” right-handed spin texture, in contrast to previous theoretical and experimental findings.

P2.30

Creation of helical Dirac fermions by interfacing two gapped systems of ordinary fermions

M. Yao (presenter) *Shanghai Jiao Tong University*

Topological insulators are a unique class of materials characterized by a Dirac cone state of helical Dirac fermions in the middle of a bulk gap. When the thickness of a three-dimensional topological insulator is reduced, however, the interaction between opposing surface states opens a gap that removes the helical Dirac cone, converting the material back to a normal system of ordinary fermions. Here we demonstrate, using density function theory calculations and experiments, that it is possible to create helical Dirac fermion state by interfacing two gapped films—a single bilayer Bi grown on a single quintuple layer Bi₂Se₃ or Bi₂Te₃. These extrinsic helical Dirac fermions emerge in predominantly Bi bilayer states, which are created by a giant Rashba effect with a coupling constant of ~ 4 eV·Å due to interfacial charge transfer. Our results suggest that this approach is a promising means to engineer topological insulator states on non-metallic surfaces.

P2.31

Graphene Sublattice Symmetry and Isospin Determined by Circular Dichroism in Angle-Resolved Photoemission Spectroscopy

C. Ast (presenter) *Max-Planck-Institute for Solid State Research*, I. Gierz *Max-Planck Research Group for Structural Dynamics*, M. Lindroos *Tampere University of Technology*, H. Höchst *Synchrotron Radiation Center Stoughton*, K. Kern *Max-Planck-Institute for Solid State Research*

The Dirac-like electronic structure of graphene originates from the equivalence of the two basis atoms in the honeycomb lattice. We show that the characteristic parameters of the initial state wave function (sublattice symmetry and isospin) can be determined using angle-resolved photoemission spectroscopy (ARPES) with circularly polarized synchrotron radiation. At a photon energy of 52 eV, transition matrix element effects can be neglected allowing us to determine sublattice symmetry and isospin with high accuracy using a simple theoretical model.

P2.32

Electron-phonon coupling at doped metal-graphene interfaces studied by angle-resolved photoemission spectroscopy

A. Grueneis (presenter) *University of Vienna*, A. Fedorov *IFW-Dresden*, D. Haberer *IFW-Dresden*, N. Verbitskiy *University of Vienna*, O. Vilkov *TU-Dresden*, D. Vyalikh *TU-Dresden*, C. Struzzi *Elettra-Sincrotrone Trieste*, S. Fabris *Elettra-Sincrotrone Trieste*, J. Fink *IFW-Dresden*, L. Petaccia *Elettra-Sincrotrone Trieste*

Graphene represents a new class of two-dimensional (2D) materials

which are only one atom thick. Since all its atoms are located on the surface, graphene can easily be functionalized chemically. We study how ionic functionalization can tailor the spectral function of graphene and show how doping of quasi-free-standing graphene by alkali and alkaline earth metals increases the carrier concentration. The electronic properties depend sensitively on whether the alkali(-ne) adatoms are located on top or under graphene. The location of these guest atoms is determined using angle-resolved x-ray photoemission spectroscopy carried out at the RBL beamline of the BESSY 2 synchrotron. High resolution ARPES data of samples prepared in the same way at the BaDElPh beamline (ELETTRA, Trieste) allow for measurements of the kink in the spectral function induced by electron-phonon coupling. To that end we performed a direct extraction of the full momentum dependent Eliashberg function from ARPES data of graphene doped up to the maximum by Li, Na, K, Rb, Cs and Ca. We discuss deviations from the rigid band model and the dependence on the guest atom location. Regarding the electron-phonon coupling constant, it is strongly dependent on the guest atom species yielding the largest values for Ca.

P2.33

Exploring unoccupied electronic structure and symmetry of valence bands of graphite using angle-resolved photoemission spectroscopy

S. K. Mahatha (presenter) *Saha Institute of Nuclear Physics*, K. S. R. Menon *Saha Institute of Nuclear Physics*

We report the observation of anomalous bands in graphite valence band structure in angle-resolved photoemission spectroscopy (ARPES) experiments. The photon energy dependence of these bands shows a constant kinetic energy nature. Our results are supported by the very low energy electron diffraction data reported on graphite surfaces which essentially map the unoccupied states representing the photoemission final states. This suggests that the ARPES technique is capable of probing the unoccupied electronic states governed by the secondary electron emission process, along with the occupied bands of solids. Whereas direct information on the symmetry of the initial electronic states are achieved by performing ARPES experiments with different polarization of light. Our experimental results shows that the σ_1 and σ_2 valence bands of graphite are of odd reflection symmetry and π valence band is of even symmetry. ARPES spectrum measured with LCP and RCP light shows intensity asymmetry. The intensity of σ_1 and σ_3 band along Γ M is reversed at the M point of the Brillouin zone upon changing the helicity of light, due to their different partial wave nature.

P2.34

POSTER SESSION 2 TUESDAY, 18:50–21:00

Can graphene be turned into a topological insulator?

C. Straßer (presenter) *Max Planck Institute for Solid State Research*, B. Ludbrook *Quantum Matter Institute, UBC*, A. Damascelli *Quantum Matter Institute, UBC*, C. Ast *Max Planck Institute for Solid State Research*, K. Kern *Max Planck Institute for Solid State Research*

In 2005, Kane and Mele [1] claimed that graphene opens a band gap at very low temperatures due to spin orbit coupling (SOC) and becomes a quantum spin Hall insulator. Since the SOC is very weak in carbon atoms the size of the gap is very small and experimentally not observable. Recently Weeks et al. [2] showed theoretically that the intrinsic SOC can be enhanced by depositing small amounts of heavy adatoms on top of a graphene sheet. The electrons which hop on the adatoms and back to the graphene sheet induce higher SOC. Calculations showed that this gives rise to a band gap of $\Delta(\text{SOC})=21$ meV at the K-point which should be observable with spectroscopic methods.

We performed angular resolved photoemission spectroscopy measurements at very low temperatures on epitaxial graphene on SiC. To induce higher SOC we decorated the sample with small amounts of Thallium. We observed n-doping due to electron transfer from the adatoms to the graphene sheet. The doping level is increasing with coverage up to a maximum of 200 meV. The band shift and careful analysis of a possible gap opening will be presented in detail.

[1] C. L. Kane et al., *Phys. Rev. Lett.* 95, 226801 (2005).

[2] C. Weeks et al., *Phys. Rev. X* 1, 021001 (2011).

P2.35 Many-body interactions in the σ -band of graphene

F. Mazzola (presenter) *Norwegian University of Science and Technology (NTNU)*, J. Wells *Norwegian University of Science and Technology (NTNU)*, S. Ulstrup *Aarhus University*, J. Miwa *Aarhus University*, R. Balog *Aarhus university*, M. Bianchi *Aarhus University*, M. Leandersson *MAX-IV Laboratory*, J. Adell *MAX-IV Laboratory*, P. Hofmann *Aarhus University*, T. Balasubramanian *MAX-IV Laboratory*

Contrary to the case of Graphene's π -band structure, the deeper lying σ -bands have attracted little attention. For example, experimental studies of many body effects (such as electron-phonon coupling), have been limited to the π -bands only.

Here we present a detailed study of the σ -band structure using angle resolved photoemission spectroscopy (ARPES). Graphene is prepared on different substrates and it is compared with graphite and quasi free standing graphene (graphene which is lifted up by oxygen intercalation after growth on Ir(111)).

We find that such bands hide an unexpected large interaction close to the Gamma-bar point. A "kink" deviates the band from the expected dispersion of a non-interacting band, and a corresponding broadening

of the line width is seen. The experiment is supported by a numerical simulation of the many-body interaction, such that the nature of the kink can be probed. We conclude that electron phonon coupling plays a significant role and can satisfactorily account for the observed kink.

P2.36 Snapshots of non-equilibrium Dirac carrier distributions in graphene

I. Gierz (presenter) *Max Planck Institute for the Structure and Dynamics of Matter*, J. C. Petersen *Max Planck Institute for the Structure and Dynamics of Matter and University of Oxford*, M. Mitrano *Max Planck Institute for the Structure and Dynamics of Matter*, C. Cacho *STFC Rutherford Appleton Laboratory*, E. Turcu *STFC Rutherford Appleton Laboratory*, E. Springate *STFC Rutherford Appleton Laboratory*, A. Stöhr *Max Planck Institute for Solid State Research*, A. Köhler *Max Planck Institute for Solid State Research*, U. Starke *Max Planck Institute for Solid State Research*, A. Cavalleri *Max Planck Institute for the Structure and Dynamics of Matter and University of Oxford*

Graphene has a conical electronic dispersion with zero density of states at the Dirac point where the valence and conduction bands touch. The resulting bottleneck for carrier recombination may enable new optical applications based on saturable absorption [1] or even optical gain at terahertz frequencies [2]. Moreover, absorbing a single photon might create multiple electron-hole pairs via impact ionization [3], considerably increasing the efficiency of graphene-based solar cells. With time- and angle-resolved photoemission spectroscopy, we can investigate the feasibility of such proposed optoelectronic devices by directly mapping out the transient occupation of electronic states as a function of momentum and energy.

We have excited slightly p-doped epitaxial graphene monolayers [4] at photon energies both below and above the threshold energy for direct interband transitions. We find that low-energy excitation at 300 meV accelerates the Dirac carriers in the mid-infrared light field, resulting in an enhanced electronic temperature followed by rapid cooling. Direct interband excitation at 950 meV produces a short-lived population inversion, relaxing to a metal-like state characterized by a single Fermi-Dirac distribution with elevated electronic temperature within 130 femtoseconds. Finally, we find no evidence for charge carrier multiplication in either of the two excitation regimes, questioning the suitability of graphene for applications in light harvesting.

[1] Z. Sun et al., *ACS Nano* 4, 803 (2010).

[2] T. Li et al., *Phys. Rev. Lett.* 108, 167401 (2012).

[3] T. Winzer et al., *Nano Lett.* 10, 4839 (2010).

[4] C. Riedl et al., *Phys. Rev. Lett.* 103, 246804 (2009).

P2.37

Hot carrier relaxation on the Dirac cone in quasi free-standing graphene probed by time- and angle-resolved photoemission

J. C. Johannsen (presenter) *École Polytechnique Fédérale de Lausanne (EPFL)*, S. Ulstrup *Aarhus University*, F. Cliento *Sincrotrone Trieste*, A. Crepaldi *Sincrotrone Trieste*, M. Zacchigna *IOM-CNR Laboratorio TASC*, B. Ressel *Sincrotrone Trieste*, C. Cacho *STFC Rutherford Appleton Laboratory*, E. Turcu *STFC Rutherford Appleton Laboratory*, E. Springate *STFC Rutherford Appleton Laboratory*, F. Fromm *University of Erlangen-Nürnberg*, C. Raidel *University of Erlangen-Nürnberg*, T. Seyller *Chemnitz University of Technology and University of Erlangen-Nürnberg*, L. Hornekaer *Aarhus University*, F. Parmigiani *Sincrotrone Trieste and Università degli Studi di Trieste*, M. Grioni *École Polytechnique Fédérale de Lausanne (EPFL)*, P. Hofmann *Aarhus University*

Electron-phonon mediated cooling in graphene is a heavily debated subject with central importance for the design of photonics and electronics devices. Recent time-resolved experiments based on the photocurrent response of graphene devices revealed that disorder assisted electron-phonon scattering, so-called supercollisions, dominate cooling processes above the Bloch-Grüneisen temperature [1-2]. Here we study this regime with momentum resolution around the Dirac point for the first time using time- and angle-resolved photoemission spectroscopy (TR-ARPES). Particularly, we probe the out-of-equilibrium electronic properties around the Dirac cone of quasi free-standing monolayer graphene on SiC, obtained by hydrogen intercalation. The sample is excited with a 0.95 eV laser pulse and probed using XUV light with a temporal resolution of 60 fs. Since the sample is p-doped (Dirac point ~250 meV above Fermi level) we study direct transitions of Dirac particles from the π to the π^* band and their relaxation dynamics.

We identify two characteristic timescales in the relaxation of the electronic temperature at the Dirac point: A 250 fs process, which we ascribe to optical phonons, and a 2.5 ps process, which we describe with a T3-dependence characteristic for supercollisions. Through our analysis we obtain the electron-phonon coupling strengths λ_1 and λ_2 describing the electron-optical phonon and supercollision mediated electron-lattice couplings, respectively. We find both λ_1 and λ_2 to be extremely low (< 0.01) in good agreement with both theoretical expectations and ARPES measurements of the same sample [3].

[1] M. W. Graham et al., *Nature Phys.* 9, 103 (2013).

[2] A. C. Betz et al., *Nature Phys.* 9, 109 (2013).

[3] J. C. Johannsen et al., *J. Phys. Condens. Matter* 25, 094001 (2013).

P2.38

Correlation effects in the spin resolved band structure of cobalt measured by spin polarized momentum microscopy

C. Tusche (presenter) *Max-Planck-Institut für Mikrostrukturphysik*, M. Ellguth *Max-Planck-Institut für Mikrostrukturphysik*, A. Krasnyuk *Max-Planck-Institut für Mikrostrukturphysik*, A. Winkelmann *Max-Planck-Institut für Mikrostrukturphysik*, C. Wiemann *Forschungszentrum Jülich*, V. Feyer *Forschungszentrum Jülich*, M. Patt *Forschungszentrum Jülich*, C. M. Schneider *Forschungszentrum Jülich*, J. Henk *Martin-Luther-Universität Halle-Wittenberg*, J. Kirschner *Max-Planck-Institut für Mikrostrukturphysik*

One of the most fundamental concepts in solid state physics is the description of the motional and energetic degrees of freedom of the electrons by the relation of the energy E vs. the crystal momentum k in a band structure of independent particles. In a real electron system, exchange- and correlation interaction are collective phenomena that lead, for instance, to effects like ferromagnetism. The 3d ferromagnets Fe, Ni, and Co, therefore represent a prototypical system of correlated electrons. For these ferromagnets, a description of the band structure in the widely used local density approximation (LDA) is of limited use, as seen by the fact that predicted well defined electronic bands are not observed experimentally. This was attributed to the finite lifetime of the quasi-particle states of the interacting system [1].

An efficient tool for the quantitative understanding of the quasi-particle band structure of ferromagnets, even in absence of sharp spectral features, is spin resolved momentum microscopy. A spin polarizing electron mirror [2] allows the simultaneous measurement of the spin polarization of the photoelectrons in the whole k_{\parallel} momentum space, for the first time. Here, we present comprehensive maps of the spin resolved band structure of cobalt grown on Cu(100), measured at the NanoESCA beamline [3] of the Elettra synchrotron. For these measurements, the imaging spin filter was installed temporarily at this instrument. The spin resolved momentum maps of cobalt show that the intensity at the Fermi surface is dominated by sharp minority bands. Already at 300 meV below E_F we observe a strong positive spin-polarization of the majority cobalt states. At larger binding energies sharp bands are only observed in the minority channel, supporting recent advanced concepts in theory for the refined treatment of spin-dependent electron correlation.

[1] J. Sánchez-Barriga et al., *Phys. Rev. B* 82, 104414 (2010).

[2] C. Tusche et al., *Appl. Phys. Lett.* 99, 032505 (2011).

[3] C. Wiemann et al., *e-J. Surf. Sci. Nanotech.* 9, 395 (2011).

POSTER SESSION 2 TUESDAY, 18:50–21:00

P2.39

Electronic and magnetic properties of isolated atoms on surfaces

S. Gardonio (presenter) *University of Nova Gorica*, T. Wehling *University of Bremen*, L. Petaccia *Elettra Sincrotrone Trieste*, S. Lizzit *Elettra Sincrotrone Trieste*, A. Goldoni *Elettra Sincrotrone Trieste*, P. Gambardella *Swiss Federal Institute of Technology Zurich*, M. Veronese *Elettra Sincrotrone Trieste*, C. Grazioli *Elettra Sincrotrone Trieste*, University of Nova Gorica, P. Moras *Consiglio Nazionale delle Ricerche*, M. Karolak *University of Hamburg*, A. Lichtenstein *University of Hamburg*, C. Carbone *Consiglio Nazionale delle Ricerche*

The magnetic and transport properties of a materials drastically change in low-dimensional surface structures, such as thin films, small clusters, and isolated adatoms. The discrete, localized states of an isolated atom brought in contact with a metal surface are known to spread into resonance levels, whose energy and width determine the survival or quenching of the magnetic moments. We have shown that by use of photoemission spectroscopy (PES), X-absorption spectroscopy (XAS) combined with X-ray magnetic circular dichroism (XMCD) it is possible to examine the electronic configuration of highly diluted magnetic atoms on surfaces [1-4]. We report here experimental and theoretical results on three model systems: Fe isolated atoms on alkali metal film, Ce atoms on Ag(100), W(110) and Rh(111) surfaces and Mn, Fe, Co and Ni atoms on Ag(100) surface. The results demonstrates that a reliable understanding of magnetic adatoms on metal surfaces requires simultaneous low and high energy spectroscopic information. We observe the interplay between delocalization, mediated by the free-electron environment, and Coulomb interaction among d and f electrons which gives rise to complex electronic configurations. We examine how the energy dependence of the impurity hybridization with the surface, together with the exchange splitting with increasing filling of 3d-shell, determines the shape of excitation spectra. With increasing hybridization we observe the quenching of the orbital moment and the screening of the local magnetic moment.

[1] P. Gambardella et al., *Phys. Rev. Lett.* 84, 047202 (2002).

[2] C. Carbone et al. *Phys. Rev. Lett.* 104, 117601 (2010).

[3] S. Gardonio et al., *Phys. Rev. Lett.* 107, 026801 (2011).

[4] S. Gardonio et al., submitted to *Phys. Rev. Lett.* (2013).

P2.40

Quantum well states in Ag thin films on MoS₂(0001) surface

S. K. Mahatha (presenter) *Saha Institute of Nuclear Physics*, K. S. R. Menon *Saha Institute of Nuclear Physics*

In-plane dispersions of quantum well (QW) states originating from the electron confinement of Ag sp electrons within the MoS₂ band gap region are investigated by means of angle-resolved photo-emis-

sion spectroscopy (ARPES). A number of QW resonances have been observed in the ARPES spectra in a binding energy range lying outside the MoS₂ energy gap which is required for full confinement of the Ag sp electrons. In spite of having the expected free electron-like behavior, these QW states show a significant increase of in-plane effective mass with increasing binding energy due to the hybridization of Ag sp electrons with the MoS₂ valence bands. The binding energy dependence of the bottom of the QW states as a function of the Ag film thickness has been analyzed. The well-established phase accumulation model has been applied for calculating the phase shifts of electrons at the boundaries. Our observations show that the total phase shift behaves differently for energies above and below the MoS₂ valence band maxima, due to the hybridization being different in nature. The structure plot calculated considering the different quantum number dependent total phase shifts provides a good description of the experimental observations.

P2.41

Why does adding transition metal to Pt increase the surface reactivity

Y. S. Kim (presenter) *Seoul National University*, S. H. Jeon *Seoul National University*, B. S. Mun *Gwangju Institute of Science and Technology*, S. Han *Seoul National University*, A. Bostwick *Lawrence Berkeley National Laboratory*, E. Rotenberg *Lawrence Berkeley National Laboratory*, P. N. Ross *Lawrence Berkeley National Laboratory*, V. R. Stamenkovic *Argonne National Laboratory*, N. Markovic *Argonne National Laboratory*, A. Walter *Lawrence Berkeley National Laboratory*, Y. J. Chang *Lawrence Berkeley National Laboratory*, T. W. Noh *Seoul National University*, H. K. Yoo *Seoul National University*

Pt-based catalyst system is one of the extensively investigated and used catalyst systems for a renewable energy and environmental technology, such as fuel cell and catalytic converter. However, the realization of a commercially viable Pt-based catalyst system requires significant lower Pt content and faster reaction kinetics.

Interestingly, recent investigations on the Pt-based alloys found that adding transition metal (TM) resulted in even higher catalytic activity in the oxygen reduction reaction (ORR) than pure Pt. It has been suggested that the modified electronic structure of Pt-TM system may contribute to the improved catalytic efficiency. However, there have been few experimental attempts to identify the surface electronic structure of Pt and Pt-TM systems and few studies on the role of TM in modifying the surface electronic structure. In addition, the nature of chemical bonding between Pt-TM and oxygen is yet to be clarified. In this presentation, using the combination of state-of-the-art angle resolved photoemission spectroscopy (ARPES) and ab initio computation, we will explain why TM-containing Pt-catalyst shows faster oxygen reaction. Based on our results, we will identify the major

contributor of the oxidation bonding process. Moreover, we will reveal that how transition metal can affect to the electronic structure and how they contribute to the key process of oxygen chemical bonding. This acquired fundamental knowledge on the chemisorbed oxygen on the Pt-alloy surface will serve as the basis for the full understanding of catalytic reactions of Pt-alloy system and search for the commercially viable Pt alternatives.

P2.42 High-resolution ARPES study of the electron self-energy and coupling parameters in palladium

K. Shimada (presenter) *Hiroshima University*, H. Hayashi *Hiroshima University*, J. Jiang *Hiroshima University*, H. Iwasawa *Hiroshima University*, Y. Aiura *National Institute of Advanced Industrial Science and Technology*, T. Oguchi *Osaka University*, H. Namatame *Hiroshima University*, M. Taniguchi *Hiroshima University*

We have investigated the electronic structure and electron self-energy of palladium single crystals using polarization-dependent high-resolution angle-resolved photoemission spectroscopy [1]. A detailed comparison between the observed and theoretical band dispersions of the Σ_1 band forming the electron-like Fermi surface indicates an electron-electron coupling parameter of ~ 0.02 . Near the Fermi level, a kink structure in the energy-band dispersion exists at ~ 20 meV, in agreement with the Debye energy. The electron-phonon coupling parameter is estimated to be 0.39 at 8 K, which is consistent with the theoretical values of 0.38 [2] and 0.40 [3]. Furthermore, analysis of the self-energy indicated a possible contribution from the electron-paramagnon interaction in the energy range of $[-50, -150]$ meV. The evaluated electron-paramagnon coupling parameter is ~ 0.06 . The sum of the obtained coupling parameters becomes ~ 0.5 for the Σ_1 band, which is fully consistent with the effective mass enhancement evaluated by the de Haas-van Alphen measurements [4].

[1] H. Hayashi et al., *Phys. Rev. B* 87, 035140 (2013).

[2] T. Takezawa et al., *Phys. Rev. B* 71, 012515 (2005).

[3] I. Yu Sklyadneva et al., *J. Phys.: Condens. Matter* 18, 7923 (2006).

[4] W. Joss and G. W. Crabtree, *Phys. Rev. B* 30, 5646 (1984).

P2.43 From surface to interface: a study of low-dimensional electron gases on SrTiO_3 and in $\text{LaAlO}_3/\text{SrTiO}_3$

N. Plumb (presenter) *Swiss Light Source, Paul Scherrer Institut*, M. Radovic *Swiss Light Source, Paul Scherrer Institut*, J. Minar *Ludwig-Maximilians-Universität München*, J. Mesot *Paul Scherrer Institute*, T. Schmitt *Swiss Light Source, Paul Scherrer Institut*, L. Patthey *SwissFEL, Paul Scherrer Institute*

Transition metal oxide surfaces, thin films, and interfaces are at the

frontier of developing next-generation multifunctional devices. A primary example is the $\text{LaAlO}_3/\text{SrTiO}_3$ (LAO/STO) interface, where a metallic electron gas capable of superconducting and magnetic behavior emerges, despite the fact that bulk LAO and STO are nonmagnetic insulators. Theories about the metallic state's origin have naturally focused on interface-specific phenomena (e.g., ion intermixing, congregation of oxygen vacancies, or the 'polar catastrophe' induced by LAO). However, recent experiments found that bare STO itself can host a universal low-dimension electron gas. This raises the possibility that the two systems are connected, and each may be able to teach us about the origins of metallicity in the other. With this in mind, we have performed a systematic study of the electronic structure of various bare STO substrates and LAO/STO interfaces. In situ high-resolution angle-resolved photoemission spectroscopy (ARPES) and resonant x-ray ARPES, as well as resonant inelastic x-ray scattering (RIXS) uncover remarkable similarities between the electron gases in these systems. Our results suggest that STO and LAO/STO are intimately connected, and we propose that confined polar (ferroelectric) structural distortions in STO play a key role in the appearance of metallicity in these systems. At the same time, however, STO and LAO/STO are not totally equivalent, and an additional structural consideration – instability toward in-plane 2×1 ordering – distinguishes LAO/STO above the classical 'critical thickness' and may be related to its unique properties.

P2.44 Momentum resolved inverse photoemission spectroscopy studies on $\text{Ni}_2\text{MnGa}(100)$ and $\text{Mn}_2\text{NiGa}(100)$ magnetic shape memory alloys

M. Maniraj (presenter) *UGC-DAE Consortium for Scientific Research*, S. W. D'Souza *UGC-DAE Consortium for Scientific Research*, A. Rai *UGC-DAE Consortium for Scientific Research*, J. Nayak *UGC-DAE Consortium for Scientific Research*, D. L. Schlögl *Iowa State University*, T. A. Lograsso *Iowa State University*, A. Chakrabarti *Raja Ramanna Centre for Advanced Technology*, S. R. Barman *UGC-DAE Consortium for Scientific Research*

Ni_2MnGa ferromagnetic shape memory alloy exhibits large magnetic field induced strain [1] and interesting properties such as spin-valve-like magnetoresistance, magnetocaloric effect, as well as existence of charge-density-wave [2]. Since the martensite transition is closely related to the states below and above the Fermi level, here, we present the unoccupied electronic band structure of $\text{Ni}_2\text{MnGa}(100)$ and compare it with a related magnetic shape memory alloy, $\text{Mn}_2\text{NiGa}(100)$ using momentum resolved inverse photoemission spectroscopy (KRIPES). For obtaining the stoichiometric atomically clean surface, we noted that preferential sputtering results in a surface that is Ni-rich and Mn deficient [3]. However, subsequent annealing to high

POSTER SESSION 2 TUESDAY, 18:50–21:00

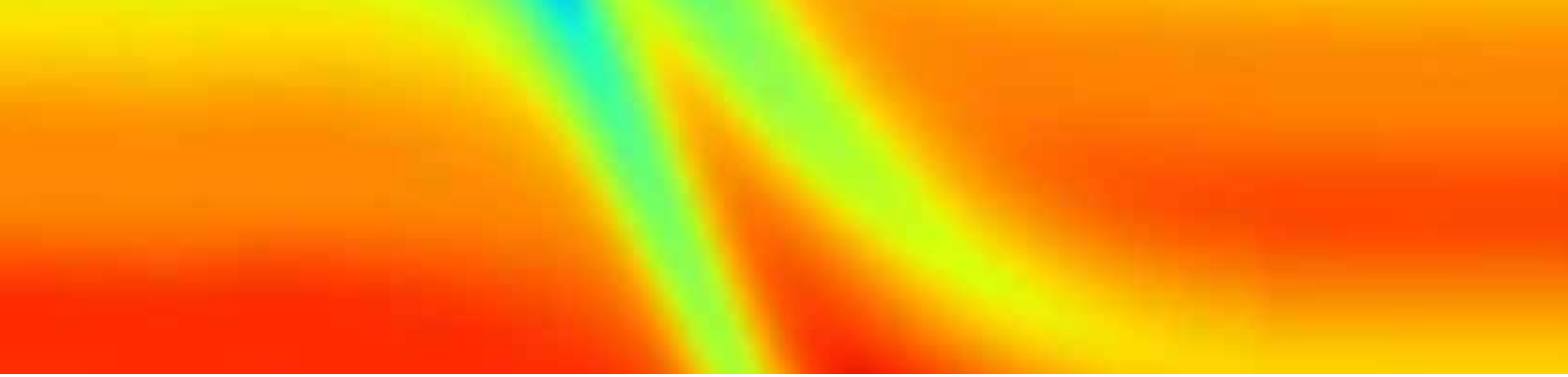
temperature results in a stoichiometric surface because Mn segregates to the surface. The surfaces have been characterized by low energy electron diffraction (LEED) and x-ray photoelectron spectroscopy. The LEED pattern shows that the surface structure changes across the martensitic phase transition, but considerable background intensity and relatively broad spots indicate presence of surface disorder. The KRIPES spectra at normal incidence of the electron beam have been acquired for different surface compositions for both Ni_2MnGa as well as Mn_2NiGa . The experimental results show that Mn related peak position is sensitive to composition, and this is explained by the theoretical calculations based on Korringa-Kohn-Rostoker method. This shift is caused by the changes in the strength of the hybridization between the Ni 3d and Mn 3d states. Further, for $\text{Ni}_2\text{MnGa}(100)$, KRIPES spectra shows significant dispersion away from the Fermi level with momentum parallel to the surface (k_{\parallel}), along $\bar{\Gamma}-\bar{X}$ high symmetry direction in the austenite phase. On the other hand, hardly any dispersion is observed within our limited resolution in the martensite phase. This is because of the increased unit cell dimension due to structural transition in the martensite phase that reduces the dimension of the Brillouin zone size so that it is comparable to the experimental k_{\parallel} resolution (0.13 \AA^{-1}). At an electron incident angle of 30° , there exists a peak just above the Fermi level, which arises due to k-conserved direction transition at the L point of the bulk Brillouin zone. In case of $\text{Mn}_2\text{NiGa}(100)$, a weak dispersion is observed along $\bar{\Gamma}-\bar{X}$ and $\bar{\Gamma}-\bar{M}$ directions.

[1] K. Ullako et al., Appl. Phys. Lett. 69, 1966 (1996); S. J. Murray et al., Appl. Phys. Lett. 77, 886 (2000).

[2] S. Singh et al., Phys. Rev. Lett. 109, 246601 (2012); S. Singh et al., Appl. Phys. Lett. 96, 081904 (2010); S. W. D'Souza et al., Phys. Rev. B 85, 085123 (2012).

[3] R. S. Dhaka et al., Surf. Sci. 603, 1999 (2009); S. W. D'Souza et al., Surf. Sci. 606, 130 (2012).

P2



LOCATION

The workshop CORPES¹³ will be held in the main auditorium of DESY in Hamburg.

DESY Hamburg
Notkestraße 85
22607 Hamburg, Germany

North: +53° 34' 29.62"

West: +9° 52' 39.28"

Link to Google maps: <http://goo.gl/maps/kx8aF>



WIRELESS INTERNET ACCESS

Please use the following parameters for wireless Internet access.

Network name: **CORPES2013**

WPA/WPA2-PSK password: **hXf4sLdzHk**



HOW TO REACH US

BY TRAIN

From Hamburg Altona station:

- » Fast, expensive: Continue by taxi, travelling time approximately 15-20 min.
- » Slow, easiest and cheap: Continue by bus line 1 (direction Schenefelder Holt) directly to the main entrance of DESY (bus stop Zum Hünengrab/DESY), travelling time approx. 25 min.
- » Or fast and cheap (see plan): Continue by S-Bahn (local city train) line S1 or S11 (direction Blankenese/Wedel) to Othmarschen. Then go on with bus line 1 (direction Schenefelder Holt).

BY PLANE

From the Hamburg airport Fuhlsbüttel:

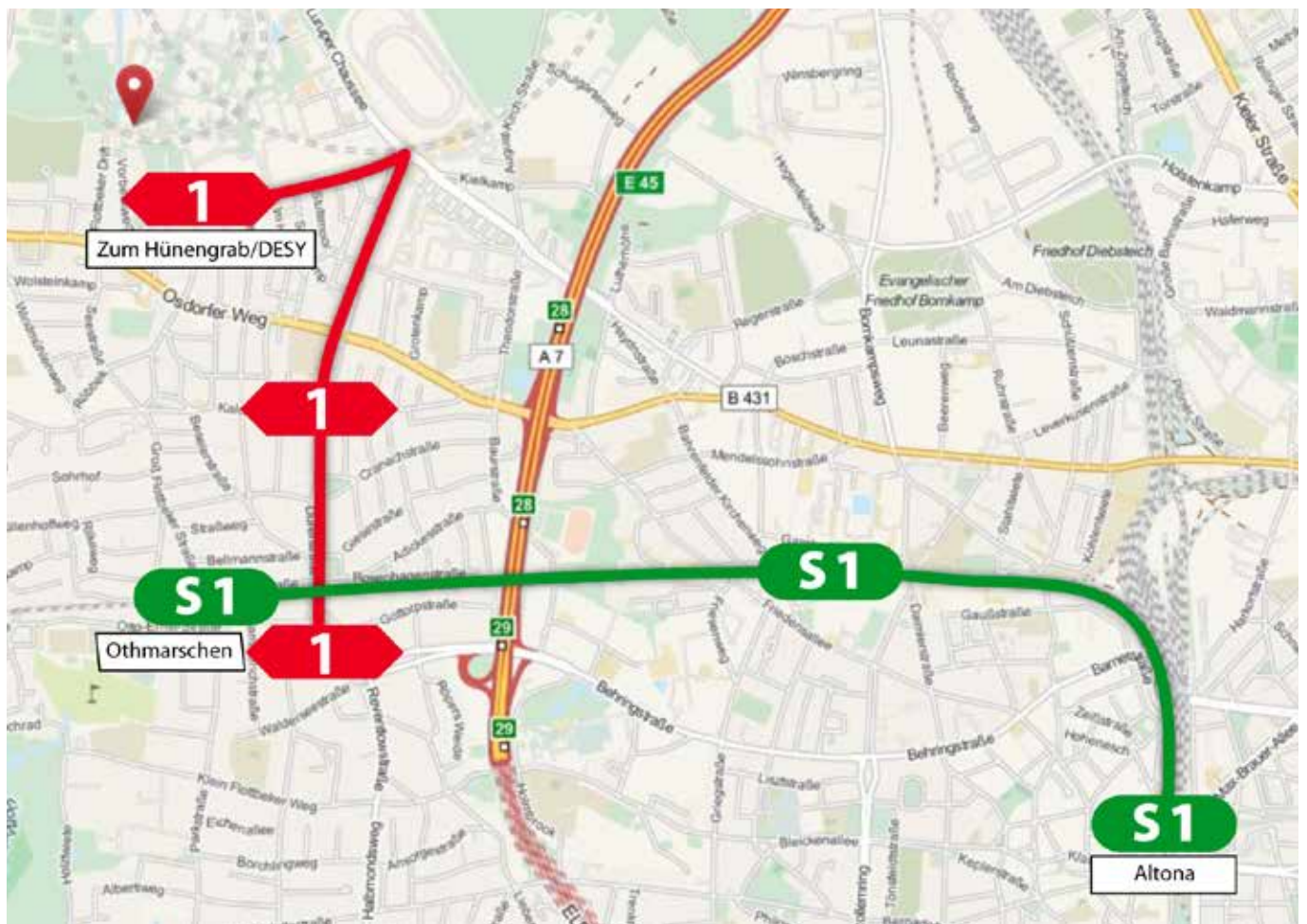
- » Continue by taxi, traveling time approx. 40-50 min.
- » Or continue with city train line S1 (direction Blankenese/Wedel) to Othmarschen station. Then go on with bus line 1 (direction Schenefelder Holt) to the main entrance of DESY (bus stop Zum Hünengrab/DESY).

BY CAR

From Autobahn (A7) exit HH-Bahrenfeld:

- » Arriving in Hamburg from the South: turn left onto the main road (Osdorfer Weg).
- » Arriving in Hamburg from the North: turn right onto the main road (Osdorfer Weg). Then turn right onto Notkestraße. The main entrance of DESY is the second road on the left.

The side entrance of DESY is located on the Luruper Chaussee. The bus line 2 stops there (bus stop „Luruper Chusse/DESY“). The side entrance is open for motorists from Monday until Friday, 06:00 to 19:00, and closed on weekends. It is open for pedestrians and cyclists at all times.



HAMBURG

Economically and culturally, Hamburg is the centre of Northern Germany. 3.5 million people live in this metropolitan region, which offers a rich cultural life. Hamburg alone has 31 theatres, 6 music halls, 10 cabarets, and numerous state and private museums.

PLACES TO SEE, THINGS TO DO

We took the freedom of selecting and adding some suggestions for some specific areas of interests. Please note that the list is not at all exhaustive!

PORT OF HAMBURG

The history of Hamburg is closely related to the development of its port. General information about the Port of Hamburg and its functioning can be found (in 7 languages, also including an overview of vessels currently in the harbor) under:

www.portofhamburg.com

HAFENCITY HAMBURG

A new downtown is growing: Hafencity—currently Europe's largest inner-city development project—is a blueprint for the development of a European city on the waterfront.

A presentation of everything currently happening between the

Elbe bridges and Kehrwiederspitze promontory is on view in the InfoCenter in Kesselhaus.

Am Sandtorkai 30, 20457 Hamburg

www.hafencity.com (InfoCenter)

ART EXHIBITIONS AND MUSEUMS

INTERNATIONAL MARITIME MUSEUM

Precious ancient paintings, model ships, instruments and exhibits related to navigation and marine research are on display in the privately owned International Maritime Museum.

Kaispeicher B, Koreastrasse 1, 20457 Hamburg

www.immhh.de

BALLIN-STADT EMIGRATION MUSEUM

The Ballin-Stadt Emigration museum is dedicated to the five million European emigrants who travelled to America between 1850 and 1934 hoping for a better future overseas. The exhibition focuses on their travelling and living conditions. Furthermore, visitors have access to the information contained in the lists the passengers setting off from Hamburg at that time. A genealogical database is also accessible from the museum research centre.

Veddeler Bogen 2, 20539 Hamburg, S-Bahn station "Veddel" (lines S3 and S31)

www.ballinstadt.net



HAMBURGER KUNSTHALLE

The valuable collection of the Hamburger Kunsthalle ranges from XIV century painting to contemporary art.

Glockengießerwall 20095, Hamburg
Hamburger Kunsthalle

BUCERIUS KUNST FORUM

The Bucerius Kunst Forum (next to the Town Hall) is mainly dedicated to temporary exhibitions—at the time of the meeting, works of Alexander Rodtschenko (1891-1956), one of the major actors of the Russian Avantgarde, will be on display.

Rathausmarkt 2, 20095 Hamburg
www.buceriuskunstforum.de

JENISCH HAUS AND THE ERNST-BARLACH HAUS

The Jenisch Haus and the Ernst-Barlach Haus are little jewels and not too far from the workshop venue.

The Jenisch Haus was built between 1831 and 1834 in neo-classical style and belonged to the Hamburger merchant and senator Martin Johann Jenisch. The interiors still witness of Empire and Biedermeier styles of that time. The museum hosts temporary exhibitions mainly related to art and culture in the 19th century. The Ernst-Barlach-Haus was built in the 60s and is currently a private museum containing key works by the expressionist sculptor, graphic artist and writer Ernst Barlach (1870–1938)

Both small museums are not too far from the Elbe river and set in the Jenisch park—which is also worth a visit, not only on sunny Summer days

Near S-Bahn station “Klein Flottbek” (lines S1 and S11)
www.altonaermuseum.de/jenisch_haus.html (in German only!)
www.barlach-haus.de

ALTONAER MUSEUM

The exhibitions at the Altonaer Museum give an overview of art and cultural history in Northern Germany over a few centuries.

Museumstraße 23, 22765 Hamburg
S-Bahn station “Altona” (lines S3, S31, S1, S11)
www.altonaermuseum.de (in German only)

OTHER PLACES OF INTEREST

HAGENBECK ZOO

Hagenbeck zoo is one of the most famous zoos in Germany and is located in a beautiful park— also including a recently re-designed polar landscape section. The tropical aquarium can be visited separately.

Lokstedter Grenzstraße 2, 22527 Hamburg
U-Bahn station “Hagenbecks Tierpark” (line U2)
www.hagenbeck.de

MODEL RAILWAY MUSEUM—MINIATUR WUNDERLAND

Miniatur Wunderland is an amazing permanent exhibition for all those who are fond of model railways and miniature landscape—with or without kids.

Kehrwieder 2-4, Block D— Speicherstadt
www.miniatur-wunderland.com

BOTANIC GARDEN HAMBURG

Free admission, opening times: daily from 9:00 a.m. to about 1 1/2 hours before sunset.

Ohnhorststraße, 22609 Hamburg
S-Bahn station “Klein Flottbek” (lines S1 and S11)
www.bghamburg.de

SPECIAL EVENTS IN HAMBURG IN 2013

INTERNATIONAL GARDEN SHOW

The 2013 international garden show (IGS) takes place in the south of Hamburg from 26 April to 13 October 2013—and enables visitors to go “around the world in 80 gardens”.

Directly close to the S-Bahn station “Wilhelmsburg” (lines S3 and S31).
www.igs-hamburg.de

INTERNATIONAL ARCHITECTURE EXHIBITION

Furthermore, the 2013 international architecture exhibition IBA including a variety of projects on different themes takes place in the south of Hamburg from 23 March 2013 to early 2014.

www.iba-hamburg.de

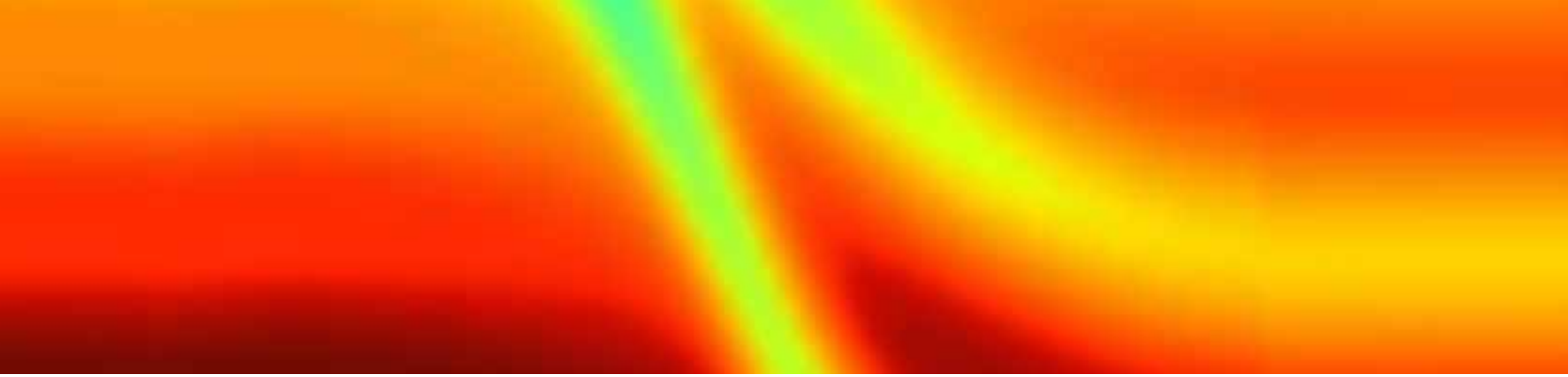
PARTICIPANTS

Aebi, Philipp // Universit  de Fribourg // philipp.aebi@unifr.ch
Allen, James // University of Michigan // jwallen@umich.edu
Antal, Agnes // EPFL // agnes.antal@epfl.ch
 rr l , Minna // Tampere University of Technology // minna.arrala@tut.fi
Ast, Christian // MPI for Solid State Research // c.ast@fkf.mpg.de
Avella, Adolfo // Universit  degli Studi di Salerno // avella@sa.infn.it
Baev, Ivan // University of Hamburg // ivan.baev@desy.de
Bascones, Elena // Instituto de Ciencia de Materiales de Madrid // leni@icmm.csic.es
Baumberger, Felix // University of Geneva // felix.baumberger@unige.ch
Bertini, Silvia // European XFEL // silvia.bertini@xfel.eu
Biermann, Silke // Ecole Polytechnique // biermann@cpht.polytechnique.fr
Birke, Michael // DESY // michael.birke@desy.de
Braun, Juergen // LMU Munich // juergen.braun@cup.uni-muenchen.de
Brouet, Veronique // Universit  Paris Sud - CNRS // veronique.brouet@u-psud.fr
Burger, Claudia // European XFEL // claudia.burger@xfel.eu
Cacho, Cephise // Central Laser Facility STFC // cephise.cacho@stfc.ac.uk
Cao, Yue // University of Colorado // ycao@colorado.edu
Cheng, Cheng-Maw // National Synchrotron Radiation Research Center // makalu@nsrrc.org.tw
Chiang, Tai // University of Illinois // tcchiang@illinois.edu
Chikina, Alla // TU Dresden // Alla.Chikina@tu-dresden.de
Claessen, Ralph // Universit t W rzburg // claessen@physik.uni-wuerzburg.de
Crepaldi, Alberto // Elettra-Sincrotrone Trieste // alberto.crepaldi@elettra.trieste.it
Das, Tanmoy // Los Alamos National Laboratory // tnmydas@gmail.com
De Jong, Nick // IoP UvA // n.dejong@uva.nl
Dessau, Dan // University of Colorado // Dessau@Colorado.edu
Di Sante, Domenico // University of L'Aquila // domenico.disante@aquila.infn.it
Dudy, Lenart // Universit t W rzburg // lenart.dudy@physik.uni-wuerzburg.de
Ebeling, Bernd // European XFEL // bernd.ebeling@xfel.eu
Eschbach, Markus // Forschungszentrum J lich // m.eschbach@fz-juelich.de
Evtushinsky, Daniil // IFW Dresden // danevt@gmail.com
Frantzeskakis, Emmanouil // University of Amsterdam // e.frantzeskakis@uva.nl
Fujimori, Atsushi // University of Tokyo // fujimori@phys.s.u-tokyo.ac.jp
Gardonio, Sandra // University of Nova Gorica // sandra.gardonio@ung.si
Gembalies, Imke // European XFEL // imke.gembalies@xfel.eu
Giannetti, Claudio // Universit  Cattolica del Sacro Cuore // claudio.giannetti@unicatt.it
Gierz, Isabella // MPI for the Structure and Dynamics of Matter // isabella.gierz@mpsd.cfel.de
Gorelov, Evgeny // Forschungszentrum J lich // e.gorelov@fz-juelich.de
Hanff, Kerstin // IEAP of the University of Kiel // hanff@physik.uni-kiel.de
Hariki, Atsushi // Osaka Prefecture University // hariki@ms.osakafu-u.ac.jp
Haverkort, Maurits W. // MPI CPFS // Maurits.Haverkort@cpfs.mpg.de
Held, Karsten // TU Wien // held@ifp.tuwien.ac.at
Hieke, Florian // Institute for Experimental physics and CFEL // florian.hieke@desy.de
Hofmann, Felix // Universit t Hamburg // fhofmann@physik.uni-hamburg.de
Hofmann, Philip // Aarhus University // philip@phys.au.dk
Hricovini, Karol // Universit  de Cergy-Pontoise // karol.hricovini@u-cergy.fr
Ideta, Shin-ichiro // Tokyo University // ideta@ap.t.u-tokyo.ac.jp

Iwasawa, Hideaki // Hiroshima University // h-iwasawa@hiroshima-u.ac.jp //
 Johannsen, Jens // EPFL // jens.johannsen@epfl.ch //
 Johannsen, Jens Christian // EPFL // jens.johannsen@epfl.ch //
 Jörg, Fink // IFW Dresden // J.Fink@ifw-dresden.de //
 Jung, Wonsig // Yonsei University // wqwsazx@gmail.com //
 Kampen, Thorsten // SPECS Surface Nano Analysis GmbH // Thorsten.Kampen@specs.com //
 Kim, Changyoung // Yonsei University // changyoung@yonsei.ac.kr //
 Kim, Timur // Diamond Light Source Ltd. // timur.kim@diamond.ac.uk //
 Kim, YongSu // Seoul National University // su0314@snu.ac.kr //
 Kong, Qingyu // Synchrotron Soleil // kong@synchrotron-soleil.fr //
 Krasovskii, Eugene // University of the Basque Country // eugene.krasovskii@ehu.es //
 Kunze, Thomas // FU Berlin // tku@zedat.fu-berlin.de //
 Kuroda, Kenta // Hiroshima University // kuroken224@hiroshima-u.ac.jp //
 Ku, Wei // Brookhaven National Laboratory // weiku@mailaps.org //
 Lahoud, Elias // Technion // eliaslah@gmail.com //
 Landolt, Gabriel // University of Zurich // gabriel.landolt@psi.ch //
 Lechermann, Frank // University of Hamburg // Frank.Lechermann@physnet.uni-hamburg.de //
 Lichtenstein, Alexander // University of Hamburg // alichten@physnet.uni-hamburg.de //
 Lindroos, Matti // Tampere University of Technology // matti.lindroos@tut.fi //
 Liu, Guodong // Chinese Academy of Sciences // gdliu_arpes@iphy.ac.cn //
 Mahalingam, Maniraj // UGC-DAE Consortium for Scientific Research // mr.maniraj@gmail.com //
 Maletz, Janek // IFW Dresden // j.maletz@ifw-dresden.de //
 Manghi, Franca // FIM Department // franca.manghi@animore.it //
 Manske, Dirk // Max Planck Institute for Solid State Research // d.manske@fkf.mpg.de //
 Matho, Konrad // Néel Institute // konrad.matho@grenoble.cnrs.fr //
 Matt, Christian // Paul Scherrer Institute // christian.matt@psi.ch //
 Millan, Samuel // Universidad Autonoma del Carmen // smillan@pampano.unacar.mx //
 Mishchenko, Andrey // RIKEN CEMS // mishchenko@riken.jp //
 Miwa, Jill // Aarhus University // miwa@phys.au.dk //
 Miyamoto, Koji // Hiroshima University // kmiyamoto@hiroshima-u.ac.jp //
 Moberg, Robert // VG Scienta AB // robert.moberg@vgscienta.com //
 Molodtsov, Serguei // European XFEL // serguei.molodtsov@xfel.eu //
 Momoh, Abraham // AM Excellent Productive Solution World // amepsworldgm@gmail.com //
 Monney, Claude // Fritz-Haber-Institut // monney@fhi-berlin.mpg.de //
 Monney, Gael // Université de Fribourg // gael.monney@unifr.ch //
 Moritz, Brian // SLAC // moritzb@slac.stanford.edu //
 Mulazzi, Mattia // Universität Würzburg // mattia.mulazzi@physik.uni-wuerzburg.de //
 Navez, Patrick // Universität Duisburg Essen // patrick.navez@uni-duisburg-essen.de //
 Nayak, Jayita // UGC-DAE Consortium for Scientific Research // jayitanayak@gmail.com //
 Nieminen, Jouko // Tampere University of Technology // jouko.nieminen@tut.fi //
 Okuda, Taichi // Hiroshima University // okudat@hiroshima-u.ac.jp //
 Oles, Andrzej M. // Jagiellonian University // a.m.oles@fkf.mpg.de //
 Pfaff, Florian // University of Würzburg // florian.g.pfaff@physik.uni-wuerzburg.de //
 Plucinski, Lukasz // FZ Juelich // l.plucinski@fz-juelich.de //
 Plumb, Nicholas // Swiss Light Source PSI // nicholas.plumb@psi.ch //
 Potthoff, Michael // University of Hamburg // michael.potthoff@physik.uni-hamburg.de //

PARTICIPANTS

Rausch, Roman // University of Hamburg // rrausch@physnet.uni-hamburg.de //
Razzoli, Elia // Université de Fribourg // elia.razzoli@unifr.ch //
Ressel, Barbara // University of Nova Gorica // barbara.ressel@ung.si //
Richter, Christine // University of Cergy-Pontoise // richter@u-cergy.fr //
Rohwer, Timm // MIT // rohwer@mit.edu //
Rotenberg, Eli // Lawrence Berkeley National Laboratory // erotenberg@lbl.gov //
Santander-Syro, Andrés Felipe // CSNSM - Université Paris Sud // andres.santander@csnsm.in2p3.fr //
Schaefer, Joerg // University of Wuerzburg // joerg.schaefer@physik.uni-wuerzburg.de //
Scharnberg, Kurt // Universität Hamburg // scharnbe@physnet.uni-hamburg.de //
Schulz, Joachim // European XFEL // Joachim.schulz@xfel.eu //
Schumann, Frank O. // Max-Planck-Institut für Mikrostrukturphysik // schumann@mpi-halle.de //
Schuppler, Stefan // Karlsruhe Institute of Technology (KIT) // stefan.schuppler@kit.edu //
Schwab, Holger // Universität Würzburg // holger.schwab@physik.uni-wuerzburg.de //
Schwier, EikeF // Hiroshima Synchrotron Radiation Center // schwer@hiroshima-u.ac.jp //
Shimada, Kenya // Hiroshima Synchrotron Radiation Center // kshimada@hiroshima-u.ac.jp //
Shimajima, Takahiro // University of Tokyo // shimajima@ap.t.u-tokyo.ac.jp //
Sing, Michael // University of Würzburg // sing@physik.uni-wuerzburg.de //
Sohn, Chang Hee // Seoul National University // sch31132@phy.snu.ac.kr //
Sorgenfrei, Florian // Helmholtz-Zentrum Berlin // florian.sorgenfrei@helmholtz-berlin.de //
Starowicz, Pawel // Jagiellonian University // pawel.starowicz@uj.edu.pl //
Stojanov, Petar // SPECS Surface Nano Analysis GmbH // petar.stojanov@specs.com //
Straßer, Carola // Max Planck Institute for Solid State Research // c.strasser@fkf.mpg.de //
Strocov, Vladimir N. // Swiss Light Source PSI // vladimir.strocov@psi.ch //
Tanaka, Yusuke // Tohoku University // y.tanaka@arpes.phys.tohoku.ac.jp //
Teichmann, Martin // FU Berlin // lkb.teichmann@gmail.com //
Thiagarajan, Balasubramanian // MAX IV Laboratory // tbalu@maxlab.lu.se //
Tohyama, Takami // Kyoto University // tohyama@yukawa.kyoto-u.ac.jp //
Tournier-Colletta, Cédric // EPFL // cedric.tournier@epfl.ch //
Tsuei, Ku-Ding // National Synchrotron Radiation Research Center // tsuei@nsrrc.org.tw //
Tsuji, Naoto // University of Tokyo // tsuji@cms.phys.s.u-tokyo.ac.jp //
Tusche, Christian // Max-Planck-Institut für Mikrostrukturphysik // tusche@mpi-halle.mpg.de //
Valenti, Roser // University of Frankfurt // valenti@itp.uni-frankfurt.de //
Van Hees, Brunhilde // European XFEL // brunhilde.van.hees@xfel.eu //
Vyalikh, Denis // TU Dresden // denis.vyalikh@gmail.com //
Wehling, TimOliver // University of Bremen // wehling@itp.uni-bremen.de //
Weinelt, Martin // Freie Universität Berlin // weinelt@physik.fu-berlin.de //
Wells, Justin // NTNU // justin.wells@ntnu.no //
Werner, Philipp // University of Fribourg // philipp.werner@unifr.ch //
Wojek, BastianM. // KTH Royal Institute of Technology // basti@kth.se //
Wurth, Wilfried // Universität Hamburg // wilfried.wurth@desy.de //
Xie, Zhuojin // Chinese Academy of Sciences // attixiezhuojin@163.com //
Xu, Nan // Paul Scherrer Institute // nan.xu@psi.ch //
Yao, Mengyu // Shanghai Jiao Tong University // yao712@gmail.com //
Yavas, Hasan // DESY // hasan.yavas@desy.de //
Ye, Zirong // Fudan University // zirongye@gmail.com //
Yoo, Hyangkeun // Seoul National University // hkyoo0419@gmail.com //



Zhang, Tong // Fudan University // tzhang18@fudan.edu.cn //
Zhao, Lin // Chinese Academy of Sciences // lzha@iphy.ac.cn //
Zhou, Xingjiang // Institute of Physics // XJZhou@aphy.iphy.ac.cn //
Zhu, Xiegang // Aarhus University // zhu@phys.au.dk //
Zhu, Zhi-Huai // University of British Columbia // zhzhu@phas.ubc.ca //



AUTHOR INDEX

- Abbamonte, P. P1.26
 Adell, J. P2.35
 Aebi, P. P1.33, P2.16
 Aiura, Y. Mo.05, P1.28, P2.42
 Akihiro, I. P1.14
 Allen, J. W. Mo.01, P2.09, P2.12
 Andersen, O. K. Mo.01, Mo.04
 Ando, Y. Mo.09
 Aoki, H. P2.03
 Arita, M. P2.21
 Arnold, G. Mo.05
 Artioli, A. Mo.08
 Ast, C. P2.31, P2.34
 Autès, G. P1.10
 Avella, A. P1.29
 Avigo, I. Th.16
 Balasubramanian, T. Tu.09, P2.35
 Balog, R. P2.35
 Bansal, N. P2.29
 Bansil, A. P1.18
 Bareille, C. Th.01
 Barman, S. R. P1.08, P2.44
 Barmettler, P. P2.03
 Barreto, L. P2.18
 Bascones, E. Th.13
 Bauer, M. P1.11, P1.13
 Baumberger, F. Tu.01
 Bazalitsky, G. P1.24
 Beck, H. P2.16
 Behnke, L. Th.03
 Behrmann, M. P1.31
 Belozarov, A. P1.32
 Berciu, M. Th.09
 Berger, H. P1.01, P1.10, P2.23
 Berntsen, M. Tu.09
 Bianchi, M. P2.18, P2.35
 Biermann, S. Th.08, P1.12
 Bihlmayer, G. P2.20
 Binder, S. P1.26
 Blügel, S. P2.20
 Boariu, F. L. Th.01
 Boothroyd, A. T. P1.32
 Bostwick, A. Mo.10, P1.10, P1.34, P2.41
 Botril, K. P1.26
 Bovensiepen, U. Th.16, P1.13
 Bowlan, J. Fr.06
 Brahlek, M. P2.29
 Braun, J. Tu.05, P2.17, P2.27
 Breese, M. P1.26
 Buczko, R. Tu.09
 Bud'ko, S. L. Th.12
 Bugnon, P. P1.01, P2.23
 Cacho, C. Fr.05, P1.01, P2.23, P2.36, P2.37
 Calderón, M. J. Th.13
 Cancellieri, C. Tu.13
 Canfield, P. C. Th.12
 Cao, G. Th.02
 Cao, Y. Mo.05, Th.02, P2.29
 Carbone, C. Mo.02, P2.39
 Carley, R. Fr.06
 Carr, A. P1.11
 Cavalleri, A. Fr.05, P1.01
 Cavalleri, A. Fr.05, P1.01, P2.36
 Chakrabarti, A. P2.44
 Chang, J. P1.23
 Chang, Y. J. P1.34, P2.41
 Chapman, R. P1.01
 Chaska, K. Tu.02
 Chatterjee, S. P2.15
 Chen, C. H. P1.05
 Cheng, C. M. P1.05
 Chiang, T. Tu.08
 Chikina, A. P2.05
 Chiu, C. C. P1.05
 Christof, N. P1.24
 Chulkov, E. P2.22
 Ciavardini, A. P1.03
 Cilento, F. P1.01, P2.23
 Ciuchi, S. P1.19
 Claessen, R. Tu.04, We.01, P1.41
 Cliento, F. P2.37
 Comin, R. P1.43
 Coreno, M. P1.03
 Cortés, R. P1.13
 Crepaldi, A. P1.10, P2.23, P2.37
 Crepaldi, C. P1.01
 Cuk, T. Fr.05
 D'Souza, S. W. P2.44
 Damascelli, A. Tu.12, P1.42, P1.43, P2.34
 Danzenbächer, S. P2.05
 Das, T. Th.10, P1.18
 De Ninno, G. P1.03
 Dendzik, M. P2.18
 Denlinger, J. Mo.01, P2.09, P2.12
 Dessau, D. Mo.05, Th.02, P2.29
 Devereaux, T. P. We.07
 Dhaka, R. Th.12
 Dhesi, S. Fr.05, P1.01
 Di Sante, D. P1.19
 Dil, J. H. P1.42, P2.19, P2.29
 Ding, H. P1.12, P1.23
 Domanski, T. P1.22
 Drachuck, G. P1.23, P1.24
 Drube, W. We.01
 Duda, L.-C. We.01
 Dudin, P. P1.06
 Dudy, L. Mo.01, P2.12
 Dziawa, P. Tu.09
 Döring, S. P2.20
 Ebert, H. Tu.05, P2.17, P2.27
 Eckstein, M. We.04, Fr.02, P2.02
 Efimov, V. P1.32
 Eich, A. P1.26
 Eisaki, H. Mo.05, P1.14, P1.26
 Elfmov, I. S. Tu.12, P1.42, P1.43
 Ellguth, M. P2.38
 Eremeev, S. P2.22
 Eremin, I. We.05, P1.13
 Evtushinsky, D. Th.06
 Fabris, S. P2.32
 Fan, Q. P1.15
 Fedorov, A. P2.32
 Feldhaus, J. P1.26
 Feng, D. L. We.03
 Ferrero, M. P1.12
 Feyer, V. P2.38
 Fink, J. Th.16, P1.13, P2.32
 Fisk, Z. P2.09
 Forster, F. P1.17
 Frantzeskakis, E. P2.10
 Freericks, J. K. We.07
 Frietsch, B. Fr.06
 Fromm, F. P1.01, P2.37
 Fujii, J. Mo.08
 Fujimaki, Y. P1.26
 Fujimori, A. Mo.06, Tu.13, P1.14
 Fujiwara, H. We.01, P1.41
 Föhlisch, A. P1.32
 Gambardella, P. P2.39
 Garcia-Fernandez, M. P1.33
 Gardonio, S. Mo.02, P1.03, P2.39
 Garnier, M. G. P1.33
 Gauthier, D. P1.03
 Ge, Q. P1.15

Geck, J.....	P2.15	Holldack, K.	P1.32	King, P.	Tu.01
Gegenwart, P.....	P1.43	Horn, K.	Mo.10, P1.08	Kipp, L.	P1.11, P1.13
Giannetti, C.....	Fr.01	Hornekaer, L.	P1.01, P2.37	Kirschner, J.	Th.03, P2.38
Gibert, M.	P1.33	Horsch, P.	Th.09, P1.29	Kittaka, S.....	P1.42
Gierz, I.	Fr.05, P1.01, P2.31, P2.36	Hricovini, K.	P2.27	Klein, M.V.....	P1.26
Gloskovskii, A.....	P1.08	Huang, Y. B.....	P1.23	Kobayashi, M.	Tu.13
Goldoni, A.	P2.11, P2.39	Hyang Keun, Y.....	P1.34	Kokh, K.....	P2.22
Goos, A.	P1.26	Hyun, S. I.....	P1.34	Kopp, T.	We.01
Goraus, J.	P1.17	Höchst, H.	P2.31	Kopprasch, J.....	P1.04
Gorelov, E.....	P1.30	Höppner, M.	P2.05	Korneta, O.....	Th.02
Gorgoi, M.....	We.01	Iacobucci, S.....	P2.11	Kowalski, B. J.....	Tu.09
Gorovikov, S.....	P2.11	Ideta, S.	P1.14	Krasovskii, E.....	Tu.06
Grazioli, C.....	P1.03, P2.39	Ivanov, R.	P1.03	Krasyuk, A.	P2.38
Green, M.....	P1.17	Iwasawa, H.....	Mo.05, P1.28, P2.42	Krutitsky, K.	P2.07
Greenblatt, M.....	Mo.01	Izquierdo, M.....	P1.32	Ku, W.	Th.11
Grioni, M.....	P1.01, P1.10, P2.23, P2.37	Janoschek, M.....	P2.12	Kumigashira, H.	Mo.06
Grueneis, A.....	P2.32	Jean-Marc, T.....	Tu.13	Kummer, K.	P1.32
Grütmacher, D.....	P2.20	Jeon, S. H.....	P2.41	Kunze, T.....	P1.04, P2.25
Gu, G. D.	Mo.05, P2.29	Jeong, D. W.	P1.34	Kuroda, K.	P2.21, P2.22
Guerassimova, N.	P1.26	Jia, G.	P1.36	Köhler, A.....	P1.01, P2.36
Haberer, D.....	P2.32	Jia, J.	Mo.12	Lahoud, E.....	Tu.02
Hafermann, H.	P2.06	Jian, J.....	Mo.03	Landolt, G.	Mo.07, P1.42, P2.19, P2.29
Hahn, S. E.....	Th.12	Jiang, J.....	P1.15, P2.42	Laubschat, C.....	P2.05
Haiyun, L.	P1.02	Jiang, R.	Th.12	Lawrenz, D.	P2.25
Hakeem, A.....	P1.38, P1.39	Johannsen, J. C.	P1.01, P2.37	Leandersson, M.	P2.27, P2.35
Han, S.....	P2.41	Jong, N. de.....	P2.28	Lechermann, F.....	P1.31
Hancock, J. N.....	P1.43	Jung, W.	P1.37	Lee, C.....	P1.14
Hanff, K.	P1.11	Kaiser, S.	Fr.05, P1.01	Lejay, P.	Th.01
Hanke, W.	Tu.04	Kalläne, M.	P1.11	Levy, G.....	P1.43
Harada, Y.....	P1.41	Kamble, B.	P1.13	Li, C.....	Th.03
Hariki, A.....	P2.01	Kaminski, A.	Th.12	Li, G.	Tu.04
Harmon, B. N.	Th.12	Kampen, T. U.....	P1.04, P2.25	Li, H. X.	Th.02
Harter, J.	P2.15	Kang, J. S.	P2.09	Lichtenstein, A. ..	Mo.02, P1.32, P2.06, P2.39
Hase, I.	P1.28	Kanigel, A.	Tu.02, P1.24	Lindroos, M.	Tu.07, P2.31
Hashimoto, M.	P1.14	Kanski, J.....	P2.27	Liu, C.	Th.12
Haverkort, M.	Mo.04	Kapteyn, H.	P1.11	Liu, F.	Mo.12
Haverkort, M. W.	Mo.01, Tu.12, P1.42	Karolak, M.....	Mo.02, P1.32, P2.39	Liu, G.	P2.14
Hayashi, H.....	P2.42	Kemper, A. F.....	We.07	Liu, H.	Fr.05, P1.01
Heckmann, O.....	P2.27	Keren, A.....	P1.23, P1.24	Lizzit, S.....	P2.39
Held, K.....	We.02	Kern, K.....	P1.01, P2.23, P2.31, P2.34	Lograsso, T. A.	P1.08, P2.44
Hellmann, S.	P1.11, P1.13	Kihou, K.....	P1.14	Longhi, E.	P1.06
Henk, J.	P2.38	Kim, C.....	Tu.10, P1.37	Lu, D.	P1.14
Herdt, A.	P2.20	Kim, J. W.	P2.09	Ludbrook, B.	P1.43, P2.34
Hildebrand, B.....	P2.16	Kim, K.....	P1.10	Ludbrook, B. M.	P1.42
Hoepfner, P.	Tu.04	Kim, K. S.	Mo.10	Luke, G.	P2.15
Hoesch, M.	P1.06, P1.40	Kim, T.	P1.06, P1.27	Luo, J. W.....	P2.29
Hofmann, F.	P2.02	Kim, Y. S.....	P1.34, P2.41	Maeno, Y.....	P1.42
Hofmann, P. Tu.03, P1.01, P2.18, P2.35, P2.37		Kimura, A.	P2.21, P2.22	Mahatha, S. K.....	P2.33, P2.40

AUTHOR INDEX

- Maletz, J. P1.16
- Manghi, F. Mo.11
- Maniraj, M. P1.08, P2.44
- Mannhart, J. We.01
- Manske, D. We.05
- Maple, B. M. P2.12
- Marchenko, D. P2.26
- Marel, D. van der. P1.43
- Mariot, J. M. P2.27
- Markiewicz, R. P1.18
- Markovic, N. P2.41
- Matho, K. P2.05
- Mazzola, F. P2.35
- McKeown Walker, S. Tu.01
- Meetej, N. Tu.02
- Meevasana, W. Tu.01
- Menon, K. S. R. P2.33, P2.40
- Menshchikova, T. P2.22
- Mesot, J. Th.15, P1.23, P2.43
- Miao, H. P1.12
- Miao, L. Mo.12
- Millan, S. P1.21
- Min, B. I. P2.09
- Min, C. H. P2.08
- Minar, J. Tu.05, P2.17, P2.27, P2.43
- Ming, S. P1.24
- Miotti, P. P1.03
- Mishchenko, A. We.06
- Mitrano, M. P1.01, P2.36
- Miwa, J. Tu.03, P2.35
- Miyamoto, K. P2.21, P2.22
- Mo, S. K. P2.29
- Molodtsov, S. P1.32
- Monceau, P. P1.10
- Monney, C. Fr.04, P2.16
- Monney, G. P2.16
- Moras, P. P2.39
- Moreschini, L. Mo.10, P1.10, P1.34
- Moritz, B. We.07
- Moser, S. P1.10
- Mueller, A. We.01
- Muff, S. P2.19
- Mulazzi, M. Mo.03, P2.13
- Mun, B. S. P2.41
- Murnane, M. P1.11
- Mussler, G. P2.20
- Nakajima, M. P1.14
- Namatame, H. P1.28, P2.21, P2.22, P2.42
- Navez, P. P2.07
- Nayak, J. P1.08, P2.44
- Nicolaou, A. P1.42
- Nie, Y. P1.19
- Nishitani, Y. P1.41
- Noh, T. W. P1.34, P2.41
- Nohara, Y. Mo.04
- Offi, F. P2.11
- Oguchi, T. P2.42
- Oh, S. P2.29
- Okuda, T. Tu.11, P2.21, P2.22
- Oleś, A. M. Th.09, P1.29
- Ortiz, I. P1.21
- Oshima, M. Tu.13
- Osterwalder, J. P2.19
- Panaccione, G. Mo.08, P2.11
- Parham, S. Mo.05, Th.02, P2.29
- Park, K. P1.38, P1.39
- Park, S. R. Th.02
- Parmigiani, F. P1.01, P2.23, P2.37
- Patt, M. P2.38
- Patthey, L. P2.43
- Pavarini, E. P1.30
- Pavlenko, N. We.01
- Peng, R. We.03
- Perez, L. P1.21
- Petaccia, L. P2.11, P2.32, P2.39
- Peter, B. Tu.13
- Petersen, J. C. Fr.05, P1.01, P2.36
- Petocchi, F. Mo.11
- Pfaff, F. P1.41
- Piefke, C. P1.31
- Plucinski, L. P2.20
- Plumb, N. Mo.05, Th.02, P1.23, P2.29, P2.43
- Poletto, L. P1.03
- Pontius, N. P1.32
- Popovic, Z. S. Mo.01
- Poteryaev, A. P1.32
- Potthoff, M. P1.07, P2.02
- Prabhakaran, D. P1.32
- Qi, T. F. Th.02
- Qian, D. Mo.12
- Qian, T. P1.12
- Queisser, F. P2.07
- Qui, D. P1.26
- Rader, O. P2.17, P2.26
- Radovic, M. P1.23, P2.43
- Rai, A. P1.08, P2.44
- Raichle, M. P1.42
- Raidel, C. P1.01, P2.37
- Rajput, P. P1.08
- Rak, J. P1.17
- Rausch, R. P1.07
- Razzoli, E. Th.12, Th.15, P1.23, P1.24
- Reber, T. Mo.05, Th.02, P2.29
- Reinert, F. Mo.03, Th.01, P1.17, P2.13
- Reinle-Schmitt, M. Tu.13
- Ren, Z. Mo.09
- Reninger, R. P1.26
- Ressel, B. P1.01, P1.03, P2.23, P2.37
- Rettig, L. Th.16, P1.13
- Richard, P. P1.12
- Richter, C. P2.27
- Rieck, C. P1.20
- Rienks, E. Th.16, P2.26
- Rizzo, A. P2.11
- Rodrigues, N. P1.01
- Roekeghem, A. P1.12
- Rohwer, T. P1.11, P1.13
- Rosen, J. A. P1.43
- Ross, P. N. P2.41
- Rossi, G. Mo.08
- Rossnagel, K. P1.11, P1.13
- Rotenberg, E. Mo.10, P1.10, P1.34, P2.41
- Ruocco, A. P2.11
- Rusydi, A. P1.26
- Rübhausen, M. P1.26
- Sadowski, J. P2.27
- Saha-Disgupta, T. Mo.01
- Saitoh, Y. We.01
- Santander-Syro, A. F. Th.01
- Sato, T. Mo.09
- Satpathy, S. Mo.01
- Scharnberg, K. P1.20
- Scherwitzl, R. P1.33
- Schlagel, D. L. P1.08, P2.44
- Schmitt, T. Tu.13, P2.43
- Schneeloch, J. P2.29
- Schneider, C. M. P2.20, P2.38
- Schnyder, A. We.05
- Scholz, M. P2.26
- Schumann, F. O. Th.03
- Schutzhold, R. P2.07
- Schwab, H. Mo.03, Th.01, P1.17, P2.13
- Schwier, E. F. P1.33
- Schäfer, J. Tu.04

Schüssler-Langeheine, C.....	P1.32	Tanaka, M.....	Tu.13	Wang, Z.....	Mo.12
Sefat, A. S.....	P1.12	Tanaka, Y.....	Mo.09	Waugh, J.....	Th.02, P2.29
Segawa, K.....	Mo.09	Taniguchi, M.....	P1.28, P2.21, P2.22, P2.42	Wehling, T.....	Mo.02, P2.39
Sekiyama, A.....	We.01	Teichmann, M.....	Fr.06, P1.04, P2.25	Weinelt, M.....	Fr.06, P1.04, P2.25
Sekiyama, A.....	P1.41	Tereshchenko, O.....	P2.22	Wells, J.....	Tu.03, P2.35
Sentef, M.....	We.07	Thaler, A.....	Th.12	Werner, P.....	We.04, Fr.02, P2.03
Seyller, T.....	Mo.10, P1.01, P2.37	Thiagarajan, B.....	P2.27	Wiemann, C.....	P2.38
Shai, D.....	P2.15	Thiel, S.....	We.01	Wilhelm, A.....	P2.06
Shen, K.....	P1.19, P2.15	Thirupathaiah, S.....	Th.16	Williams, T.....	P2.15
Shen, Z.....	P1.14	Tjernberg, O.....	Tu.09	Willmott, P.....	Tu.13
Shi, M.....	Tu.13, Th.12, Th.15, P1.23	Tohyama, T.....	P1.25	Willmott, P. R.....	We.01
Shim, J. H.....	P1.34, P2.09	Tomioka, Y.....	P1.14	Winkelmann, A.....	P2.38
Shimada, K.....	Mo.03, P1.28, P2.21, P2.42	Tournier-Colletta, C.....	P1.10	Wojek, B. M.....	Tu.09
Shimajima, T.....	Th.07	Trabant, C.....	P1.32	Wolf, M.....	Th.16
Shirai, K.....	P2.21	Treusch, R.....	P1.26	Wolf, T.....	P1.13
Shu, L.....	P2.12	Trinckauf, J.....	P2.15	Wurth, W.....	Fr.03
Sichkar, S.....	P2.04	Trioni, M. I.....	P2.11	Xu, H.....	We.03
Simmons, M.....	Tu.03	Triscone, J.....	P1.33	Xu, M.....	P1.15
Simoes e Silva, W.....	P2.18	Trivedi, N.....	Tu.02	Xu, N.....	P1.12
Simoncig, A.....	Fr.05, P1.01	Trousselet, F.....	Th.09	Xu, Z.....	Fr.05, P2.29
Sing, M.....	We.01, P1.41	Tsuei, K. D.....	P1.05	Yamasaki, A.....	We.01, P1.41
Singh, S.....	P1.08	Tsuji, N.....	We.04, P2.03	Yang, A.....	P2.29
Singh, Y.....	P1.43	Turcu, E.....	Fr.05, P1.01, P2.23, P2.36, P2.37	Yao, M.....	P2.30
Slomski, B.....	P1.42, P2.19	Tusche, C.....	P2.38	Yarlagadda, S.....	P1.09
Sohn, C. H.....	P1.34, P1.35	Uchida, S.....	P1.14, P1.26	Yashina, L.....	P2.26
Sohrt, C.....	P1.11	Ueda, Y.....	P2.21	Yazyev, O.....	P1.10
Spezzani, C.....	P1.03	Ulstrup, S.....	P1.01, P2.18, P2.35, P2.37	Ye, Z.....	We.03, P1.15
Spiwek, M.....	P1.32	Unnikrishnan, M.....	Mo.08	Yoo, H. K.....	P1.35, P2.41
Springate, E. .	Fr.05, P1.01, P2.23, P2.36, P2.37	Uozumi, T.....	P2.01	Yoon, S.....	P1.39
Stamenkovic, V. R.....	P2.41	Uueda, S.....	P2.21	Yoshida, T.....	Mo.06, P1.14
Stange, A.....	P1.11	Valenti, R.....	Th.05	Yoshida, Y.....	Mo.05, P1.28
Starke, U.....	P1.01, P2.36	Valenzuela, B.....	Th.13	Yoshimatsu, K.....	Mo.06
Starowicz, P.....	P1.17	Varykhalov, A.....	P2.26	Yuh, J. Y.....	P1.05
Stefani, G.....	P2.11	Veenstra, C. N.....	P1.42, P1.43	Zacchigna, M.....	P1.01, P2.23, P2.37
Stensgaard, M.....	P2.18	Verbitskiy, N.....	P2.32	Zajdel, P.....	P1.17
Story, T.....	Tu.09	Veronese, M.....	P2.39	Zegenhagen, J.....	P1.08
Straßer, C.....	P2.34	Vilkov, O.....	P2.32	Zhang, G.....	P1.30
Stricker, D.....	P1.43	Vilmercati, P.....	P2.11	Zhang, P.....	P1.12
Strocov, V. N.....	Tu.13	Vobornik, I.....	Mo.08, P1.17	Zhang, T.....	We.03
Struzzi, C.....	P2.32	Volykhov, A.....	P2.26	Zhang, W.....	P1.12
Stöhr, A.....	P1.01, P2.36	Vyalikh, D.....	Th.04, P2.05, P2.32	Zhang, X. W.....	P2.29
Suga, S.....	We.01, P1.41	Vydrova, Z.....	P1.33	Zhang, Y.....	We.03, P1.15
Sun, Z.....	Mo.05	Walter, A.....	Mo.10, P1.10, P2.41	Zhou, X.....	Th.14
Szczerbakow, A.....	Tu.09	Wang, C.....	P1.21	Zhu, X.....	P2.18
Sánchez-Barriga, J.....	P2.17, P2.26	Wang, D. J.....	P1.05	Zhu, Z.....	Tu.12, P1.42, P1.43
Takahashi, T.....	Mo.09	Wang, H.....	P1.06	Zubko, P.....	P1.33
Tamai, A.....	Tu.01	Wang, Q.....	Mo.05, Th.02, P2.29	Zunger, A.....	P2.29
Tan, S.....	We.03	Wang, W.....	P2.27		

